

**ORGANOTIN COMPOUNDS:- THEIR ANALYSES AND EFFECT ON
MODEL BIOMEMBRANES**

BY

BASIL UGWUNNA NWATA

B.Sc (Hons), University of Ilorin, Nigeria, 1981

M.Sc, University of Ibadan, Nigeria 1984

M.Sc, University of British Columbia, Canada 1989

**A THESIS SUBMITTED IN PARTIAL FULFILLMENT OF THE
REQUIREMENTS FOR THE DEGREE OF DOCTOR OF PHILOSOPHY
IN THE FACULTY OF GRADUATE STUDIES
DEPARTMENT OF CHEMISTRY**

We accept this thesis as conforming to the required standard

THE UNIVERSITY OF BRITISH COLUMBIA

JUNE 1994

© Basil Ugwunna Nwata, 1994

In presenting this thesis in partial fulfilment of the requirements for an advanced degree at the University of British Columbia, I agree that the Library shall make it freely available for reference and study. I further agree that permission for extensive copying of this thesis for scholarly purposes may be granted by the head of my department or by his or her representatives. It is understood that copying or publication of this thesis for financial gain shall not be allowed without my written permission.

(Signature)

Department of CHEMISTRY

The University of British Columbia
Vancouver, Canada

Date 9th AUG. 1994

ABSTRACT

Studies involving the analyses of organotin compounds in marine organisms of British Columbia, and the effect of organotin compounds on the permeability of model biological membranes are presented in this thesis.

Analysis of organotin compounds by gas chromatography-selected ion monitoring mass spectrometry (GC-MS SIM) affords a very specific technique for the identification and quantitation of organotin compounds, by using the peculiar isotope pattern for tin compounds. This methodology is therefore able to distinguish organotin compounds from other compounds that may co-elute with them from the gas chromatograph.

Although some British Columbian locations such as Hastings Arm, Alice Arm, etc showed no organotin contamination, the major organotin pollutants found for some coastal areas such as Denman Island, Dundas Island, etc were tributyltin and dibutyltin species. The butyltin body content for Blue mussels in the contaminated areas range from 14.4 to 37.3 ng/g (wet wt as Sn) for tributyltin and 6.7 to 67.3 ng/g (wet wt as Sn) for dibutyltin species. Dicyclohexyltin levels of 3.5 ng/g and 21.3 ng/g (wet wt as Sn) were found only at Wreck Beach Vancouver, and Anyox respectively.

The effect of organotin compounds on egg phosphatidylcholine (EPC) liposomes or organotin-EPC liposomes, were established by studying the efflux of a probe compound; dimethylarsinic acid (DMA) trapped inside these liposomes, by using ^1H NMR spectroscopy. The probe compound at pH 7.4 exists as two chemical species; DMAH and DMA^- which are capable of diffusing from these liposomes.

When the organotin compounds were added externally to the EPC liposomes, tributyltin chloride caused an increased permeability of the liposomes, which was linearly dependent on the concentration of the externally added tributyltin chloride solution. Monobutyltin trichloride decreased the permeability coefficient of DMAH to the EPC liposomes from 1.7×10^{-8} to 4×10^{-9} cm/s, while trimethyltin cation facilitated the efflux of DMA^- from the liposomes.

For TBT-EPC liposomes formed by a mixture of tributyltin chloride and EPC, the efflux of DMA^- from these liposomes was facilitated by the tributyltin cation only if the liposomes were not in contact with externally added tributyltin chloride solution. When in contact with externally added tributyltin chloride, the ability of the tributyltin cation to act as carrier for DMA^- was lost. The activation energy for the passive efflux of DMAH from TBT-EPC liposomes varied from 52.3 to 64.4 kJ/mol depending on the tributyltin content of the liposome.

For the monobutyltin trichloride-EPC liposomes (MBT-EPC), the monobutyltin cation did not exhibit any ability to act as carrier for DMA^- irrespective of whether it was externally added to the liposomes or not. The DMAH species permeate by passive diffusion with activation energy of 106.8 to 121.5 kJ/mol.

A modified batch hydride generation-graphite furnace atomic absorption spectrophotometric method (HG-GFAAS) is described for total tin determination. In this method, tin hydride was adsorbed and pre-concentrated on graphite furnace tubes pre-coated with palladium or sodium tungstate matrix modifiers, prior to their atomization in the graphite furnace.

TABLE OF CONTENTS

Abstract	ii
Table of contents	iv
List of Tables	xiv
List of Figures	xix
List of Abbreviations	xxiii
Acknowledgements	xxvi
Dedication	xxvii
Chapter 1	
General Introduction	1
1.1 Historical background of the organotin compounds	1
1.2 Industrial applications and use of organotin compounds	1
1.3 Need for a chemical antifouling agent	3
1.3.1 Contact leaching antifouling paints	5
1.3.2 Ablative formulation	5
1.3.3 Self polishing co-polymer paints	6
1.4 Toxicity of organotin compounds	6
1.5 Metabolism and behaviour of tributyltin compounds in the environment	9
1.6 Analytical methods for organotin compounds	11
1.6.1 Molecular spectrophotometry and spectrofluorimetric techniques	12
1.6.2 Electrochemical techniques	13

1.6.3	Atomic spectrometry	14
1.6.4	Gas chromatography	17
1.6.4.1	Hydride generation gas-chromatography (HG-GC)	17
1.6.4.2	Conversion to tetraalkyltin compounds	19
1.6.4.2(a)	Gas chromatography with flame photometric detection (GC-FPD)	20
1.6.4.2(b)	Gas chromatography with atomic absorption spectrometric detection (GC-AAS)	21
1.6.4.2(c)	Gas chromatography with mass spectrometric detection (GC-MS)	21
1.6.5	Liquid chromatography (LC)	21
1.6.6	Thin layer chromatography (TLC) and high performance thin layer chromatography	24
1.7	Tributyltin and government regulations	25
1.8	Objectives and scope of the present study	26
Chapter 2	Speciation and quantitation of butyltin and cyclohexyltin compounds in marine organisms by using capillary column GC-MS SIM	29
2.1	Introduction	29
2.2	Experimental	30
2.2.1	Instrumentation	30
2.2.1.1	Gas chromatography (GC)	30

2.2.1.2	NMR and mass spectrometry	30
2.2.1.3	Gas chromatography-mass spectrometry (GC-MS)	31
2.2.1.4	Mechanical shaker and blender	31
2.2.2	Materials and reagents	32
2.2.3	Synthesis of standard organotin compounds	33
2.2.3.1	Synthesis of tributylmethyltin	33
2.2.3.2	Synthesis of dibutyldimethyltin	33
2.2.3.3	Synthesis of tricyclohexylmethyltin	34
2.2.3.4	Synthesis of dicyclohexyldimethyltin	34
2.2.3.5	Synthesis of the internal standards	34
2.2.3.5(a)	Synthesis of tetrapropyltin	34
2.2.3.5(b)	Direct synthesis of deuterated internal standards	35
2.2.3.6	Synthesis of methylmagnesium iodide	36
2.3	Analytical procedure	36
2.3.1	Gas chromatography	36
2.3.1.1	Establishment of elution profile and retention data	36
2.3.1.2	Suitability of tetrapropyltin as internal standard	37
2.3.1.3	Suitability of $(C_4^2H_9)_3SnCH_3$ and $(C_4^2H_9)_2Sn(CH_3)_2$ as internal standards	37
2.3.2	Low resolution mass spectrometry	38
2.3.3	GC-MS retention data, calibration curves and precision	38
2.3.4	Recovery studies	39

2.3.5	Extraction of the organotin compounds from marine animals	41
2.4	Results and discussion	43
2.4.1	Characterization of the standard tetraorganotin compounds	43
2.4.2	Fragment ions and intensities of the standard tetraorganotin compounds	48
2.4.3	GC-MS elution profile and masses of selected fragment ions used for selected ion monitoring	51
2.4.4	Suitability of tetrapropyltin as internal standard as studied by gas chromatography	53
2.4.5	Detection limit, calibration curves, and precision for the GC-MS SIM analysis	57
2.4.5.1	Detection limit and calibration curves obtained by GC-MS SIM	57
2.4.5.2	Precision of the GC-MS SIM method	62
2.4.6	Recovery studies on the extraction procedure	63
2.4.7	Organotin concentrations in some marine organisms of British Columbia, Canada	67
2.4.7.1	Organotin concentrations in oysters	67
2.4.8	Spread of organotin compounds in the Canadian environment	71
2.4.9	Organotin concentrations in various organisms from the same locations	79

2.4.10	Distribution of organotin compounds in marine animals studied over a period of three years	81
Chapter 3	Effect of tributyltin chloride, monobutyltin trichloride and trimethyltin hydroxide on the permeability of egg phosphatidylcholine liposomes	83
3.2	Dimethylarsinic acid (DMA) as a probe for studying the effect of organotin compounds on the membranes of liposomes	84
3.3	Liposomes as models for biological membranes	85
3.4	Types of liposomes and methods of preparation	87
3.4.1	Multilamellar vesicles (MLVs)	88
3.4.2	Small unilamellar vesicles (SUVs)	88
3.4.3	Large unilamellar vesicles (LUVs)	89
3.5	Transport processes in membranes	90
3.5.1	Simple or passive diffusion	90
3.5.2	Facilitated diffusion	91
3.5.2.1	Solute translocation through channels	92
3.5.2.2	Translocation through carriers	92
3.5.3	Active transport	93
3.6	Solute transport across liposomal membranes	94
3.6.1	Transport of non-ionic solutes	94
3.6.2	Transport of ions	97

3.7	Properties of liposomes capable of yielding investigative information	99
3.8	Butyltin compounds: the need for the present study	99
3.9	Theoretical description of the diffusion experiment applicable to NMR spectrometry	101
3.9.1	Passive diffusion	101
3.9.2	Facilitated diffusion	101
3.10	Experimental	111
3.10.1	Instrumentation	111
3.10.1.1	Nuclear magnetic resonance spectrometry (NMR)	111
3.10.1.2	Lipid extruder and membrane filters	111
3.10.1.3	UV-Visible spectrophotometry	111
3.10.2	Chemicals and reagents	112
3.10.3	Preparation of large unilamellar vesicles (LUVs) from egg phosphatidylcholine (EPC) and the encapsulation of dimethylarsinic acid	112
3.10.4	Preparation of butyltin-EPC LUVs and the encapsulation of DMA	114
3.10.5	The NMR water suppression and spectral acquisition conditions for DMA efflux from EPC and butyltin-EPC liposomes	116

3.10.6 Determination of phospholipid concentrations	
by phosphorus assay	117
3.10.6.1 Extraction of phospholipid from liposomes prior to phosphorus determination	117
3.10.6.2 Lipid concentration determination	117
3.10.7 Processing of the NMR spectra	118
3.10.8 Analysis and treatment of data	120
3.10.8.1 Determination of rate constants and mode of permeation	120
3.10.8.2 Determination of permeability coefficients	124
3.11 Results and Discussion	125
3.11.1 The use of DMA as a probe in permeability studies of EPC liposomes in the presence and absence of organotin compounds in the extraliposomal aqueous compartment	125
3.11.2 Effect of organotin concentration on the efflux of DMA	135
3.11.3 Efflux of DMA from tributyltin chloride-EPC liposomes (with tributyltin chloride absent in the extraliposomal compartment)	139
3.11.4 Efflux of DMA from monobutyltin trichloride-EPC liposomes	145
3.11.5 Effect of the butyltin chloride concentrations of the liposome on permeability properties of TBT-EPC and MBT-EPC liposomes	149

3.11.6	Effect of temperature on the permeability of organotin-EPC liposomes	151
3.11.7	Activation energies for the permeation of butyltin chloride-EPC liposomes	153
3.11.8	Relevance of this NMR study to the environmental toxicity of butyltin compounds	158
Chapter 4	Hydride generation methods of atomic absorption spectrophotometry for total tin determination	160
4.1	Introduction	160
4.2	Experimental	162
4.2.1	Instrumentation	162
4.2.1.1	Continuous hydride generation atomic absorption spectrophotometry (HG-AAS)	162
4.2.1.2	Batch hydride generation-graphite furnace atomic absorption spectrophotometry (HG-GFAAS)	164
4.2.2	Materials and Reagents	165
4.2.3	Methodology for HG-AAS	166
4.2.3.1	Continuous hydride generation method (HG-AAS)	166
4.2.3.2	Batch hydride generation-graphite furnace method (HG-GFAAS)	166
4.2.4	Preparation of matrix modifiers and standard tin solutions	168
4.2.4.1	Preparation of palladium modifier	168

4.2.4.2	Preparation of sodium tungstate modifier	165
4.2.4.3	Preparation of standard tin solutions	169
4.2.5	Optimum concentration of reagents used in HG-AAS	169
4.2.6	Use of L-cysteine to remove interferences	170
4.2.6.1	Optimum concentration of L-cysteine required to remove interferences	171
4.2.7	Optimum conditions for the batch HG-GFAAS	171
4.2.7.1	Optimization of reagent concentrations for HG-GFAAS	172
4.2.7.2	Optimization of the trapping temperatures and trapping time for tin hydride in the graphite furnace tube	172
4.2.8	Treated graphite furnace tubes:- coating the graphite furnace tubes with solutions of sodium tungstate and palladium modifiers	172
4.2.8.1	Optimum modifier treatment of graphite furnace tubes	173
4.2.8.2	Calibration curves for the HG-GFAAS method	173
4.3	Sample digestion and preparation	174
4.4	Results and Discussion	175
4.4.1	Optimum concentrations of sodium borohydride and HCl necessary for the production of stannane in the continuous hydride generator	175
4.4.2	Optimum concentration of L-cysteine required to eliminate interferences in HG-AAS	177

4.4.3	HG-AAS determination of total tin in oysters and standard reference material (Tort 1)	179
4.4.4	Batch hydride generation-graphite furnace atomic absorption spectrophotometry (HG-GFAAS)	182
4.4.4.1	Optimum concentrations of reagents needed for tin hydride production in the HG-GFAAS method	184
4.4.4.2	Optimum flow rate of sodium borohydride into the batch hydride generator	185
4.4.4.3	Optimum temperature for trapping tin hydride in the pre-treated graphite furnace tubes	186
4.4.4.4	Optimum trapping time	187
4.4.4.5	Pre-treatment of graphite furnace tubes with modifiers	188
4.4.4.6	Determination of total tin content of a standard reference material by the HG-GFAAS method	192
Chapter 5	Summary and conclusions	195
	References	202
Appendix A	Map of locations sampled for organotin pollution	220
Appendix B	The NMR spectral acquisition and water suppression parameters for the efflux of dimethylarsinic acid from liposomes	221
Appendix C	Michaelis-Mentons equations for enzyme kinetics	223
Appendix D	Wet ashing apparatus with air cooled reflux condenser used for digestion of marine animals	224

	LIST OF TABLES	PAGE
2.1	¹¹⁹ Sn NMR chemical shifts for the standard organotin compounds	44
2.2	Major fragment ions of tributylmethyltin	48
2.3	Major fragment ions for dibutyldimethyltin and tricyclohexylmethyltin	49
2.4	Major fragment ions for dicyclohexyldimethyltin and tetrapropyltin	50
2.5	Retention time and retention time window used for GC-MS SIM analysis	51
2.6	Fragment ions and masses used to detect and quantitate each organotin compound in GC-MS SIM	53
2.7	Regression data for graphs obtained with various concentrations of the internal standard tetrapropyltin	54
2.8	Detection limits for organotin compounds by GC-MS SIM	60
2.9	Calibration equations used for the quantitation of environmental samples by GC-MS SIM	61
2.10	Precision of the GC-MS SIM	63
2.11	Recovery of organotin compounds spiked into Shrimp	64
2.12	Organotin concentrations in the oyster <u>Crassostrea gigas</u> from some coastal areas of British Columbia	68
2.13	Organotin concentration, spread and speciation in some	

locations of British Columbia	72
2.14 Some organotin concentrations reported for the Blue mussels <u>Mytilus edulis</u>	77
2.15 Organotin concentrations in the Blue mussel <u>Mytilus edulis</u> converted to $\mu\text{g/g}$ wet wt as organotin cation	78
2.16 Organotin distribution in marine animals from Camano Sound British Columbia	79
2.17 Organotin distribution in marine animals from Tasu Sound British Columbia	80
2.18 Organotin body burden for soft shell clams from Quatsino Sound, British Columbia studied over a period of three years	81
3.1 Efflux data for the diffusion of DMAH from EPC liposomes in the absence of organotin compounds	126
3.2 Effect of $33.2 \mu\text{M}$ tributyltin chloride on the efflux of DMAH from EPC liposomes	127
3.3 Effect of $33.2 \mu\text{M}$ monobutyltin trichloride on the efflux of DMAH from EPC liposomes	131
3.4 Data for the efflux of DMA from EPC liposomes in the presence of $33.2 \mu\text{M}$ trimethyltin hydroxide	135
3.5 Effect of tributyltin chloride concentration on	

	DMAH efflux	136
3.6	Effect of monobutyltin trichloride concentration on the efflux of DMAH	138
3.7	Diffusion parameters for the efflux of DMA from tributyltin chloride-EPC liposomes by a mixture of passive and facilitated diffusion	141
3.9	Parameters for the efflux of DMAH from TBT-EPC B liposomes in the presence of externally added tributyltin chloride (16 μ M)	145
3.9	Permeability data for efflux of DMAH from MBT-EPC B liposomes (with monobutyltin trichloride absent in the extraliposomal compartment)	148
3.10	Permeability data for efflux of DMAH from MBT-EPC B liposomes (with monobutyltin trichloride present in the extraliposomal compartment)	148
3.11	Effect of tributyltin chloride concentration on the permeability of tributyltin chloride-EPC liposomes with tributyltin chloride also present in the extraliposomal volume	150
3.12	Effect of monobutyltin trichloride concentration on the permeability of monobutyltin trichloride-EPC liposomes with monobutyltin trichloride also present in the extraliposomal	

volume	150
3.13 Effect of temperature on the permeability properties of TBT-EPC A liposomes	151
3.14 Effect of temperature on the permeability properties of TBT-EPC B liposomes	151
3.15 Effect of temperature on the permeability properties of MBT-EPC A liposomes	152
3.16 Effect of temperature on the permeability properties of MBT-EPC B liposomes	152
3.17 Effect of tributyltin chloride content of liposome on the activation energy for efflux of DMAH from TBT-EPC liposomes	155
3.18 Effect of monobutyltin trichloride content of liposomes on the activation energy for efflux of DMAH from MBT-EPC liposomes	155
3.19 Arrhneius pre-exponential factor for DMAH efflux from TBT-EPC liposomes	157
3.20 Arrhneius pre-exponential factor for DMAH efflux from MBT-EPC liposomes	157
4.1 Graphite furnace atomization program for tin determination by HG-GFAAS	167
4.2 Operating conditions for the continuous hydride generation	

	-atomic absorption spectrophotometry (HG-AAS)	170
4.3	Total tin content of samples analyzed by the HG-AAS method	181
4.4	Reagent ratios needed to maximize tin hydride generation	184
4.5	Comparison of palladium and sodium tungstate-treated graphite furnace tubes showing the atomic absorbance of tin hydride generated from 14 $\mu\text{g/mL}$ tin solution	192
4.6	Total tin content of a standard reference material Tort 1 obtained by different authors	193
4.7	Comparison of figures of merit obtained with the two atomic absorption spectrophotometric methods used in this study	194

	LIST OF FIGURES	PAGE
Figure 2.1	Flow diagram for the extraction of organotin from marine animals	42
Figure 2.2	Mass spectra (EI) of tricyclohexylmethyltin	45
Figure 2.3	¹ H NMR spectra of dicyclohexyldimethyltin	46
Figure 2.4	Mass spectra (EI) of dicyclohexyldimethyltin	47
Figure 2.5	GC-MS elution profile of the standard tetraorganotin compounds	52
Figure 2.6	Effect of internal standard concentration on the linearity of calibration curves for tributylmethyltin	55
Figure 2.7	Effect of internal standard concentration on the linearity of calibration curves for tributylmethyltin	56
Figure 2.8	GC-MS calibration curves for (a) dibutyldimethyltin and (b) tributylmethyltin	58
Figure 2.9	GC-MS calibration curves for (a) dicyclohexyldimethyltin and (b) tricyclohexylmethyltin	59
Figure 2.10	Selected ion current chromatogram of standard organotin compounds spiked into shrimp	65
Figure 2.11	Mass spectra of peak A in Figure 2.10	65
Figure 2.12	Mass spectra of (i) peaks C and (ii) peak D in Figure 2.10	66
Figure 2.13	(a) Selected ion current chromatogram of extract from Blue mussel from Wreck Beach, Vancouver. (b) Mass spectra of	

	peak D in Figure 2.13(a)	76
Figure 3.1	Structure of a phospholipid (phosphatidylcholine)	86
Figure 3.2	Liposome	87
Figure 3.3	Schematic diagram of facilitated diffusion (efflux) mediated by a carrier	93
Figure 3.4	Passive diffusion of a permeant HA across a liposomal membrane	96
Figure 3.5	Proposed mechanism of tributyltin mediated efflux of dimethylarsinate (DMA^-) from a liposome and the equilibria of the carrier-permeant interactions	103
Figure 3.6	^1H NMR spectra of DMA as it diffuses out of EPC liposomes	119
Figure 3.7	Log plot for the efflux of DMA from EPC liposomes	121
Figure 3.8	Chemical species of dimethylarsinic acid present at pH 7.4	123
Figure 3.9	Efflux of DMA from EPC liposomes (organotin compounds are absent in the extraliposomal compartment)	126
Figure 3.10	Time course for the efflux of DMA from EPC liposomes (tributyltin chloride present in the extraliposomal compartment)	128
Figure 3.11	Time course for the efflux of DMA from EPC liposomes (monobutyltin trichloride present in the extraliposomal compartment)	128
Figure 3.12	Log plot of DMA efflux from EPC liposomes ($33.2 \mu\text{M}$ trimethyltin hydroxide present in extraliposomal volume)	133

Figure 3.13	Time course for DMA efflux from EPC liposomes (33.2 μM trimethyltin hydroxide present in extraliposomal volume)	133
Figure 3.14	Effect of tributyltin chloride concentration on the permeability of EPC liposomes (tributyltin chloride was added into the extraliposomal compartment)	137
Figure 3.15	Effect of monobutyltin trichloride on the permeability of EPC liposomes (monobutyltin trichloride was added into the extraliposomal compartment)	137
Figure 3.16	Log plot of DMA efflux from TBT-EPC C liposomes	140
Figure 3.17	Time course for DMA efflux from TBT-EPC C liposomes	140
Figure 3.18	Contribution of passive and facilitated diffusion to the efflux of DMA from TBT-EPC liposomes of different tributyltin chloride composition	142
Figure 3.19	Log plot for efflux of DMA from TBT-EPC C liposomes when 16.7 μM tributyltin chloride is present in the extraliposomal compartment	143
Figure 3.20	Time course for efflux of DMA from TBT-EPC C liposomes when 16.7 μM tributyltin chloride is present in the extraliposomal compartment	144
Figure 3.21	Log plot of DMA efflux from MBT-EPC B liposomes	147
Figure 3.22	Time course for DMA efflux from MBT-EPC B liposomes	147

Figure 3.23	Arrhenius plot for DMAH efflux from TBT-EPC B liposomes	154
Figure 3.24	Arrhenius plot for DMAH efflux from MBT-EPC B liposomes	154
Figure 4.1	Schematic diagram of the apparatus used for the HG-AAS method	163
Figure 4.2	Schematic diagram of the hydride generator used for the HG-GFAAS method	163
Figure 4.3	Effect of sodium borohydride and HCl concentrations on the absorbance of tin hydride produced from 4 $\mu\text{g/mL}$ tin solution	176
Figure 4.4	Effect of the concentration of L-cysteine on the absorbance of tin hydride	178
Figure 4.5	Effect of sodium borohydride flow rate on absorbance	185
Figure 4.6	Effect of trapping temperature on the atomic absorbance of tin hydride	187
Figure 4.7	Effect of trapping time on absorbance	188
Figure 4.8	Effect of sodium tungstate concentration on absorbance	191
Figure 4.9	Effect of palladium on absorbance	191

LIST OF ABBREVIATIONS

b.p	Boiling point
Calcd	Calculated value
cm	Centimeter
Conc	Concentration
Contd	Continued
DMA	Dimethylarsinic acid or equilibrium mixture of DMA ⁻ and DMAH
DMA ⁻	Dimethylarsinate; negatively charged species of dimethylarsinic acid present in solution at pH 7.4
DMAH	Undissociated dimethylarsinic acid present in solution at pH 7.4
EI	Electron ionization
EPC	Egg phosphatidylcholine
GC	Gas chromatograph/chromatography
GC-MS	Gas chromatography with mass spectrometric detection
	or
	Gas chromatograph coupled to a mass spectrometer
GC-MS SIM	Gas chromatography with mass spectrometric detection in the selected ion monitoring mode.
GFAAS	Graphite furnace atomic absorption spectrophotometry
h	hour

HEPES	N-2-Hydroxyethylpiperazine-N'-2-ethanesulphonic acid
HG-AAS	Hydride generation atomic absorption spectrophotometry
HG-GFAAS	Hydride generation-graphite furnace atomic absorption spectrophotometry
Hz	Hertz
i.d	internal diameter
LUVs	Large unilamellar vesicles
M	Molar (mol L^{-1})
MBT	Monobutyltin trichloride
MBT-EPC liposome	Liposome formed by a mixture of monobutyltin trichloride and egg phosphatidylcholine
min	minutes
MS	Mass spectrometer/spectrometry
ND	Not detected
NMR	Nuclear magnetic resonance spectrometer/spectrometry
ppb	Parts per billion
ppm	Parts per million
psi	Pounds per square inch
RSD	Relative standard deviation
SIM	Selected ion monitoring
TBT	Tributyltin chloride
TBT-EPC liposome	Liposome formed by a mixture of tributyltin chloride and

	egg phosphatidylcholine
tris	Tris(hydroxymethyl)aminomethane
TSP	Deuterated 3-(trimethylsilyl) propionic acid sodium salt
v/v	Volume to volume ratio
w/v	Weight to volume ratio

ACKNOWLEDGEMENTS.

I wish to express my gratitude to my research supervisor Professor W.R. Cullen for his guidance and interest in this research, and for my financial support.

I would like to thank Dr Gunther Eigendorf for his advice on mass spectrometry, and for his kindness towards me.

I am also grateful to Madiba Saidy, Ryan Males, and the following people: Dr.'s Christopher Harrington, Bruce Todd, Roshan Cader, Kian Pang for their help in the various stages of this thesis, and to the past and present members of Professor Cullen's research group for many helpful discussions.

My gratitude also goes to the following people; Ms Lina Madilao, Mr Steve Rak, Kim Wong and Gary Hewitt for their help in the various technical aspects of this work, and to Dr P.R. Cullis and Professor F.G. Herring for the use of their facilities.

I am thankful to the Department of Chemistry, University of British Columbia, Canada for financial support and provision of research facilities.

I also wish to express my sincere gratitude to my mother, brothers and sisters, and brother-in-law Dr A.N. Ewunonu, for their encouragement to me.

To my wife Joyce, and children; Edoziem and Chima, I owe you much gratitude for the encouragement and moral support you gave me.

DEDICATION

This thesis is dedicated to the memory of my beloved father

Chief Nelson Ukachi Nwata.

Your departure before the task could be completed was very painful, but the daily remembrance of you is my source of inspiration. Rest in perfect peace.

CHAPTER 1**GENERAL INTRODUCTION.****1.1. HISTORICAL BACKGROUND OF THE ORGANOTIN COMPOUNDS.**

The synthesis of diethyltin diiodide by Frankland¹ in 1849, marked the introduction of a new class of compounds that were later to occupy a significant position in industry and agriculture. By definition, organotin compounds are those compounds that have a carbon-tin covalent bond in the molecule. Progress in the chemistry of organotin compounds was enhanced by the discovery of Grignard reagents which made possible the production of a variety of organotin compounds of formula R_4Sn , from which lower alkyl- or aryl- tin compounds could easily be made.

The first industrial application of organotin compounds was made in 1936, when Yngve of the Carbide and Carbon Chemical Company, U.S.A., discovered the heat stabilizing effect of organotin compounds on polyvinyl chloride (PVC) and other chlorinated hydrocarbon polymers². The organotin compounds that have been found useful in this application are the mono and dibutyltin compounds and the dioctyltin compounds.

1.2 INDUSTRIAL APPLICATIONS AND USE OF ORGANOTIN COMPOUNDS.

The organotin compounds find a wide range of use in the manufacturing

industry, agriculture and medicine. Because of their very low toxicity, the dioctyltin derivatives are used as stabilizers for food packaging polymers. Organotin compounds are also used for cold curing of silicone rubber and as polymerisation catalysts; for example, butylchlorotin dihydroxide³. Dibutyltin diacetate is a catalyst for flexible foams. Some organotin dihalides having the formula $R_2SnX_2L_2$ (R=ethyl or phenyl, X=chloride or bromide, L_2 = o-phenanthroline or 2-(2-pyridyl) benzimidazole exhibit anti-tumour and anti-herpes activity in vitro⁴. Dibutyltin dilaurate is also effective in the removal of intestinal worms in poultry³. Dicyclohexyltin derivatives of dipeptides having the formula Cy_2SnL (L=glycylglycine, glycylalanine, glycylphenylalanine and glycyltyrosine) exhibit high cytotoxicity in vitro to breast cancer cells⁵.

The triorganotin compounds are the most important of the organotin compounds in agricultural applications. For example, tricyclohexyltin compounds are effective as miticides and possess marked acaricidal action against plant-feeding mites, but have very little effect on predacious mites and insects³. They also have been reported as antifeedants for the Gypsy moth Porthetria dispar⁶. The pesticide Plictran[®] marketed by Dow Chemical Company has tricyclohexyltin hydroxide as the active ingredient⁷, and has been used in Canada for crop protection on apples and pears⁸. Peropal[®], a pesticide marketed by Bayer AG has 1-tricyclohexyltin-1,2,4-triazole as the active ingredient.

The triphenyltin compounds show antifungal activity. The fungicide Brestan[®] marketed by Hoechst A.G, Germany, contains triphenyltin acetate and has been used against a broad range of fungal organisms in sugar beet and potatoes³. Du-Ter[®], a

fungicide marketed by Philips-Duphar, Holland contains triphenyltin hydroxide as the active ingredient³. The use of triphenyltin hydroxide as an antifeedant for the Colorado beetle Leptinotarsa decemlineata has also been reported⁹.

The tributyltin compounds are fungicides, algaeicides and slimicides, and have been widely used as wood preservatives. Presently, their major use is in marine antifouling paint formulations for protecting the hulls of ships and boats from algae, fungi, sponges, molluscs, barnacles, diatoms, shipworms etc. Such fouling has the effect of increasing weight and drag, causing the ship to consume more fuel to maintain speed. The tributyltin compounds used in marine paint formulations are bis(tributyltin) oxide, bis(tributyltin) dodeceny succinate, bis(tributyltin) sulphide, tributyltin fluoride, tributyltin resinate, tributyltin methacrylate, bis(tributyltin) adipate. Unfortunately the tributyltin compounds are the major organotin compounds of concern from the point of view of environmental marine pollution. When used as antifouling agents, they pollute the marine environment. They do not remain localized but spread throughout the marine environment causing considerable problems such as imposex in marine gastropods¹⁰ and the deformation and decline of oyster stock¹¹.

1.3 NEED FOR A CHEMICAL ANTIFOULING AGENT.

The nuisance caused by the growth of unwanted marine organisms is a major problem in the maritime industry. One of the early approaches taken to prevent fouling in wooden ships, was the use of copper metal sheathing¹² on the ship's hulls.

This achieved moderate success in the control of fouling. In steel ships, the use of copper metal sheathing is not appropriate because of the severe galvanic corrosion of steel when in contact with copper and sea water¹². The usual method of fouling prevention in steel ships is to use chemical agents which are usually incorporated in the paints used to paint the hulls. These antifouling paints act by releasing biocides, which kill the larvae and spores of any marine animals and plants attempting to settle on the ship's hull.

Among the early biocides employed for this purpose was cuprous oxide¹². Cuprous oxide exhibits a wide spectrum of toxicity to animals, but many plants are resistant to it. Continuous use of the copper oxide results in the formation of insoluble greenish salts within the surface layers of the paint film. The build up of these salts on the surface prevents further controlled release of fresh biocide. This process limits the life time, and the efficiency of the paint. The search for biocides to boost the performance of cuprous oxide led to the screening of the organotin compounds for biocidal activity. Tributyltin compounds were found to be suitable biocides because they exhibit low mammalian toxicity, but high toxicity to fungi and algae at low concentrations. They are also typically colorless and can therefore be incorporated into brightly colored paints.

In the course of searching for efficient ways to deliver tributyltin compounds to the target organisms, the following antifouling paint formulations have become available.

1.3.1 Contact leaching antifouling paints.

In this design, the antifouling system is composed of a tough insoluble film-forming resin such as a chlorinated rubber within which tributyltin fluoride is physically dispersed¹². When immersed in water, the freely dispersed molecules of tributyltin fluoride near the surface of the paint are able to diffuse out of the matrix of the paint film. As the biocide leaches out of the film, it leaves behind microscopic pores within the paint matrix. The inflow of sea water into these tiny pores causes the release of fresh tributyltin biocide from beneath the surface layers of the film. A major disadvantage of this paint design is that with the passage of time, the microscopic pores become clogged with insoluble materials thereby making it difficult for biocide in the deeper strata of the paint matrix to be released. As a result, contact leaching antifouling paints work best only during the early part of their life span. When the antifouling action of the paint fails, a large amount of the biocide is still trapped in the inner matrix thereby creating a severe problem in the proper disposal of spent antifouling paints¹².

1.3.2 Ablative formulation.

In this design, the tributyltin compound is dispersed into a film matrix composed of a mixture of soluble polymeric materials which are designed to break down over time¹². As the film matrix breaks down, the biocide is released. A disadvantage of this design is that it is difficult to control the actual breakdown of the paint film and the release of the biocide because the rate of paint film

breakdown is affected by water conditions and vessel speed⁴.

1.3.3 Self polishing copolymer paints.

In self polishing copolymer paints, the paint film is composed of a copolymer of methylmethacrylate and tributyltin methacrylate which also is the source of the biocide. At the surface of the paint, sea water interacts with the hydrophobic copolymer and initiates a saponification reaction which cleaves tributyltin cation from the co-polymer backbone, releasing it into the sea. The release rate of the tributyltin cation is gradual thereby enabling the biocidal action of the antifouling paint to last a long time.

1.4 TOXICITY OF ORGANOTIN COMPOUNDS.

In general, the toxicity of the organotin compounds R_nSnX_{4-n} increases with the increase in the number of alkyl or aryl substituents bonded directly to the tin atom¹⁵. Maximum toxicity is obtained when $n=3$. On increasing the number of alkyl or aryl substituents above $n=3$, the toxicity drops. Therefore, tetraorganotin compounds on their own have no toxicity. The toxicity observed with the tetraorganotin compounds is believed to be due to their in vivo metabolism to triorganotin compounds¹³. As the number of carbon atoms in the alkyl chain is increased above three, mammalian toxicity decreases.

The type of R- group on the tin atom determines the level of toxicity to specific organisms⁸. The trimethyltin compounds are the most toxic to insects while

the triethyltin compounds are the most toxic to mammals⁸. For gram-negative bacteria, the tripropyltin compounds are the most toxic⁸. The tri-n-butyltin compounds are the most toxic to gram-positive bacteria and fungi⁸.

The toxic effect of the trialkyltin compounds is attributed to the inhibition of mitochondrial oxidative phosphorylation, and subsequent disruption of a fundamental energy process¹³. The trialkyltin compounds bind to a number of proteins, and mortality may arise from direct reaction of the organotin species with proteins¹³. Differences in protein binding sites among groups of organisms would result in the varying spectrum of effectiveness of the triorganotin compounds to different organisms^{13,14}.

Another mechanism by which trialkyltin compounds may derive their toxicity has been described by Selwyn *et al*¹⁵, and Tosteson and Weith¹⁶. According to these authors tributyltin^{15,16}, tripropyltin and triphenyltin¹⁵ cations mediate chloride-hydroxide exchange in the mitochondria and smectic mesophases (liposomes)¹⁵, and in planar lipid bilayers¹⁶. Also, the tripropyltin cation has been reported to mediate chloride-chloride exchange across a lipid bilayer¹⁷. The ability of the trialkyltin cations to mediate anion transport is the subject of study in chapter three of this thesis.

The dialkyltin compounds R_2SnX_2 also show a similar trend of decreasing toxicity with increasing length of the alkyl chain⁸. The mode of toxicity of the dialkyltin compounds has been shown to be different from that of trialkyltin compounds¹⁸. The toxic action of the lower dialkyltin compounds is due to their

ability to combine with enzymes possessing two thiol groups in the correct conformation^{8,18}. The biochemical effect of this is an interference with α -keto acid oxidation^{8,18}.

The mono-organotin compounds RSnX_3 , do not show any important toxic effect⁸.

The organotin compounds do not appear to show any carcinogenic or teratogenic effect⁸. However, di- and tri- alkyl and aryl tin compounds have been shown to induce chromosomal contraction in human lymphocytes¹⁹. Alterations in the spermatocyte chromosomes of the mesogastropod Truncatella subcylindrica induced by dibutyltin dichloride and tributyltin chloride have also been reported by Vitturi *et al*²⁰, thus demonstrating the genotoxicity of these compounds.

Of particular interest in the marine environment are the tributyltin compounds. Tributyltin compounds are very toxic to marine life at very low concentrations, and are suspected of inducing imposex in the female dogwhelk Nucella lapillus^{21,22}. Tributyltin compounds have also been reported to induce shell malformations in the oyster Crassostrea gigas at very low concentrations^{23,24}, and have also been reported to have caused high mortality in the larvae of the common mussel Mytilus edulis²⁵. The toxicity of tributyltin species to the following non-target marine organisms at the ppb level has been reported:- amphipod larvae²⁶, lobster larvae and zoeal shore crab²⁷, and the sheepshead minnow Cyprinodon variegatus²⁸. At the low ppb levels, tributyltin species cause sublethal effects in the zoeal mud crab Rhithropanopeus harrisi²⁹ and copepods Acartia tonsa³⁰.

1.5 METABOLISM AND BEHAVIOUR OF TRIBUTYLTIN COMPOUNDS IN THE ENVIRONMENT.

On introduction into the marine environment, tributyltin compounds are removed from the water column by photolysis and assimilation by plants and animals²¹, and by adsorption to the sediment, and particulate matter. Hydrolysis and volatilization do not appear to be major degradative pathways²². The affinity of tributyltin compounds for sediments and particulate matter makes them far less bioavailable to organisms in the upper water layer, but bottom feeding organisms are exposed to higher concentrations of tributyltin compounds. Therefore, the feeding habit of a marine organism is an important factor in determining its tributyltin body burden. According to Maguire³¹, tributyltin species adsorb so firmly to particles that under abiotic conditions, there was no desorption of tributyltin oxide from harbour sediments over a period of ten months. However, under biotic conditions there was microbial degradation resulting in the liberation of butylated and methylated products. Tributyltin cation is hydrophobic, and therefore has a high tendency to preferentially accumulate in the surface microlayer of natural waters³². Its octanol-water partition coefficient ($K_{ow}=5500-700$)³³ and sediment-water partition coefficient ($K_{oc} = 1600$)³⁴ values favour accumulation in the surface microlayer. The surface microlayer attracts and sequesters hydrophobic species such as tributyltin species. The preferential accumulation of tributyltin compounds in the surface microlayer is expected to render tributyltin species unavailable to most organisms. However, bioaccumulation has been observed for a variety of organisms. Bacteria

and phytoplankton accumulate tributyltin species to concentrations 600 times and 30,000 times respectively, greater than their exposure concentrations^{32,33}. Also, a bioaccumulation factor of 4400 has been reported by Evans and Laughlin³⁶ for the hepatopancreas of the mud crab Rhithropanopeus harrisii. Accumulation of tributyltin species up to a concentration factor of 12,000 by the plant Eelgrass Zostera marina has been reported³⁷.

Tributyltin compounds have been found to exhibit preferential accumulation in certain tissues. Ward et al³⁸ observed that the viscera of the sheepshead minnow contained higher concentrations of tributyltin oxide than the cranial or muscle tissues. The reported bioaccumulation factors for tributyltin compounds are high enough to warrant concern with regard to their persistence and accumulation in food chains. However, they are degraded in vivo by bacteria³⁹, fungi⁴⁰, algae³⁵ and fish³⁴. The detoxification route for tributyltin compounds involves their conversion to the less toxic dibutyltin, monobutyltin, and inorganic tin species. Getzendaner and Corbin⁴¹ have also reported similar detoxification pattern for tricyclohexyltin species. Barug⁴⁰ has observed the degradation of tributyltin oxide to monobutyltin derivatives by the bacteria Pseudomonas aeruginosa. However, tributyltin chloride was not degraded under anaerobic conditions by the same bacteria. Maguire et al³⁵ have observed the in vivo degradation of tributyltin species by a green algae with the major degradation product being dibutyltin species.

Tributyltin compounds do not appear to be amenable to biomagnification. Macek et al⁴² have presented data indicating that chemicals with short or moderate

half-lives in vivo do not pose a biomagnification problem. Tributyltin species have a half-life considerably shorter than forty days by aerobic metabolism⁴³.

1.6 ANALYTICAL METHODS FOR ORGANOTIN COMPOUNDS.

The early analytical methods available for the determination of tin were classical gravimetric or volumetric procedures that gave only total inorganic tin concentrations. Beginning in the early 1930s, and extending into the early 1960s, optical spectrographic methods for total tin determination were extensively used for the determination of geological samples. With the passage of time, the more sensitive colorimetric, fluorimetric, neutron activation and flame atomic absorption techniques were introduced. The wide use of flame atomic absorption spectrometry was hampered by the low sensitivity of the tin absorption lines⁴⁴.

For the organotin compounds, early analytical methods relied on the conversion of the organotin compounds to inorganic tin, usually by digestion with mineral acids followed by ignition. Later, more diversified techniques such as electrochemical, chromatographic, and mass spectrometric techniques capable of providing speciation information were introduced. Recently, a tandem mass spectrometry (MS-MS) technique⁴⁵ has been applied to a mixture of standard organotin compounds with a view to analyzing them without prior derivatization to volatile species or prior chromatographic separation. This method relies on the fixed relationship between parent and daughter ions of any compound under fixed experimental conditions. The applicability of this technique to the analysis of

environmental samples has not yet been demonstrated.

Not much attention has been given to the qualitative analysis of organotin compounds. However, infrared spectroscopy⁴⁶, Mossbauer spectrometry^{46,47}, nuclear magnetic resonance spectrometry^{48,49,50} and electron spin resonance spectrometry⁵¹ have been applied to provide information on molecular structure and speciation.

The various quantitative analytical methods applied over the years are described in the following sections.

1.6.1 Molecular spectrophotometry and spectrofluorimetric techniques.

These methods rely on the attachment of a chromophoric ligand to the organotin compound. This makes it possible to analyze the organotin compounds by using uv-visible, or fluorescence spectroscopy, since the alkyl groups of the organotin compounds are not of much spectroscopic importance. A variety of ligands have been employed for this purpose. Aldridge and Cremer⁵² were the first to use dithizone for the spectrophotometric determination of diethyltin and triethyltin species. Diethyltin and triethyltin chlorides react with dithizone to form colored complexes. Analysis of the complexes is effected following partitioning between aqueous potassium hydroxide and chloroform. The diethyltin species partition into the alkali layer, while the triethyltin species migrate to the chloroform layer. The separated organotin compounds can then be determined by uv-spectrophotometry. A modified method for the reaction between dithizone and the organotin compounds has been reported by Havir and Vretal⁵³ for the determination of bis(tributyltin) oxide. Skeel and Bricker⁵⁴

developed a spectrophotometric method for the determination of dibutyltin dichloride by using diphenyl carbazone. This method achieved a sensitivity in the microgram range. Other colorimetric reagents that have been used in the analyses of the organotin compounds are dithiol⁵⁵, haematoxylin⁵⁶, 8-hydroxyquinoline⁵⁷, phenylfluorone⁵⁸, pyrocatechol violet^{59,60}, flavinol⁶¹ (3-hydroxyflavone).

For the fluorimetric determination of the organotin compounds, 3-hydroxyflavone⁶² and morin⁶³ (2',3,4,4',5,7,-pentahydroxyflavone) have been applied to the determination of phenyltin, and alkyltin compounds respectively.

A major disadvantage of the spectrophotometric and spectrofluorimetric techniques is the lack of specificity of these organic ligands to organotin compounds. However, limited selectivity can be achieved by employing various extraction techniques prior to spectrophotometry or spectrofluorimetry.

1.6.2 Electrochemical techniques.

Electrochemical techniques rely on the difference in the redox potentials of the various organotin compounds for speciation. Polarography, in the various modes such as anodic stripping voltammetry^{64,65}, and potentiometric titrations^{66,67} have been used for the determination of organotin compounds in aqueous and non-aqueous media.

Diethyltin dichloride was the first organotin compound whose polarographic reduction was recorded⁶⁸. The polarographic behavior of other organotin compounds has also been described⁶⁹. The ease of the polarographic reduction of the organotin

compounds has been found to be a function of the alkyl moiety on the tin atom⁷⁰. The ease of reduction follows the order⁷⁰ ethyl > propyl > butyl. Polarography, in the differential pulse mode has also been applied to the determination of organotin compounds^{71,72,73}.

Potentiometric titration of organotin compounds in dimethylsulfoxide (DMSO) has been reported to show well defined differential pulse polarographic peaks whose heights are linearly dependent on concentration⁷⁴. Quantitation of organotin compounds based on this observation has also been accomplished⁷⁴.

The half wave potentials of some organotin compounds have been determined by Abeed *et al*⁷⁵, by using voltammetry, and cyclic voltammetry at rotating disc electrodes (gold and glassy carbon electrodes) in non aqueous solvents. Their results showed that the reduction becomes more difficult as the electron donating ability of the alkyl or aryl groups attached to the tin atom increases (phenyl→ methyl→butyl). The variation of the anion attached to the tin atom had little effect on the half wave potentials. The application of electrochemical techniques to organotin analysis is restricted by the sample matrix. Organic matter present in environmental samples coats the electrode surface causing broadening of peaks, and shifts in peak potentials.

1.6.3 Atomic spectrometry.

Atomic absorption spectrometry has been used extensively in the analysis of organotin compounds. Atomic absorption spectrometry is not capable of speciation unless a prior separation of the organotin compounds is achieved. The methods

usually employed to separate organotin compounds prior to their determination by atomic spectrometry include solvent-solvent extractions or conversion to organotin hydrides. The first analytical speciation and quantitation of organotin compounds by atomic absorption spectrometry after their derivatization to organotin hydrides was developed by Hodge *et al*⁷⁶. The method involved the reaction of organotin compounds in natural water, acid digest of sediment or macroalgae with sodium borohydride. The organotin hydrides produced were collected in a hydride trap which was cooled in liquid nitrogen. The hydride trap was warmed to release the organotin hydrides into a quartz tube furnace according to their boiling points. Since the publication of this analytical method by the authors⁷⁶, numerous atomic absorption methods based on hydride generation and the boiling point differences of the organotin hydrides have been reported ^{77,78,79,80,81,82,83,84}.

Many gas chromatographic techniques based on the hydride generation method of Hodge *et al*⁷⁶ are presently in use (Section 1.6.4.1).

The speciation of butyltin compounds by liquid-liquid extraction prior to atomic absorption spectrometry has been described by McKie⁸⁵. This method⁸⁵ involved the extraction of butyltin species into acidified hexane and the subsequent removal of dibutyltin and monobutyltin species by washing with 3% sodium hydroxide solution. The hexane layer was evaporated and the solution of the residue in nitric acid was analyzed for tributyltin species by using graphite furnace-Atomic absorption spectrometry (GFAAS). The matrix modifier used in this determination was $\text{NH}_4\text{H}_2\text{PO}_4$. An analytical method similar to the technique reported by McKie⁸⁵ has

been applied to the determination of tributyltin species in shellfish and sediments by Stewart and de Mora⁸⁶. These authors⁸⁶ employed $K_2Cr_2O_7$ as a matrix modifier.

The use of atomic absorption spectrometry for the determination of organotin compounds is usually affected by severe matrix interferences. To overcome this problem, various matrix modifiers have been introduced. One of such matrix modification methods was the coating of the interior surfaces of a graphite furnace tube with zirconyl acetate⁸⁷. This has been shown to increase the atomization efficiency of tin⁸⁷. Peetre and Smith⁸⁸ have reported that there is a relationship between the atomic absorption sensitivity and the structure of an organotin compound. According to this report⁸⁸, the atomic absorption sensitivity decreased as the energy of the alkyl-tin bond decreased.

Atomic emission spectrometry of the organotin compounds has not been popularly used except in plasma emission^{89,90,91,92} detection or flame photometric detection in gas chromatography (Section 1.6.4.2a). Atomic emission spectrographic method has been described for the determination of bis(tributyltin) oxide⁹³. Prior separation of other organotin compounds present in the sample is necessary if speciation is desired because emission spectrography on itself, is not capable of distinguishing between the different organotin compounds.

1.6.4 Gas chromatography.

Organotin compounds are usually converted to volatile hydrides or tetraalkyltin compounds prior to gas chromatographic separations. In a few reports,

the analysis of organotin compounds without prior derivatization to hydrides or tetraalkyltin compounds has been accomplished^{94,95,96,97,98}. In such methods, the chromatograms are usually characterized by peak broadening and tailing. The column efficiency is also decreased.

Both packed and capillary gas chromatographic columns have been used with various detection techniques. The chromatographic techniques employed in the analyses of the organotin compounds are discussed below.

1.6.4.1 Hydride generation gas chromatography (HG-GC).

This method involves the conversion of the organotin compounds to volatile hydrides by the use of excess borohydride to produce alkyltin hydrides of the formula R_nSnH_{4-n} . The generated hydrides are purged from solution with the help of an inert gas, and can be cryoscopically trapped. The cold trap is subsequently warmed, to release the organotin hydrides into the column of the gas chromatograph. Detection of the separated organotin hydrides is achieved by using various gas chromatographic detectors.

Woollins and Cullen⁹⁹ have described a hydride generation-GC flame ionization detection technique based on the method previously developed by Hodge *et al*⁷⁶ for the analysis of organotin compounds. Hattori *et al*¹⁰⁰ have also described the determination of organotin compounds in environmental water and sediments, on a packed column by using HG-GC electron capture detection. An ultratrace method for the analysis of aquatic butyltin by HG-GC with flame photometric

detection has been described by Matthias et al¹⁰¹. A novel on-column hydride generation analysis of organotin compounds by gas chromatography-atomic absorption spectrometry (GC-AAS) has been described by Clark et al¹⁰², and Takami et al¹⁰³. In the method described by Takami et al¹⁰³, fish samples were extracted with hydrochloric acid-ethanol mixture. The extracted organotin compounds in the fish were transferred to ethylacetate/hexane by using liquid-liquid extraction, and then applied onto a sulfonated cation exchange column where the organotin compounds were trapped. On-column hydride generation was effected by passage of an ethanolic sodium borohydride solution through the cation exchange resin. The generated hydrides were extracted into hexane, and analyzed by GC-MS.

The GC-hydride generation method of organotin determination has been very extensively used by numerous authors^{104, 105, 106, 107, 108, 109}.

Two detection methods have widely been used in gas chromatography for the analyses of organotin compounds after their conversion to volatile derivatives. These are flame photometric detection (FPD) and atomic absorption spectrometry (AAS). Coupling the gas chromatograph directly to an atomic absorption spectrometer (GC-AAS) appears to be the most popular technique for element specific speciation of the organotin compounds after hydridization.

Methyltin species in natural water have been determined after hydride derivatization by using GC-graphite furnace atomic absorption spectrometry (GC-GFAAS)¹¹⁰. Butyltin species in natural water and sediments have been analyzed by Quevauviller and Donard¹¹¹, by using GC-HG-quartz tube atomic absorption

spectrometry.

In environmental samples, production of volatile hydrides may be inhibited by severe matrix interferences¹¹². Such matrix interferences can be eliminated by the use of L-Cysteine¹¹³.

1.6.4.2 Conversion to tetraalkyltin compounds.

Conversion of organotin compounds to tetraalkyltin derivatives is usually accomplished by reacting the organotin compounds with a Grignard reagent, or sodium tetraethylborate. The reaction of monoalkyltin, dialkyltin, and trialkyltin species with the Grignard reagent proceeds to completion at very low concentrations, and no rearrangement of the original alkyl groups attached to the tin atom is usually observed¹¹⁴. The tetraalkyltin derivatives formed are usually stable in organic solvents^{114,115}. Various alkyl groups such as methyl^{116,117}, ethyl¹¹⁸, pentyl^{119,120}, and n-hexyl^{121,122}, have been attached to the butyltin compounds to facilitate their analyses. Detection of the derivatized tetraalkyltin compounds is usually accomplished by the use of various gas chromatographic detectors. The GC-detector systems that have been used for tetraalkyltin analyses are described below.

1.6.4.2(a) Gas chromatography with flame photometric detection (GC-FPD).

The flame photometric detector has been used extensively for the detection and quantitation of organotin compounds in the environment following their derivatization to tetraalkyltin compounds. Developed by Aue and Flinn¹²³, flame

photometric detection has been used for tin-specific detection in gas chromatographic analyses of butyltin species in fish^{118,120}, water^{120,121,122,124}, sediments^{120,122,125}, and for the determination of methyltin species in water¹²⁶.

A disadvantage of the flame photometric detector is the decrease in sensitivity which may be caused by the accumulation of SnO₂ on the internal surfaces of the detector, and by tropolone, a ligand sometimes used in the extraction of organotin compounds¹²⁷.

Flame photometric detection of the organotin compounds relies on the conversion of tin to SnH in air/hydrogen flame. SnH yields a red emission line in the gas phase at about 610 nm and almost all analyses for tin have been carried out at this wavelength. Earlier, Aue and Flinn¹²³ had described another emission line for tin at 390 nm in the flame photometer. This emission line was unstable, irreproducible and easily quenched¹²³, and was later attributed to a quartz surface induced tin luminescence¹²⁸. Jang *et al*¹²⁹ have described a sensitive flame photometric analysis involving the 390 nm emission line. According to the authors, a clean quartz surface is required in the vicinity of the flame to achieve stability of the emission line, and only the Shimadzu flame photometric detector has this feature. The detection limit was claimed to be about thirty times better than that at the 610 nm emission line.

1.6.4.2(b) Gas chromatography with atomic absorption spectrometric detection (GC-AAS).

Analysis of organotin compounds by GC-AAS after conversion to tetraalkyltin

compounds is not popular and has only been seldomly used. Forsyth *et al*¹³⁰ have applied this method to the determination of organotin compounds in fruit juices.

1.6.4.2(c) Gas chromatography with mass spectrometric detection (GC-MS).

GC-MS affords a very reliable method in the analysis of the organotin compounds, since detection is based both on retention data and fragmentation pattern. The first application of GC-MS to the analysis of organotin compounds was described by Meinema *et al*¹¹⁶. In this procedure, benzene extracts of pure butyltin compounds were converted to their butylmethyltin derivatives by using methylmagnesium bromide. The derivatized butylmethyltin compounds were analyzed by using GC-MS with dibutylhexylmethyltin as the internal standard. The application of GC-MS to the determination of organotin compounds in environmental samples has been reported by Cullen *et al*¹¹⁷, Forsyth *et al*¹³⁰, Muller¹³¹, Unger *et al*¹³².

1.6.5 Liquid chromatography (LC).

Liquid chromatography of the organotin compounds does not require derivatization to volatile species, and hence could be useful for the analysis of non-volatile organotin compounds. The alkyltin species are difficult to detect by uv-visible spectroscopy therefore, derivatization might be necessary to enhance their detection. Various liquid chromatographic detectors have been used for the analysis of organotin compounds. An indirect photometric method for the determination of alkyltin compounds has been described by Whang *et al*¹³³ for tributyltin, tripropyltin,

triethyltin, and trimethyltin species after their separation on a strong cation exchange column.

For high sensitivity, inductively coupled plasma-mass spectrometers (ICP-MS)^{134,135,136}, inductively coupled plasma-atomic emission spectrometers (ICP-AE)^{135,136} and atomic absorption spectrometers^{137,138,139,140,141} have been used to detect organotin compounds in high performance liquid chromatography (HPLC). Direct coupling of the liquid chromatograph to a mass spectrometer or atomic absorption spectrometer is associated with problems such as solvent interferences. The large amount of solvent and sometimes non-volatile buffers that go into the detector systems are also a major concern. This concern can be addressed by interfacing the LC and the detector systems, or by the use of a microbore column. The small solvent flow rate (10-100 $\mu\text{L}/\text{min}$) in microbore HPLC has been shown to be compatible with direct effluent introduction to a flame atomic absorption spectrophotometer¹⁴².

A coupled LC-AAS technique with enhanced laser ionization detection has been described by Epler *et al*¹⁴³, for the analysis of tributyltin species in sediment. In their technique, tributyltin species in a sediment sample were extracted into 1-butanol, separated on a strong cation exchange column and detected by using a premixed air-acetylene flame which was irradiated with two pulsed lasers. The enhanced ionization of the tin atom in their technique¹⁴³ was attributed to a rapid collisional ionization of the excited tin atoms in the flame.

Another method of solving the problem of excessive solvent introduction into

the detector system, is by the post column derivatization of the organotin compounds to volatile hydrides which can then be introduced into an atomic absorption spectrometer¹⁴⁴. This method has been applied to the determination of methyltin species¹⁴⁴.

Organotin compounds adsorb strongly onto unmodified silica gel columns therefore, most liquid chromatographic separations are performed on reversed phase columns, size exclusion columns, and other modified columns such as cyano bonded silica gel columns. Jessen *et al*¹⁴⁵ have studied the adsorption behavior of alkyltin halides on various chromatographic columns, and concluded that silica based octadecyl (ODS) and cyano columns are not sufficiently inert to alkyltin halides while silica gel columns pyrolytically coated with carbon black are inert. However, the organotin halides have been reported to adsorb on a commercially available graphitized carbon black¹⁴⁶. The ability of organotin halides to adsorb on graphitized carbon black was the basis for a selective determination of the organotin compounds by Ferri *et al*¹⁴⁶.

The separation of the alkyltin halides on a cyanopropyl bonded silica gel column and their detection by fluorescence spectrometry after on-column complexation with morin has been described by Langseth¹⁴⁷. It has been reported by Jessen *et al*¹⁴⁵, that rearrangement of the alkyl groups on the tin atom can occur especially if tetraalkyltin compounds are co-injected with other organotin compounds into the LC column.

1.6.6 Thin layer chromatography (TLC) and high performance thin layer chromatography (HPTLC).

Thin layer chromatography is not widely used for the quantitative analysis of the organotin compounds. However, it has been applied to qualitatively identify organotin compounds. The separation of butyltin compounds and their colorimetric detection after complexation with pyrocatechol violet has been reported by Laughlin *et al*¹⁴⁸.

Speciation of the mammalian organotin metabolic products has been reported by Kimmel *et al*¹⁴⁹. Their method involved both normal and two dimensional TLC techniques, and visual detection of the organotin species after complexation with colorimetric reagents such as pyrocatechol violet or dithizone. Vasundhara *et al*⁵⁶ have demonstrated the good resolving power of the TLC for a series of tri- and di-organotin compounds. Detection of the separated organotin compounds was by treatment of the TLC plate with haematoxylin.

High performance thin layer chromatography (HPTLC) has not been popularly used for qualitative analyses of the organotin compounds. However the quantitation of butyltin compounds in a wood matrix, by using HPTLC has been reported by Ohlsson *et al*¹⁵⁰. Their method involved the post column development photolysis and complexation of the butyltin species with pyrocatechol violet, followed by colorimetry of the tin-pyrocatechol violet complex.

A HPTLC method of quantitation has also been described by Tomboulian *et al*¹⁵¹ for phenyltin compounds. Quantitation was by fluorescence scanning

densitometry, following in situ complexation of the phenyltin compounds with morin.

1.7 TRIBUTYLTIN AND GOVERNMENT REGULATIONS.

Tributyltin compounds dissolved in marine waters exhibit acute toxicity to a variety of aquatic life. Available data in the literature tend to suggest that fish and larger crustacea are less sensitive to tributyltin compounds than bivalves, molluscs, phytoplankton and small crustaceans. It has been established that molluscs are generally very sensitive to organotin compounds¹⁵². Following the establishment of a correlation between tributyltin compounds, shell malformation and abnormal growth in oysters, the French Government in 1982 banned the use of antifouling paints containing more than 3% by weight of tributyltin compound on boats less than 25 tons. In 1987, a total ban on the use of organotin paints on vessels less than 25 metres came into effect in France¹⁵².

In 1986, the Government of England prohibited the retail sale of some antifouling paints containing tributyltin compounds. In 1987, the use of tributyltin-containing paints on small boats and mariculture equipment was banned¹⁵³.

The use of organotin compounds in fresh water antifouling paints is prohibited in Germany and Switzerland¹⁵⁴.

In Canada, tributyltin compounds are registered under the Pest Control Products Act for use as a slimicide and for general lumber preservation. Its use as a preservative for nets is not allowed⁴⁴. In 1989, the Canadian Government prohibited the use of tributyltin compounds on vessels less than 25 metres in length,

and also stipulated a maximum release rate of 4 μg tributyltin compound per square centimetre of ship's hull¹⁵⁵.

1.8 OBJECTIVES AND SCOPE OF THE PRESENT STUDY.

Tributyltin compounds have been shown to cause shell malformation in oyster, and other molluscs^{11,23,24}, and have also been linked to imposex in the marine gastropods such as the female dogwhelk¹⁰. Cullen *et al*¹¹⁷ have reported the presence of butyltin and cyclohexyltin species in some coastal areas of British Columbia, Canada. The toxic effect of the cyclohexyltin species is not known with certainty. Therefore, it is necessary to provide data on the extent of organotin pollution in the coastal areas of British Columbia, Canada.

Chapter 2 of this thesis provides information on the levels of butyltin and dicyclohexyltin species in some marine locations of British Columbia.

Although the trialkyltin compounds are thought to exert their toxicity by the inhibition of mitochondrial oxidative phosphorylation, little attention has been given to the effect of the alkyltin compounds on biomembranes. Early studies by Selwyn¹⁵, and Tosteson and Wieth¹⁶ showed that tributyltin, triphenyltin cations act as carriers for Cl^- and OH^- , and therefore mediate Cl^-/OH^- , while the propyltin cation mediates Cl^-/Cl^- exchange across artificial biomembranes called liposomes. Later, Tosteson and Weith¹⁵⁶ showed that tributyltin chloride affects the dipole potential of phosphatidylethanolamine lipid bilayer, and lowers it by about 70 millivolts. The effect of organotin compounds on the other properties of membranes such as

permeability, elasticity, etc has not been reported. A knowledge of the effect of the organotin compounds on the other properties of the membrane is important for a complete understanding of the mechanisms of their toxicity.

Arakawa *et al*¹⁵⁷ have reported the inhibition of intracellular calcium mobilization by tributyltin chloride and dibutyltin dichloride. Arakawa and Wada¹⁵⁸ then surmised that the inhibition of Ca^{2+} mobilization may be due to changes in the membrane structure caused by the butyltin compounds. Also, the authors¹⁵⁸ had suggested that the toxicity of the alkyltin compounds should depend on their solubility in biological fluids, and their extent of incorporation into cells.

Therefore, the experiments described in Chapter 3 of this thesis are concerned with providing information on the permeability changes of model biomembranes known as liposomes, and the effect of organotin incorporation into these liposomes on membrane permeability.

It is necessary to use liposomes as models for biological membranes because of their similarity with true biomembranes (Chapter 3 Section 3.3). Also, the use of liposomes eliminates complications that may arise in interpreting experimental data if true biomembranes are used for permeability studies.

The ease or difficulty of efflux of an encapsulated probe permeant; dimethylarsinic acid (DMA) from these liposomes in the presence and absence of the organotin compounds, is an indication of how the membrane permeability responds to the presence of the organotin compounds.

Since the advent of organotin pollution in the marine environment, every

effort by workers in the field of environmental pollution has been directed towards providing data on the level and speciation of the organotin compounds. The total tin content of marine animals has been largely neglected. Therefore, Chapter 4 of this thesis is concerned with total tin determination in oysters, and the analytical method development for total tin determination by hydride generation-atomic absorption spectrophotometry.

CHAPTER 2

**SPECIATION AND QUANTITATION OF BUTYLTIN AND
CYCLOHEXYLTIN COMPOUNDS IN MARINE ORGANISMS BY USING
CAPILLARY COLUMN GC-MS SIM.**

2.1 INTRODUCTION.

The work reported in this section involved the analysis of marine animals for organotin compounds, and the synthesis of standard tetraorganotin compounds which were used as calibration standards for quantitation. The speciation and quantitation procedure involved a prior extraction of the organotin compounds from the marine organisms by the use of methylene chloride. The extracted organotin compounds were reconstituted in n-hexane and subjected to Grignard methylation, a well known chemical reaction to yield tetraorganotin compounds. Speciation and quantitation were by capillary column GC-MS SIM.

The high sensitivity and specificity of the mass spectrometric detector especially for tin compounds makes it the detector of choice. Tin has thirteen stable isotopes which in mass spectrometry give rise to a very characteristic isotope pattern. The isotope pattern for tin is very diagnostic for distinguishing tin compounds from other compounds that may co-elute with them during chromatographic separations. The use of the mass spectrometer as a detector for gas chromatographic separations is accomplished by the direct coupling of the GC capillary column to the ion source of the mass spectrometer.

2.2 EXPERIMENTAL.

2.2.1 Instrumentation.

2.2.1.1 Gas chromatography (GC).

The gas chromatograph used to establish the retention times, and the optimum chromatographic conditions for organotin separation was a Hewlett Packard Model 5890 instrument equipped with a flame ionization detector (FID). Data acquisition from the gas chromatograph was achieved by using a Hewlett Packard 3393A integrator. The GC column was a DB-1 polysiloxane stationary phase wall coated open tubular (WCOT) capillary column (15 m \times 0.25 mm i.d) purchased from J & W Scientific, Folsom, California. The carrier gas was helium at a linear velocity of 30 cm/s. The column temperature was held at 50°C for 10 minutes, and then increased at the rate of 20°C per minute to a final temperature of 240°C until complete elution was obtained.

2.2.1.2 NMR and mass spectrometry.

^1H NMR spectra were run at 300 MHz by using a Varian XL 300 spectrometer. Chemical shifts are quoted relative to tetramethylsilane as external reference. ^{119}Sn NMR spectra were obtained on the same instrument. ^{119}Sn chemical shifts are quoted relative to tetramethyltin as external reference.

Low resolution mass spectra (using electron ionization, EI) for characterizing

the calibration standards were obtained on a Kratos MS 50 mass spectrometer.

2.2.1.3 Gas chromatography-mass spectrometry (GC-MS).

The GC-MS system consisted of a Carlo-Erba Fractovap series 4160 gas chromatograph interfaced to a Kratos MS 80 RFA double focusing mass spectrometer equipped with a Kratos DS55 data system. The mass spectrometer was operated in EI under selected ion monitoring mode (SIM), and was calibrated by introducing perfluorokerosine into the ion source. The operating conditions for the mass spectrometer were; calibration range = 118-331, sweep = 1500 ppm, cycle time = 1 second, filament current = 1-2 Amp., electron voltage = 70 eV., ion source temperature = 180 °C.

The gas chromatograph was operated in the temperature programming mode. The temperature of the column was kept constant at 50 °C for 10 minutes, and then increased to 240 °C at a rate of 20 °C per minute until complete elution was obtained. The injector temperature was maintained at 250 °C. The GC column is as described in section 2.2.1.1, and was connected to the mass spectrometer via a capillary interface. The carrier gas was helium at a linear velocity of 30 cm/s.

2.2.1.4 Mechanical shaker and blender.

The mechanical shaker employed during the extraction step of the organotin compounds from environmental samples was a Magniwhirl reciprocating shaker (Blue M Electric Company, Blue Island, Illinois, U.S.A.).

The blender used to homogenize the biological samples was obtained commercially.

2.2.2 Materials and reagents.

Dibutyltin dichloride and tributyltin chloride were purchased from M & T Chemicals Inc., Rahway, New Jersey, and Ventron (Alfa Inorganics) Beverly Massachusetts, U.S.A. respectively. Tin metal (20 mesh) was obtained from Mallinckrodt Chemical Works, St Louis, Missouri, U.S.A.. Tricyclohexyltin chloride (Technical Grade) and methylmagnesium bromide (3M in diethyl ether) were obtained from Aldrich Chemical Company, Milwaukee, U.S.A.. Dicyclohexyltin dibromide was purchased from Johnson Matthey (Alfa products), Danvers, Massachusetts, U.S.A.. The following chemicals silica gel (230-400 mesh) and sodium chloride (Reagent Grade) were purchased from BDH, Poole, England. Iodobutane-d9 and 2-ethoxyethanol were supplied by Merck Frosst Canada Inc. (MSD isotope division) Montreal, Canada and Matheson, Coleman and Bell Manufacturing Chemists, Norwood, Ohio, U.S.A. respectively. The following reagents and solvents were procured from Fisher Scientific, Fair Lawn, New Jersey, U.S.A :- methyl iodide (Certified Grade), anhydrous magnesium sulfate (Certified Grade), anhydrous diethyl ether (Reagent Grade), n-hexane (HPLC Grade), n-pentane (Spectrograde), n-heptane (HPLC Grade).

2.2.3 Synthesis of standard organotin compounds.

2.2.3.1 Synthesis of tributylmethyltin, $(C_4H_9)_3SnCH_3$.

Tributyltin chloride (2.99 g, 0.0092 mol) was dissolved in n-hexane (100 mL) in a 250 mL Erlenmeyer flask. Excess methylmagnesium bromide (6 mL of 3M, 0.0180 mol) in ether was added to the reaction mixture and stirred for six hours at room temperature, after which the excess methylmagnesium bromide was destroyed by the gradual addition of sulphuric acid (1 M) while the reaction flask was cooled in an ice bath. The reaction mixture was transferred to a separatory funnel where the aqueous layer was removed, and the hexane layer was washed five times with hydrochloric acid (10 mL of 10% HCl), dried with anhydrous sodium sulphate and filtered into a round bottom flask (250 mL). The hexane was removed on a rotary evaporator to yield the crude product which was distilled twice at reduced pressure to obtain 1.70 g (61% yield) tributylmethyltin, b.p 58°C / 10 mm Hg. Analysis: % Found: C, 51.40; H, 9.80. % Calcd: C, 51.18; H, 9.91.

2.2.3.2 Synthesis of dibutyldimethyltin $(C_4H_9)_2Sn(CH_3)_2$.

Dibutyltin dichloride (1.46g, 0.0048 mol) and excess methylmagnesium bromide (15 mL of 0.045 mol) were reacted for six hours as described in Section 2.2.3.1 to yield a crude product which was distilled twice to obtain 0.9 g of dibutyldimethyltin (71% yield), b.p 33°C / 4 mm Hg. Analysis: % Found: C, 45.83; H, 9.30. % Calcd: C, 45.67; H, 9.20.

2.2.3.3 Synthesis of tricyclohexylmethyltin (C_6H_{11})₃SnCH₃.

Tricyclohexyltin chloride (2.02g, 0.0050 mol) and excess methylmagnesium bromide (10 mL of 3M, 0.030 mol) were reacted for 12 hours as described in Section 2.2.3.1. The crude product was distilled to obtain 1 g tricyclohexylmethyltin (52% yield), b.p 128°C / 0.6 mm Hg. Analysis: % Found: C, 59.93; H, 9.47. % Calcd: C, 59.56; H, 9.47.

2.2.3.4 Synthesis of dicyclohexyldimethyltin (C_6H_{11})₂Sn(CH₃)₂.

Dicyclohexyltin dibromide (2.00g, 0.0045 mol) and excess methylmagnesium bromide (10 mL of 3M, 0.030 mol) were reacted for 12 hours as described in Section 2.2.3.1. The obtained crude product was distilled to obtain 0.87g dicyclohexyldimethyltin (61% yield), b.p 88°C / 0.06 mm Hg. which was identified by mass spectrometry and NMR spectrometry (Section 2.4.1).

2.2.3.5 Synthesis of the internal standards.

2.2.3.5(a) Synthesis of tetrapropyltin (C_3H_7)₄Sn.

Tetrapropyltin was synthesized according to the method described for tetraethyltin¹⁵⁹, by reacting magnesium turnings (8.26 g, 0.34 mol), n-propyl bromide (46.74 g, 0.38 mol) and tin(IV) chloride (13.81 g, 0.053 mol) in anhydrous diethyl ether. The obtained crude product was distilled twice to yield 8.5 g tetrapropyltin, b.p 108°C / 11 mm Hg. Analysis: % Found: C, 49.61; H, 9.76. % Calcd: C, 49.52; H,

9.70.

2.2.3.5(b) Direct synthesis of $(C_4^2H_9)_2SnI_2$ and $(C_4^2H_9)_3SnI$ and the subsequent synthesis of deuteriated internal standards $(C_4^2H_9)_3SnCH_3$ and $(C_4^2H_9)_2Sn(CH_3)_2$.

This synthesis was carried out according to the method reported by Oakes and Hutton¹⁶⁰ for dibutyltin diiodide. Deuteriated butyliodide (3.13g, 0.017 mol) and 2-ethoxyethanol (1 mL) were mixed together in a round bottom flask (50 mL). Lithium (0.097g, 0.014 mol) and tin metal (0.89g, 0.0075 mol) were also added to the round bottom flask. The contents of the flask were refluxed for two hours with stirring, and vacuum distilled to obtain 0.77 g of a mixture of the crude products $(C_4^2H_9)_2SnI_2$ (71% yield) and $(C_4^2H_9)_3SnI$ (29% yield) as identified by GC-MS. The crude products in pentane were treated with aqueous potassium hydroxide (2% w/v) to precipitate the deuteriated dibutyltin dihydroxide ($m/z=286$). The pentane solution was filtered and evaporated under reduced pressure to give deuteriated tributyltin hydroxide as identified by mass spectrometry ($m/z=335$).

Aliquots (0.18 g) of the deuteriated tributyltin hydroxide and dibutyltin dihydroxide were each reacted with methylmagnesium bromide (0.3 mL, 0.0009 mol) in hexane as described in Section 2.2.3.1 to give $(C_4^2H_9)_3SnCH_3$ and $(C_4^2H_9)_2Sn(CH_3)_2$ respectively as identified by GC-MS.

2.2.3.6 Synthesis of methylmagnesium iodide.

Magnesium turnings in slight excess (0.062g, 1.50 mol) and methyl iodide (210.07g, 1.48 mol) were reacted in anhydrous diethyl ether according to standard procedure¹⁶¹ to obtain the Grignard reagent, methylmagnesium iodide.

2.3 ANALYTICAL PROCEDURE.

2.3.1 Gas chromatography.

2.3.1.1 Establishment of elution profile and retention data.

Appropriate amounts of the well characterized standard tetraorganotin compounds $(C_4H_9)_3SnCH_3$, $(C_4H_9)_2Sn(CH_3)_2$, $(C_6H_{11})_3SnCH_3$, $(C_6H_{11})_2Sn(CH_3)_2$ and $(C_3H_7)_4Sn$ were each dissolved in n-heptane in different volumetric flasks (25 mL) to form the stock solutions (50 $\mu\text{g/mL}$ as Sn). A working solution (5 $\mu\text{g/mL}$ as Sn) of each tetraorganotin compound was prepared in n-heptane from the stock solutions.

Aliquots of each working solution (1 μL) of each standard tetraorganotin solution (5 $\mu\text{g/mL}$ as Sn) were injected into the capillary column of the gas chromatograph by using splitless injection. The retention time of each standard organotin compound was noted.

Aliquots of each stock solution were pipetted into the same volumetric flask (5 mL) to form a mixture of all the standard tetraorganotin compounds (5 $\mu\text{g/mL}$ as Sn). This mixture (1 μL) was separated on the capillary column of the gas

chromatograph. Each of the tetraorganotin compounds was detected and identified on the basis of the earlier established retention times.

2.3.1.2 Suitability of tetrapropyltin as internal standard.

The suitability of tetrapropyltin as internal standard was verified on the tributylmethyltin solutions according to the following procedure:-four sets of tributylmethyltin solutions in heptane were prepared. Each set of solutions contained 2, 4, 6, 8, 10 $\mu\text{g/mL}$ (as Sn) tributylmethyltin, and also contained the internal standard tetrapropyltin at only one of the following concentration levels:- 2, 4, 6, 50 $\mu\text{g/mL}$ as Sn. Each mixture of tributylmethyltin and the internal standard (1 μL) was injected into the capillary column of the gas chromatograph and separated. Three replicate injections of each sample solution were made. The peak area ratios of the tributylmethyltin to the internal standard were plotted against the various concentrations of the tributylmethyltin solutions (Section 2.4.4).

2.3.1.3 Suitability of $(\text{C}_4^2\text{H}_9)_3\text{SnCH}_3$ and $(\text{C}_4^2\text{H}_9)_2\text{Sn}(\text{CH}_3)_2$ as internal standards.

A mixture of the deuterated compound $(\text{C}_4^2\text{H}_9)_3\text{SnCH}_3$, and tributylmethyltin in heptane was injected into the capillary column of the gas chromatograph. No separation was obtained. Similarly, no separation was obtained for a mixture of $(\text{C}_4^2\text{H}_9)_2\text{Sn}(\text{CH}_3)_2$ and dibutyldimethyltin. Although no separation was obtained on the gas chromatographic column, the deuterated butyltin compounds can still be used

as internal standards if high instrument sensitivity is not desired, because under conditions of GC-MS SIM, the butyltin compounds and their analogous deuterated compounds co-elute, and are simultaneously detected by the mass spectrometer. Therefore at a given retention time, only a few number of scans can be obtained for each fragment ion, thereby leading to decreased sensitivity.

2.3.2 Low resolution mass spectrometry: selection of fragment ions used for selected ion monitoring GC-MS.

The tetraorganotin compounds, as neat liquids were subjected to low resolution mass spectrometry. The fragment ions, and their intensities were recorded (Section 2.4.2 Tables 2.2 to 2.4). Fragment ions possessing the highest intensities were selected to be monitored in the GC-MS SIM analysis.

2.3.3 GC-MS retention data, calibration curves, and precision.

Appropriate amounts of the well characterized standard tetraorganotin compounds, $(C_4H_9)_3SnCH_3$, $(C_4H_9)_2Sn(CH_3)_2$, $(C_6H_{11})_2Sn(CH_3)_2$ and $(C_6H_{11})_3SnCH_3$ were each dissolved in n-heptane in separate volumetric flasks (25 mL) to form standard solutions. Appropriate amounts of each standard solution were pipetted into the same volumetric flask (50 mL), and made up to the mark with n-heptane to form the stock solution (5 $\mu\text{g/mL}$ as Sn, of each of the standard tetraorganotin compounds). Appropriate amounts of the stock solution were placed into six different volumetric flasks (10 mL) together with aliquots of the tetrapropyltin solution in

heptane, so that each volumetric flask contained 0.2 $\mu\text{g}/\text{mL}$ (as Sn) of the internal standard, and 0.2 to 1.2 $\mu\text{g}/\text{mL}$ of a mixture of all the tetraorganotin standards.

Each mixture of the standard organotin compounds and the internal standard (1 μL) was analyzed by GC-MS SIM. Only the fragment ions shown in Table 2.7 (Section 2.4.3) were monitored at the retention times shown in Table 2.6. The peak area ratios of the standard organotin compounds to the internal standard were plotted against the standard tetraorganotin concentrations (Section 2.4.5, Figures 2.8 and 2.9) to afford the calibration curves.

2.3.4 Recovery studies.

Recovery studies were performed in duplicate at one level of organotin concentration (1.5 μg as Sn). Shrimp (Pandalus tridens) (40 g, wet wt) from a batch whose prior analysis by GC-MS revealed the absence of any organotin compound was homogenized in a blender, and transferred to an Erlenmeyer flask (1 L). The shrimp homogenate was spiked with 1.5 μg (as Sn) of each of the following compounds: tributyltin chloride, dibutyltin dichloride, tricyclohexyltin chloride, and dicyclohexyltin dibromide all dissolved in n-heptane. The solution was vortex mixed and sodium chloride (20 g) was added together with concentrated hydrochloric acid (50 mL) and methylene chloride (100 mL). The resulting slurry was shaken on a mechanical shaker for one hour and filtered through a pyrex glass wool into a separatory funnel (1 L) where the lower methylene chloride layer was removed. The shrimp residue, and the glass wool were returned to the Erlenmeyer flask (1 L). The aqueous layer

from the separatory funnel was also returned to the Erlenmeyer flask (1 L) and the extraction procedure repeated twice more. All the methylene chloride layers were pooled together, dried with anhydrous magnesium sulfate and filtered through a Whatman No 1 filter paper into a round bottom flask (500 mL), and evaporated off by using a rotary evaporator to obtain an oily residue which was dissolved in n-hexane solution.

Aliquots of the shrimp extract in n-hexane (5 mL), and a solution of the internal standard (0.5 mL of 2.2 $\mu\text{g}/\text{mL}$ as Sn) and methylmagnesium iodide in diethyl ether (3 mL) were added to the Erlenmeyer flask. The reaction mixture was left standing with intermittent shaking for one hour, after which excess methylmagnesium iodide was destroyed by the gradual addition of dilute sulphuric acid (1 M) and de-ionized water (about 10 mL). The hexane solution in the Erlenmeyer flask was transferred to a separatory funnel (50 mL) where the aqueous bottom layer was removed, and the upper hexane layer passed through a silica gel column (2 cm x 0.5 cm i.d) pre-equilibrated with n-pentane. The hexane solution was drained down the silica gel column, and then eluted with n-pentane (15 mL) into a sample vial. The solution in the sample vial was concentrated down to about 0.2 mL by blowing a gentle stream of nitrogen. About 0.3 mL of n-heptane were added to the sample vial, to bring the total volume of the solution to about 0.5 mL. The heptane solution (1 μL) was analyzed in duplicate by GC-MS SIM.

2.3.5 Extraction of the organotin compounds from marine animals.

About 2-5 frozen marine bivalves were thawed, and then shucked. Portions of the soft tissue weighing between 18-137 g were placed in a blender together with 100 mL de-ionized water, and homogenized for about 3 minutes. The homogenized tissue slurry was transferred to an Erlenmeyer flask (1 L). Sodium chloride (20 g), concentrated hydrochloric acid (50 mL), and methylene chloride (100 mL) were added into the tissue slurry and mixed by shaking. The tissue slurry was then shaken on a mechanical shaker for one hour, and then extracted and processed as described in Section 2.3.4 above. A flow diagram for the extraction of organotin compounds from marine animals is given in Figure 2.1.

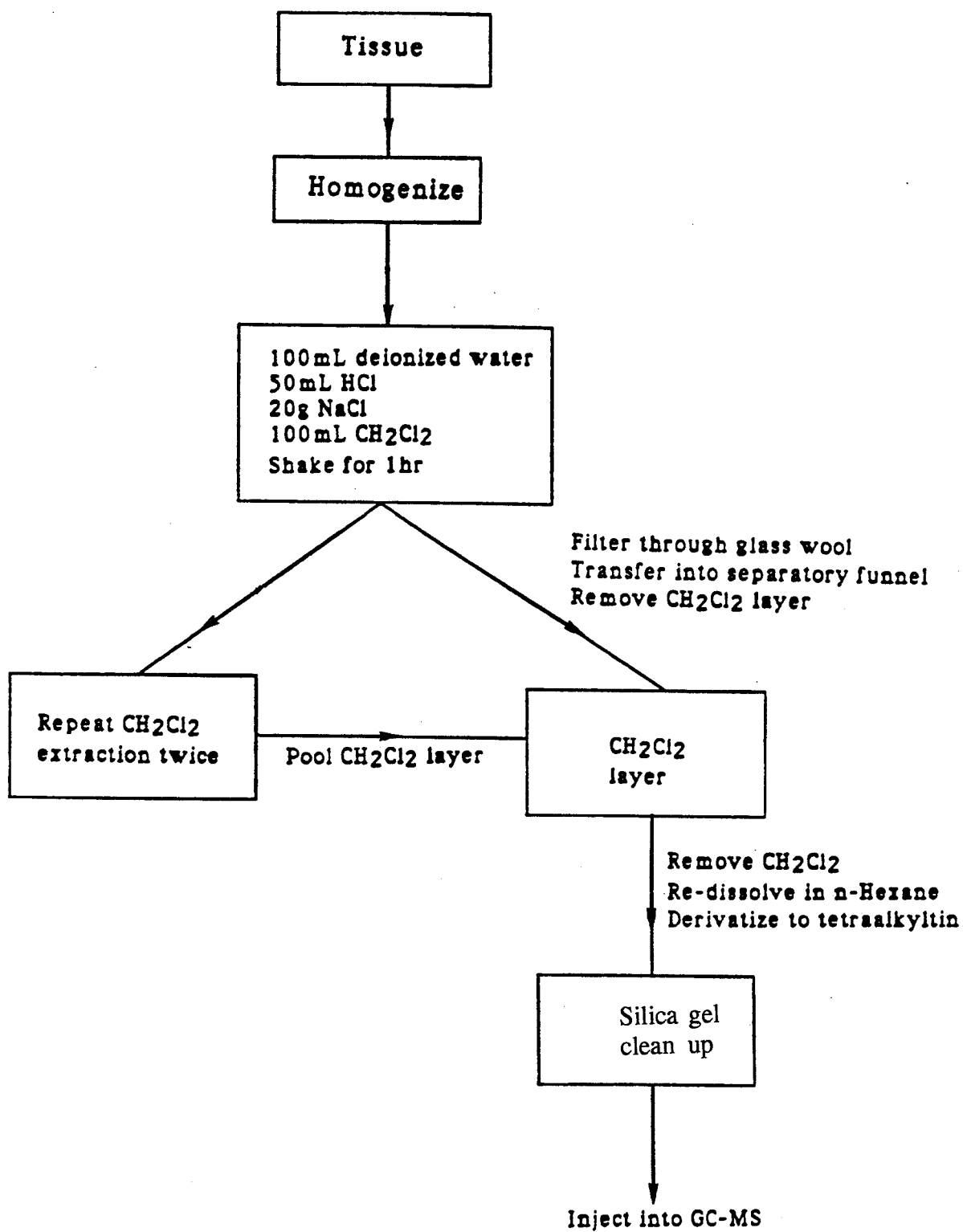


Figure 2.1 Flow diagram for the extraction of organotin from marine animals.

2.4 RESULTS AND DISCUSSION.

2.4.1 Characterization of the standard tetraorganotin compounds.

The standard tetraorganotin compounds were synthesized by Grignard methylation of butyltin and cyclohexyltin halides as described in Section 2.2.3. above. The butylmethyltin and the tetrapropyltin compounds afford good elemental analyses.

Tricyclohexylmethyltin was characterized by elemental analysis and mass spectrometry (Figure 2.2). Dicyclohexyldimethyltin was characterized by ^1H NMR (Figure 2.3) and mass spectrometry (Figure 2.4). The integrated peak area ratios of the methyl group protons, and the cyclohexyl group protons in the ^1H NMR spectra of dicyclohexyldimethyltin were used to confirm the number of protons on the cyclohexyl group. The number of protons on the cyclohexyl group of dicyclohexyldimethyltin was 22 as expected. In the NMR spectra of the free cyclohexane¹⁶², all the protons are equivalent, and give rise to a singlet at $\delta=1.4\text{ppm}$ in CCl_4 . In substituted cyclohexane such as bromocyclohexane, two groups of protons are observed¹⁶². In dicyclohexyldimethyltin three groups of cyclohexyl protons are observed. The peaks are strongly coupled, and the multiplets observed cannot be explained on the basis of a first order coupling. The cyclohexyl group proton on the carbon atom directly bonded to the tin atom is deshielded and resonates at low field ($\delta=1.8\text{ ppm}$).

Further characterization of the butylmethyltin and cyclohexylmethyltin compounds was provided by ^{119}Sn NMR (Table 2.1) as this information is not yet

available in the literature. From the chemical shift data shown in Table 2.1, it can be inferred that the cyclohexyl group has a more deshielding effect on the tin atom, than the n-butyl group.

Table 2.1 ^{119}Sn NMR chemical shifts for the standard organotin compounds^a.

Compound	δ (ppm)	Conc. (M)
$(\text{C}_4\text{H}_9)_3\text{SnCH}_3$	-6.128	1.10
$(\text{C}_4\text{H}_9)_2\text{Sn}(\text{CH}_3)_2$	-2.539	0.58
$(\text{C}_6\text{H}_{11})_3\text{SnCH}_3$	-44.378	0.77
$(\text{C}_6\text{H}_{11})_2\text{Sn}(\text{CH}_3)_2$	-16.393	0.30
$(\text{C}_3\text{H}_7)_4\text{Sn}$	-18.072	1.98

^a ^{119}Sn NMR was obtained on deuterated chloroform solutions of the organotin compounds, and referenced relative to tetramethyltin.

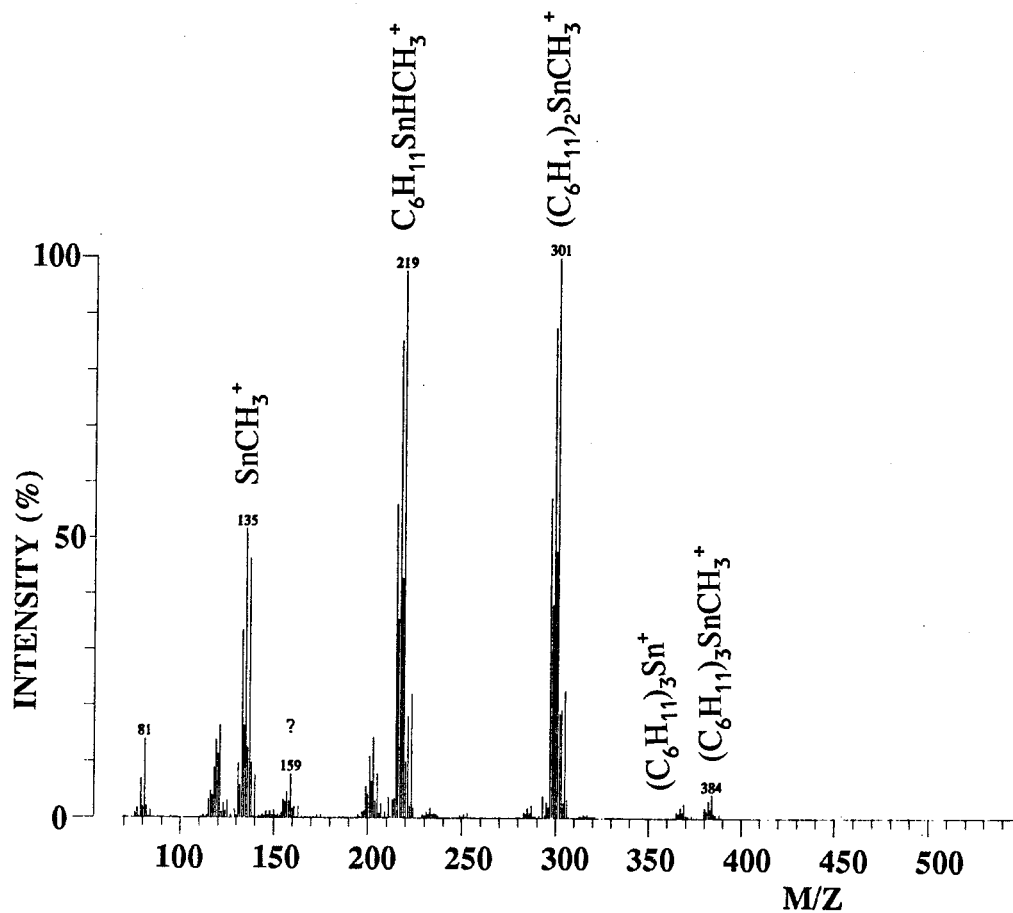


Figure 2.2 Mass spectra (EI) of tricyclohexylmethyltin.

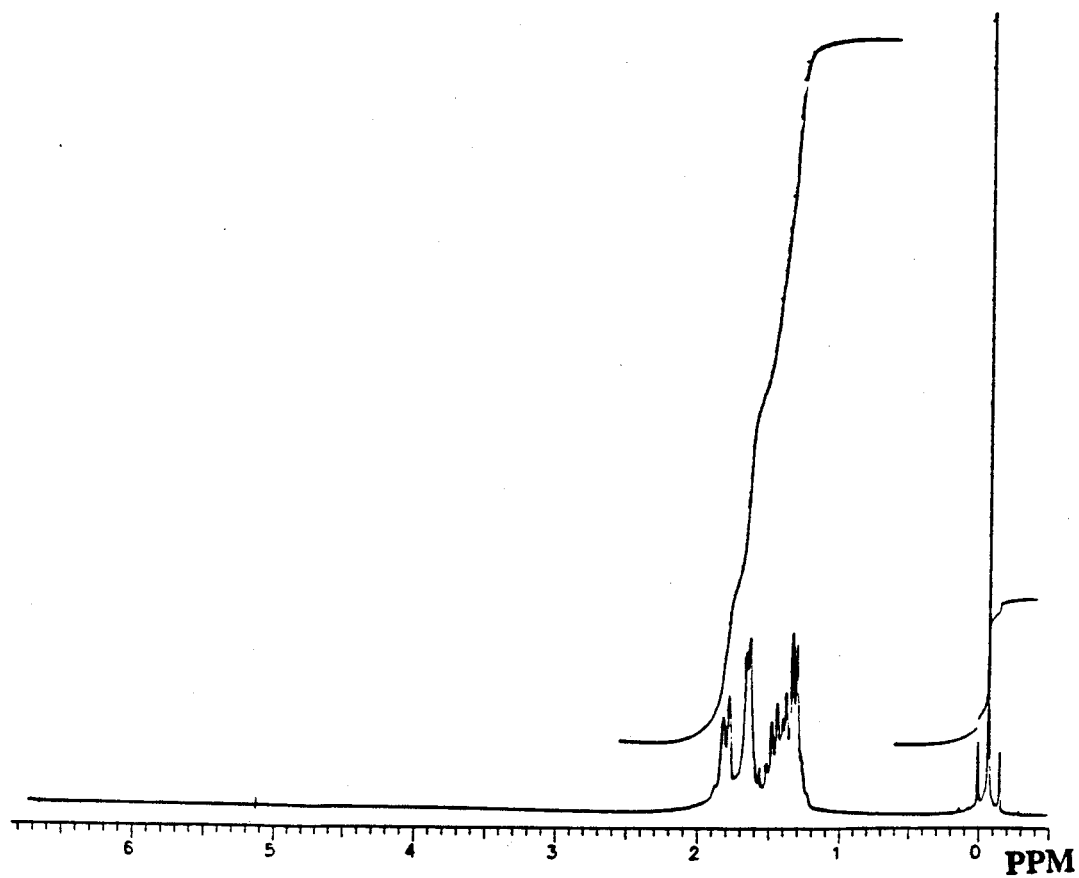


Figure 2.3 ^1H NMR spectra of dicyclohexyldimethyltin.

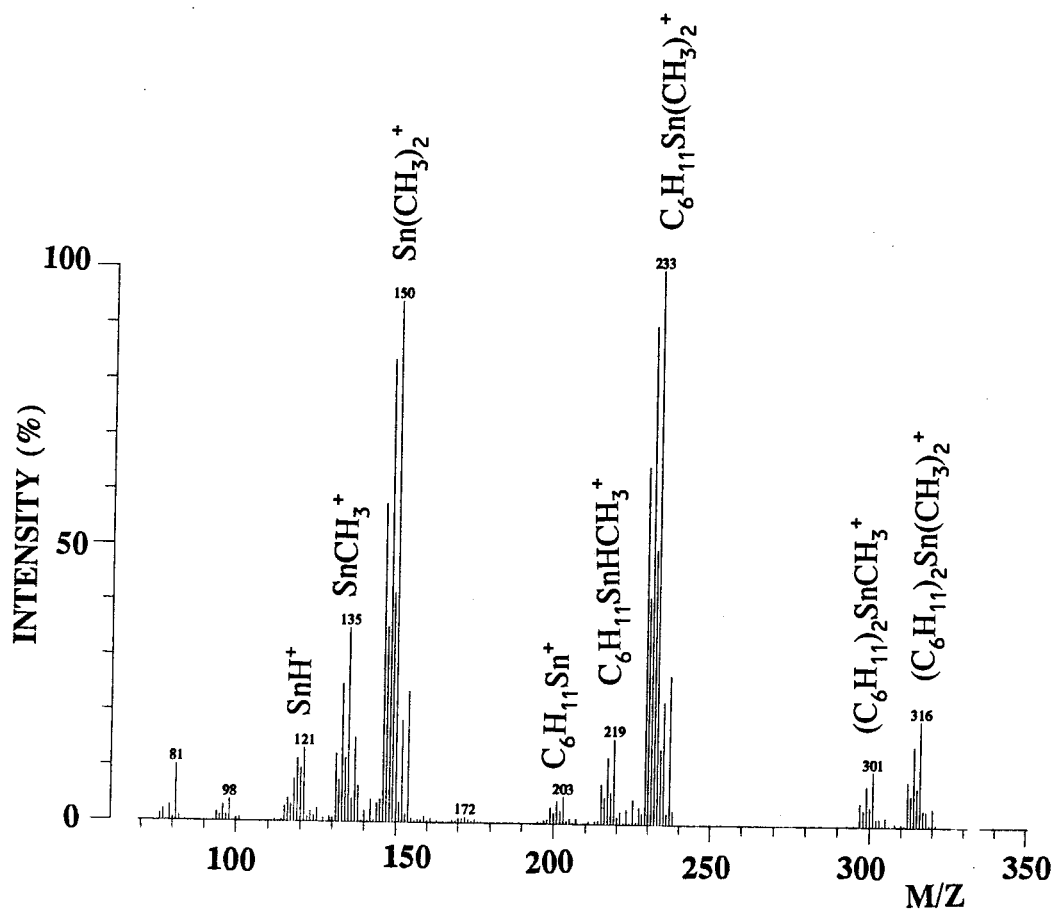


Figure 2.4 Mass spectra (EI) of dicyclohexyldimethyltin.

2.4.2 Fragment ions and intensities of the standard tetraorganotin compounds.

The standard tetraorganotin compounds were subjected to low resolution mass spectrometry. The molecular ions were of low intensity, and therefore were not used for the GC-MS analysis. The fragmentation involves the loss of butyl or cyclohexyl or methyl groups from the tin atom. The fragment ions and intensities relative to the base peak are given in Tables 2.2, 2.3 and 2.4.

Table 2.2 Major fragment ions of tributylmethyltin.

Standard compound	M/Z	Fragment ion	Relative Intensity (%)
$(C_4H_9)_3SnCH_3$ (MW=306) ^a	121	SnH^+	79
	135	CH_3Sn^+	100
	177	$C_4H_9Sn^+$	65
	193	$C_4H_9SnHCH_3^+$	99
	235	$(C_4H_9)_2Sn^+$	12
	249	$(C_4H_9)_2SnCH_3^+$	93
	291	$(C_4H_9)_3Sn^+$	9
	306	$(C_4H_9)_3SnCH_3^+$	0.7

a = Molecular weight and all fragment ion assignments are based on ^{120}Sn .

Table 2.3 Major fragment ions for dibutyldimethyltin and tricyclohexylmethyltin.

Standard compound	M/Z	Fragment ion	Relative Intensity (%)
$(C_4H_9)_2Sn(CH_3)_2$ (MW = 264) ^a	121	SnH^+	35
	135	CH_3Sn^+	70
	150	$(CH_3)_2Sn^+$	99
	177	$C_4H_9Sn^+$	14
	193	$C_4H_9SnHCH_3^+$	52
	207	$C_4H_9Sn(CH_3)_2^+$	100
	249	$(C_4H_9)_2SnCH_3^+$	39
	264	$(C_4H_9)_2Sn(CH_3)_2^+$	5
$(C_6H_{11})_3SnCH_3$ (MW = 384) ^a	121	SnH^+	17
	135	CH_3Sn^+	52
	219	$C_6H_{11}SnHCH_3^+$	100
	301	$(C_6H_{11})_2SnCH_3^+$	98
	369	$(C_6H_{11})_3Sn^+$	3
	384	$(C_6H_{11})_3SnCH_3^+$	4

a = Molecular weight and all fragment ion assignments are based on ^{120}Sn .

Table 2.4 Major fragment ions for dicyclohexyldimethyltin and tetrapropyltin.

Standard compound	M/Z	Fragment ion	Relative Intensity (%)
$(C_6H_{11})_2Sn(CH_3)_2$ (MW = 316) ^a	121	SnH^+	13
	135	CH_3Sn^+	35
	150	$(CH_3)_2Sn^+$	94
	203	$C_6H_{11}Sn^+$	5
	219	$C_6H_{11}SnHCH_3^+$	15
	233	$C_6H_{11}Sn(CH_3)_2^+$	100
	301	$(C_6H_{11})_2SnCH_3^+$	10
	316	$(C_6H_{11})_3Sn^+$	19
$(C_3H_7)_4Sn$ (MW = 292) ^a	121	SnH^+	46
	135	CH_3Sn^+	9
	163	$C_3H_7Sn^+$	91
	207	$(C_3H_7)_2SnH^+$	91
	249	$(C_3H_7)_3Sn^+$	100
	292	$(C_3H_7)_4Sn^+$	3

a = Molecular weight and all fragment ion assignments are based on ^{120}Sn

2.4.3 GC-MS elution profile and masses of fragment ions used for selected ion monitoring.

The elution profile of the standard tetraorganotin compounds is shown in Figure 2.5. The retention times and the retention time window (the time frame within which the retention time can vary and still be valid) used for the GC-MS analyses of the organotin compounds are shown in Table 2.5.

Table 2.5 Retention time and retention time window used for GC-MS SIM analysis.

Compound	Retention time (min)	Retention time window (min)
$(C_4H_9)_2Sn(CH_3)_2$	12.42	11.50-13.33
$(C_3H_7)_4Sn$	13.97	13.33-14.25
$(C_4H_9)_3SnCH_3$	14.60	14.25-15.50
$(C_6H_{11})_2Sn(CH_3)_2$	16.13	15.50-17.00
$(C_6H_{11})_3SnCH_3$	18.93	17.00-20.00

The fragment ions chosen for GC-MS SIM were selected on the basis of their high intensities in low resolution mass spectrometry (Tables 2.2, 2.3, 2.4). The fragment ions and masses monitored for each organotin compound are shown in Table 2.6.

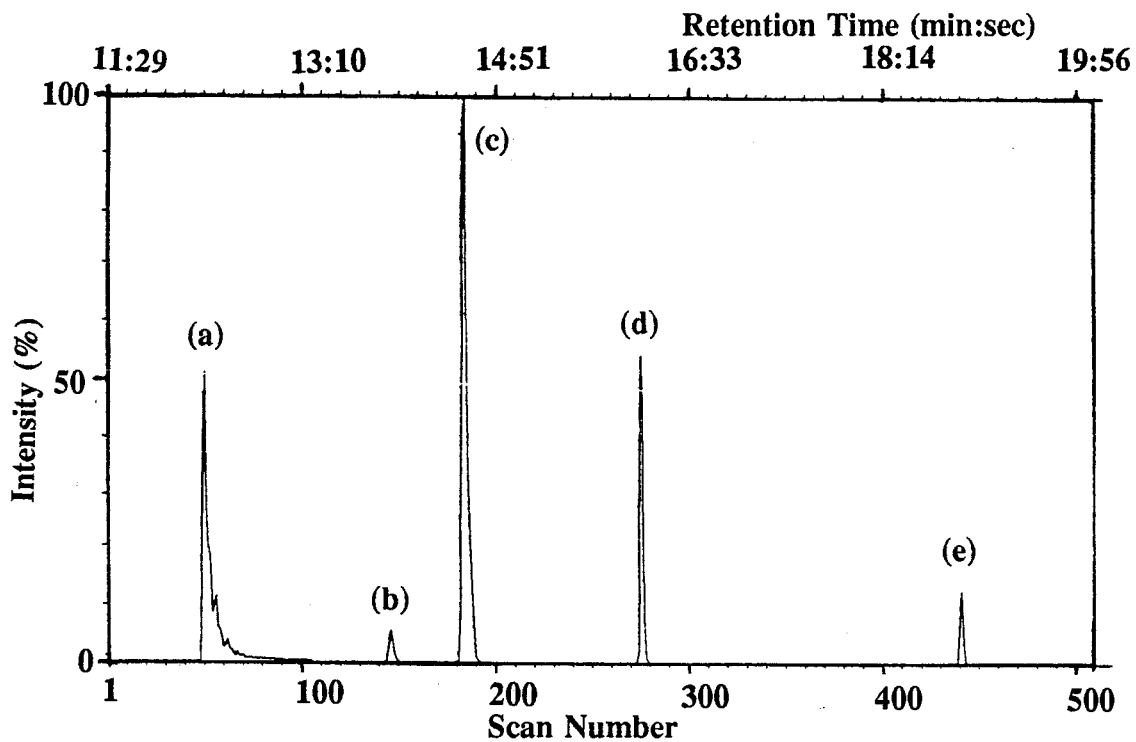


Figure 2.5 GC-MS elution profile of the standard tetraorganotin compounds. Peaks a, b, c, d, e, correspond to dibutyldimethyltin, tetrapropyltin, tributylmethyltin, dicyclohexyldimethyltin, and tricyclohexylmethyltin respectively.

For each fragment ion, masses corresponding to tin 116, 118 and 120 isotopes were monitored (Table 2.6).

Table 2.6 Fragment ions and masses used to detect and quantify each organotin compound in GC-MS SIM.

Compound	M/Z monitored	Fragment ion
$(C_4H_9)_3SnCH_3$	193, 191, 189	$C_4H_9SnHCH_3^+$
$(C_4H_9)_2Sn(CH_3)_2$	207, 205, 203	$C_4H_9Sn(CH_3)_2^+$
$(C_6H_{11})_3SnCH_3$	219, 217, 215	$C_6H_{11}SnHCH_3^+$
$(C_6H_{11})_2Sn(CH_3)_2$	233, 231, 229	$C_6H_{11}Sn(CH_3)_2^+$
$(C_3H_7)_4Sn$	249, 247, 245	$(C_3H_7)_3Sn^+$

2.4.4 Suitability of tetrapropyltin as internal standard as studied by using gas chromatography (GC).

The use of internal standards eliminates the effect of variations in the instrument's operating parameters on the analyte. In GC or GC-MS, variations in injection volume, ion source temperature, carrier gas flow rate, could cause considerable errors from run to run, if not eliminated by the method of internal standardization. Ideally, compounds used as internal standards should be structurally

similar to the analyte and their spectroscopic response should also be similar to that of the analyte. Also, the internal standard should not be naturally present in the analyte. Tetrapropyltin satisfies these conditions closely. No natural source of tetrapropyltin in the marine environment is known, and its gas chromatographic retention time is in the range of the retention times of the analytes (Fig 2.5). This ensures that the internal standard and the analytes experience similar broadening effects on the capillary column. Also, calibration graphs obtained for tributylmethyltin solutions by using different concentrations of tetrapropyltin (2 - 50 $\mu\text{g/mL}$ as Sn) as internal standard, gave high correlation coefficients (Table 2.7).

Table 2.7 Regression data for graphs obtained with various concentrations of the internal standard tetrapropyltin.

Conc. $(\text{C}_3\text{H}_7)_4\text{Sn}$ ($\mu\text{g/mL}$ as Sn)	Regression equation for $(\text{C}_4\text{H}_9)_3\text{SnCH}_3$	Regression coefficient
2	$Y=0.4964X - 0.0924$	0.9980
4	$Y=0.2514X - 0.0521$	0.9910
6	$Y=0.1659X - 0.0322$	1.0000
50	$Y=0.0190X - 0.0023$	1.0000

The calibration curves obtained for tributylmethyltin by using different concentrations of the internal standard are shown in Figures 2.6 and 2.7. The error

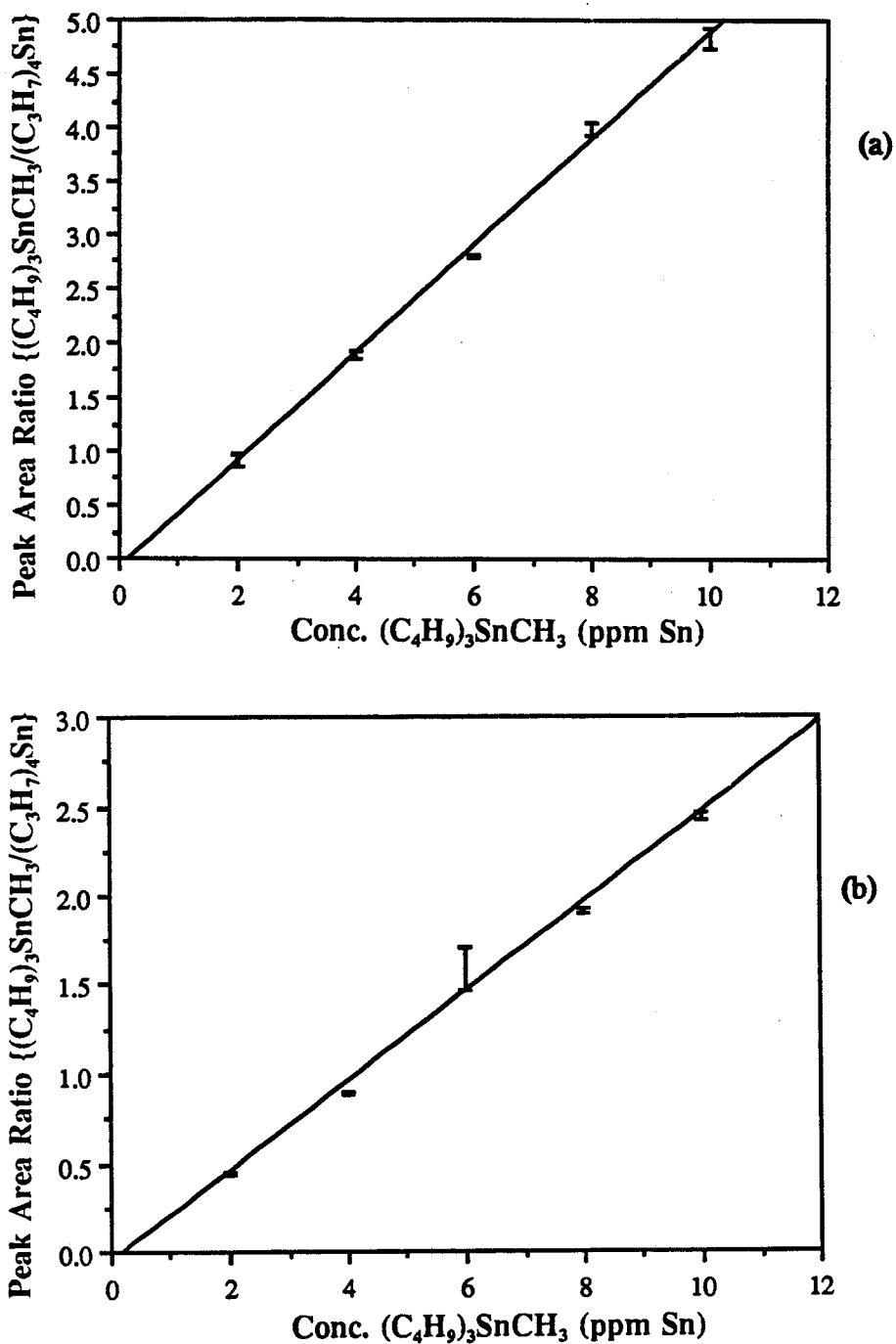


Figure 2.6 Effect of internal standard concentration on the linearity of calibration curves for tributylmethyltin. Graphs a and b were obtained by using 2 $\mu\text{g/mL}$ (as Sn) and 4 $\mu\text{g/mL}$ (as Sn) tetrapropyltin respectively.

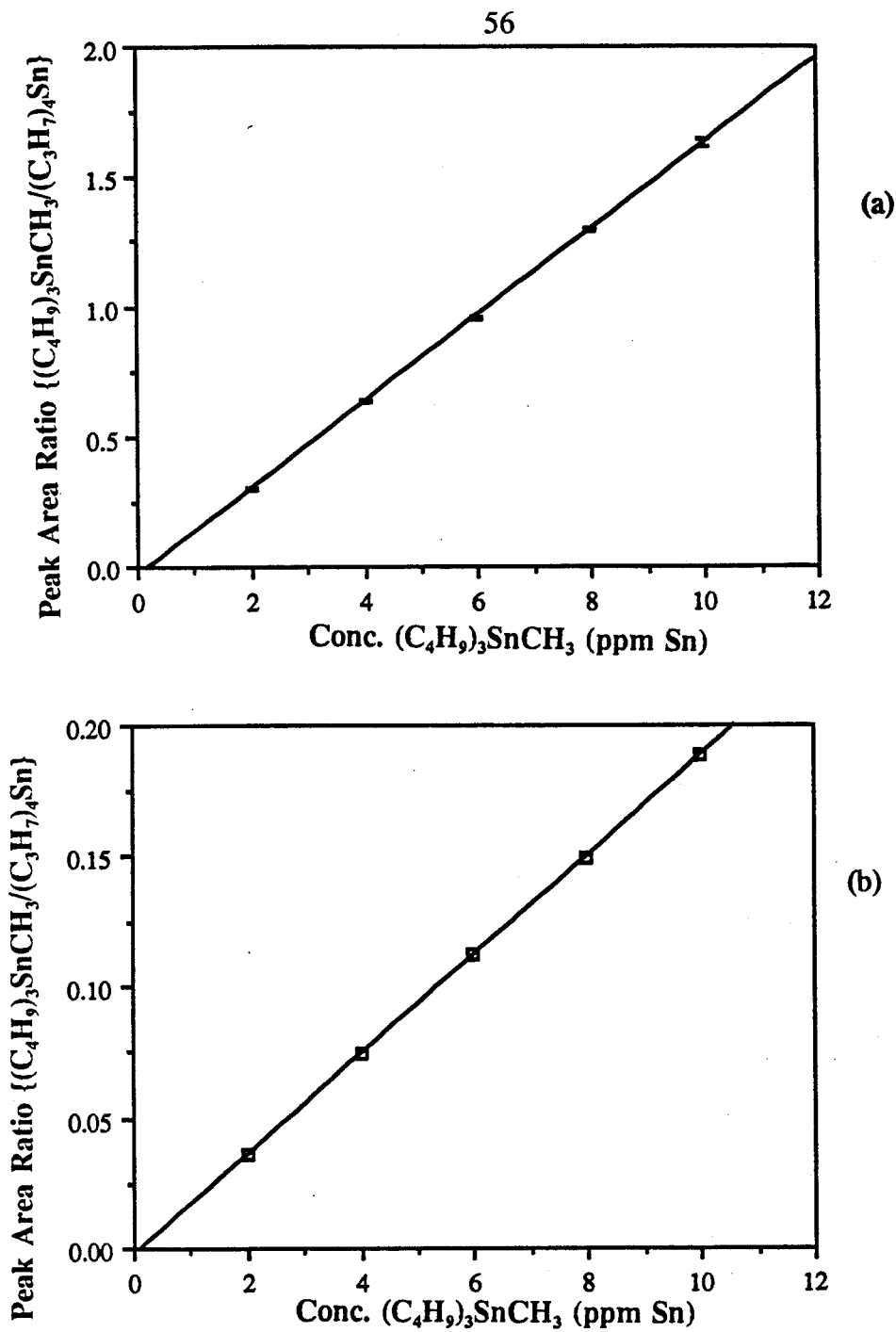


Figure 2.7 Effect of internal standard concentration on the linearity of calibration curves for tributylmethyltin. Graphs a and b were obtained by using 6 $\mu\text{g/mL}$ (as Sn) and 50 $\mu\text{g/mL}$ (as Sn) tetrapropyltin respectively.

bars in Figures 2.6 and 2.7 represent the standard error for three replicate determinations. All the calibration graphs for tributylmethyltin obtained by using the various concentrations of tetrapropyltin ($2 \mu\text{g/mL}$ to $50 \mu\text{g/mL}$ as Sn) as internal standard gave good linearity (Figures 2.6 and 2.7). Thus, the internal standard could be applied in concentrations up to $50 \mu\text{g/mL}$ (as Sn) without introducing non-linearity in the calibration curves. The regression equations obtained for the graphs are shown in Table 2.7.

An ideal internal standard would have been an analogous stable isotope of the butyltin or cyclohexyltin compounds because it would be chemically very similar to the analyte. Deuterated tributylmethyltin was examined for use as internal standard in GC-MS SIM, but was found to be unsuitable because it caused a decrease in the instrument's sensitivity to tributylmethyltin detection as explained in Section 2.3.1.3.

2.4.5 Detection limit, calibration curves, and precision for the GC-MS SIM analysis.

2.4.5.1 Detection limit and calibration curves obtained by GC-MS SIM.

The limit of detection was obtained from a plot of the peak area ratio of the standard tetraorganotin compounds to the internal standard versus the concentration of the standard tetraorganotin solutions (Figures 2.8 and 2.9). The error bars represent the standard error for three replicate determinations.

The detection limit defined as the analyte concentration which gives a signal equal to the signal of the blank, plus thrice the standard deviation of the blank, was

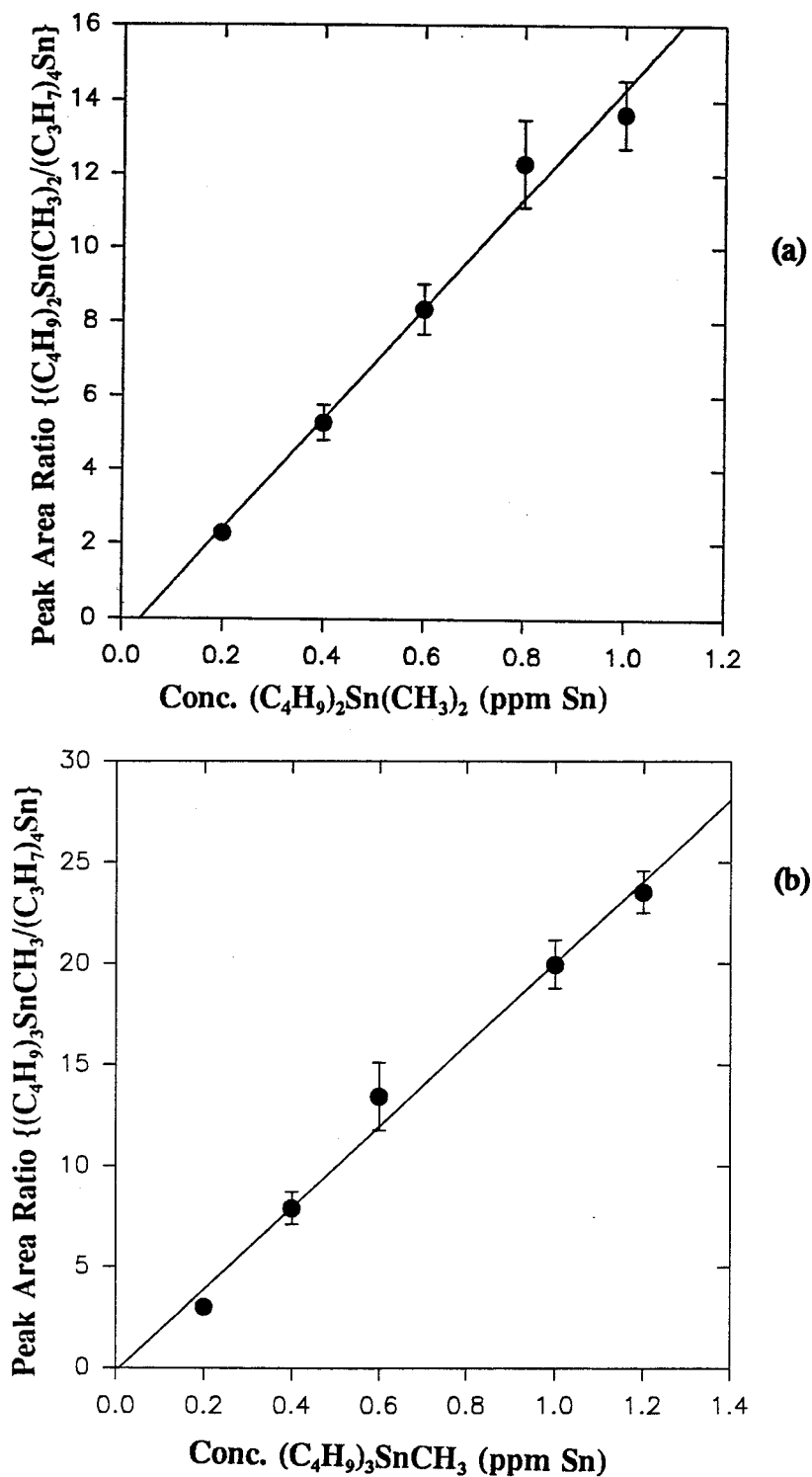


Figure 2.8 GC-MS calibration curves for (a) dibutyldimethyltin and (b) tributylmethyltin.

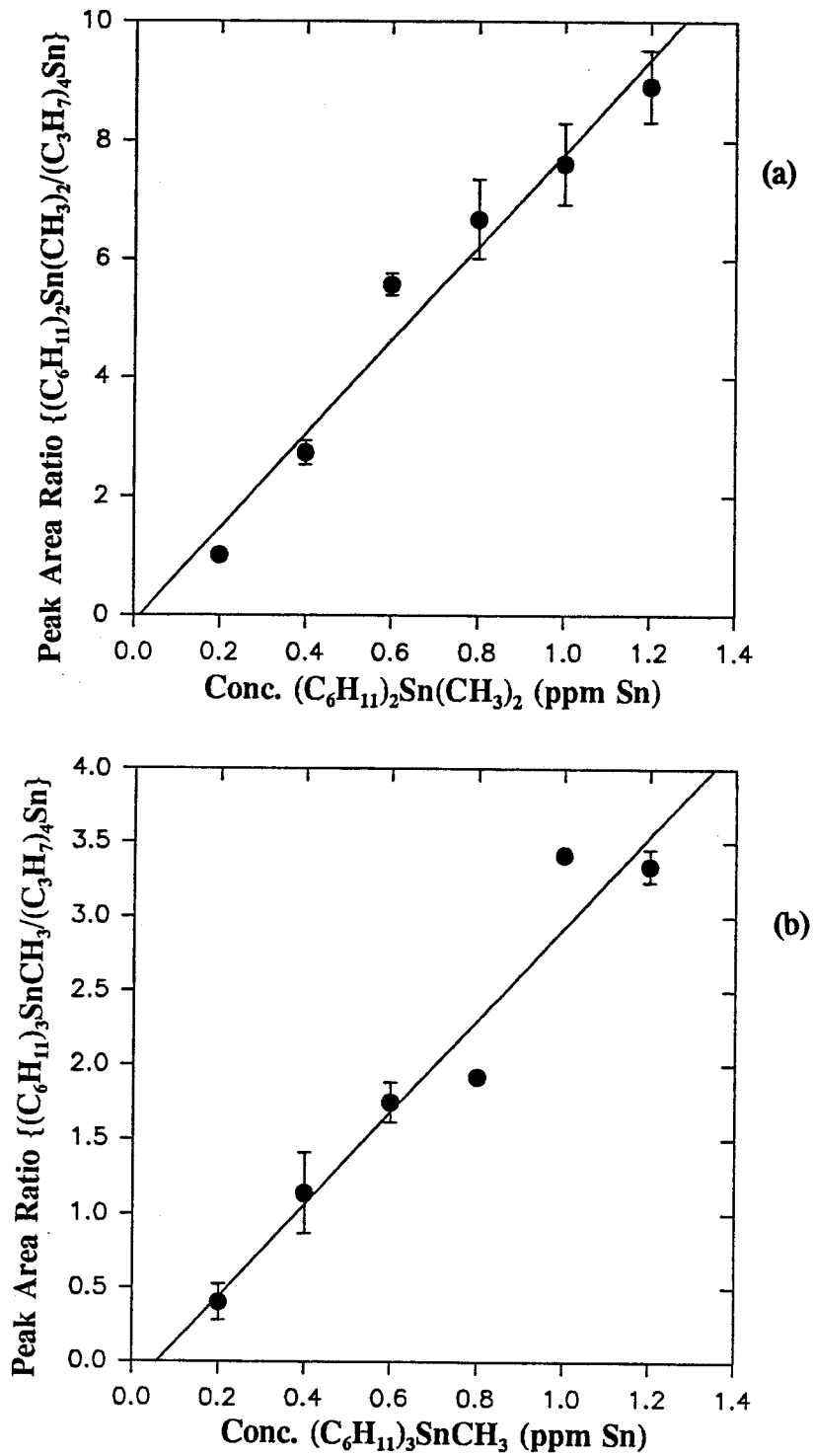


Figure 2.9 GC-MS calibration curves for (a) dicyclohexyldimethyltin and (b) tricyclohexylmethyltin.

calculated according to the method previously described by Miller and Miller¹⁶³ from the calibration curves (Figures 2.8 and 2.9). According to these authors¹⁶⁶, at the limit of detection the analyte signal is given by the equation $Y = Y_B + 3S_B$ where Y is the analyte signal at the limit of detection, Y_B is the blank signal and S_B is the standard deviation of the blank. The standard deviation of the blank S_B can be calculated as the standard deviation of the y residuals $S_{y/x}$. The blank signal Y_B may be taken to be the intercept of the graph on the y axis. From the working calibration curves of the analytes (Figures 2.8 and 2.9), the intercept of the graph on the y-axis is obtained, and the standard deviation of the y-residuals $S_{y/x}$ is calculated. Then, the detection limit is determined (Table 2.8).

Table 2.8 Detection limits for organotin compounds by GC-MS SIM.

Compound	Detection limit ($\mu\text{g/mL}$ as Sn)
$(\text{C}_4\text{H}_9)_3\text{SnCH}_3$	0.053
$(\text{C}_4\text{H}_9)_2\text{Sn}(\text{CH}_3)_2$	0.028
$(\text{C}_6\text{H}_{11})_2\text{Sn}(\text{CH}_3)_2$	0.049
$(\text{C}_6\text{H}_{11})_3\text{SnCH}_3$	0.064

Typical calibration curves obtained by the least squares method, for the quantitation of the organotin compounds from environmental samples by GC-MS SIM are shown in Figures 2.8 and 2.9. A linear relationship is obtained over the concentration

Table 2.9 Calibration equations used for the quantitation of environmental samples by GC-MS SIM.

Compound	Calibration equation	Regression coefficient
$(C_4H_9)_3SnCH_3$	$RA = 4.0378RC - 0.1554$	0.9944
$(C_4H_9)_2Sn(CH_3)_2$	$RA = 2.9721RC - 0.5492$	0.9989
$(C_6H_{11})_2Sn(CH_3)_2$	$RA = 1.5812RC - 0.1093$	0.9817
$(C_6H_{11})_3SnCH_3$	$RA = 0.6196RC - 0.1742$	0.9685

RA =Relative peak area ratio of organotin compound to internal standard, and is plotted as y-axis.

RC =Relative concentrations of organotin compound to internal standard, and is the x-axis.

range studied. The regression equations obtained from a direct plot of the peak area ratios of the tetraorganotin compounds to the internal standard versus the various concentrations of the tetraorganotin compounds were modified to obtain the working

calibration equations by substituting RC (concentration ratio of tetraorganotin to internal standard) for X in the general form of a straight line equation $Y=MX + C$. The resulting calibration equations are shown in Table 2.9.

An obvious characteristic of the calibration curves in Figures 2.8 and 2.9 is the failure of the regression line to pass through the graph's origin despite various optimization steps in the GC-MS operating conditions. This phenomenon was very reproducible in calibration curves obtained at various times and consequently is unlikely to affect its use for quantitation. A possible consequence of this effect is the difficulty in attaining a very low detection limit required for trace metal speciation.

2.4.5.2 Precision of the GC-MS SIM method.

The precision of the GC-MS SIM analysis was determined by analyzing replicate injections of mixtures of the standard tetraorganotin compounds and the internal standard dissolved in n-heptane. The precision was determined at two concentrations 0.2 $\mu\text{g/mL}$ and 1.2 $\mu\text{g/mL}$ (as Sn). The relative standard deviation for six replicate injections was calculated (Table 2.10). There was no significant difference in precision at the two organotin concentrations as tested by means of a two-tailed F-test at 5% probability level¹⁶³.

The sensitivity of the GC-MS SIM method as shown in the slope of the calibration graphs (Table 2.9) follows the order tributylmethyltin > dibutyldimethyltin > dicyclohexyldimethyltin > tricyclohexylmethyltin.

Table 2.10 Precision for six replicate injections of organotin compounds as determined by GC-MS SIM.

Compound	Precision (RSD %)	
	0.2 $\mu\text{g/mL}$ as Sn	1.2 $\mu\text{g/mL}$ as Sn
$(\text{C}_4\text{H}_9)_3\text{SnCH}_3$	5.4	8.1
$(\text{C}_4\text{H}_9)_2\text{Sn}(\text{CH}_3)_2$	9.4	10.5
$(\text{C}_6\text{H}_{11})_2\text{Sn}(\text{CH}_3)_2$	11.1	10.0
$(\text{C}_6\text{H}_{11})_3\text{SnCH}_3$	14.8	7.4

2.4.6 Recovery studies on the extraction procedure.

Recovery studies of the organotin compounds were carried out at the concentration level of 1.5 μg (as Sn) per 40 g (wet wt) of shrimp as described in section 2.3.4 above. The extraction procedure affords good recoveries for tributyltin, dibutyltin and dicyclohexyltin species (Table 2.11). The detection of the tricyclohexyltin species was hampered by the elution of other unidentified compounds from the sample matrix in its retention window (Fig 2.10). Thus in Figure 2.10, there is an unidentified peak E, of very high intensity which elutes at the same retention time as tricyclohexylmethyltin and completely masks the peak due to this tin compound. Therefore, the quantitation of tricyclohexyltin was not carried out. The

other peaks labelled A, B, C and D on the diagram (Figure 2.10) are due to dibutyldimethyltin, tetrapropyltin, tributylmethyltin and dicyclohexyldimethyltin respectively. The unlabelled peaks in Figure 2.10 are unknown and their mass spectra do not show tin isotope pattern. The mass spectra for peaks A, C and D (Figure 2.10) are shown in Figures 2.11 and 2.12 (i) and (ii) respectively.

Table 2.11 Recovery of organotin compounds spiked into Shrimp (Pandalus tridens) by extraction with methylene chloride.

Compound	Percentage recovery \pm (RSD %) ^a
$(C_4H_9)_3SnCH_3$	96.9 \pm 2.1
$(C_4H_9)_2Sn(CH_3)_2$	99.9 \pm 1.6
$(C_6H_{11})_2Sn(CH_3)_2$	93.0 \pm 9.1

a = Relative standard deviation of two extractions, each of two replicate injections into the GC-MS.

RSD = Relative standard deviation.

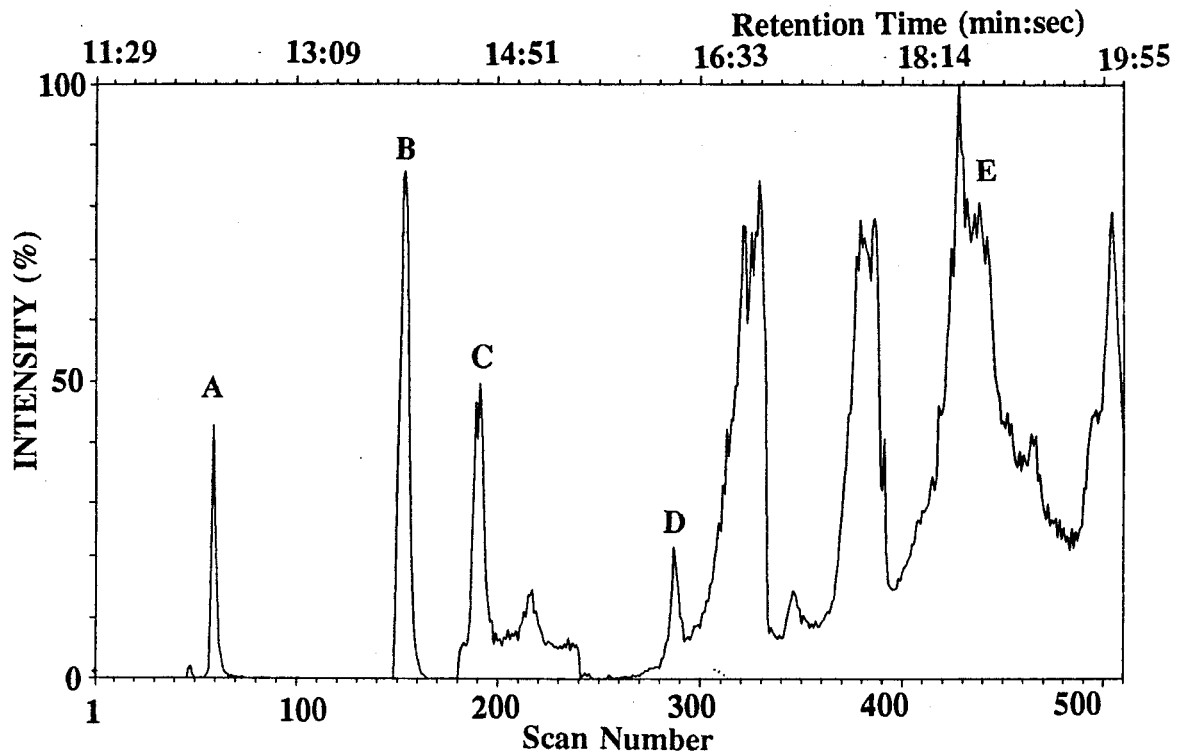


Figure 2.10 Selected ion current chromatogram of standard organotin compounds spiked into shrimp. Peak B corresponds to the internal standard.

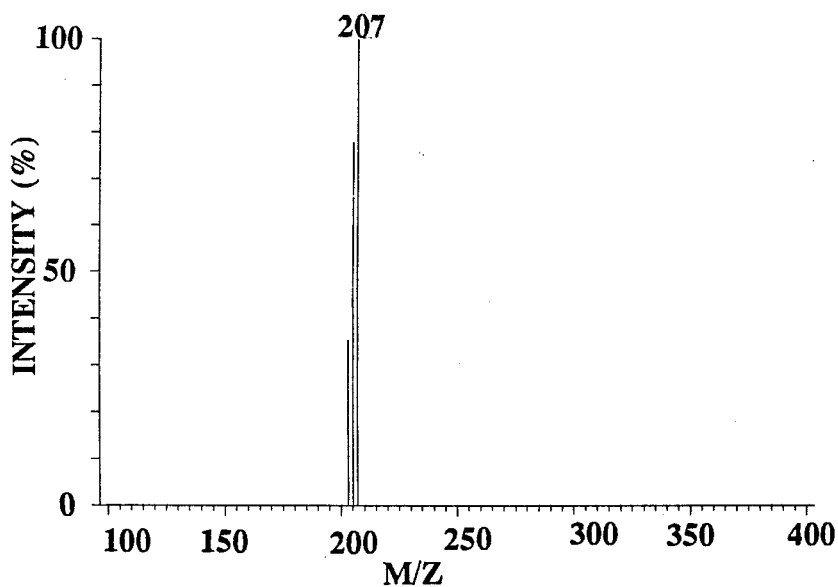


Figure 2.11 Mass spectra of peak A in Figure 2.10. The peak at $m/z=207$ indicates the presence of dibutyltin.

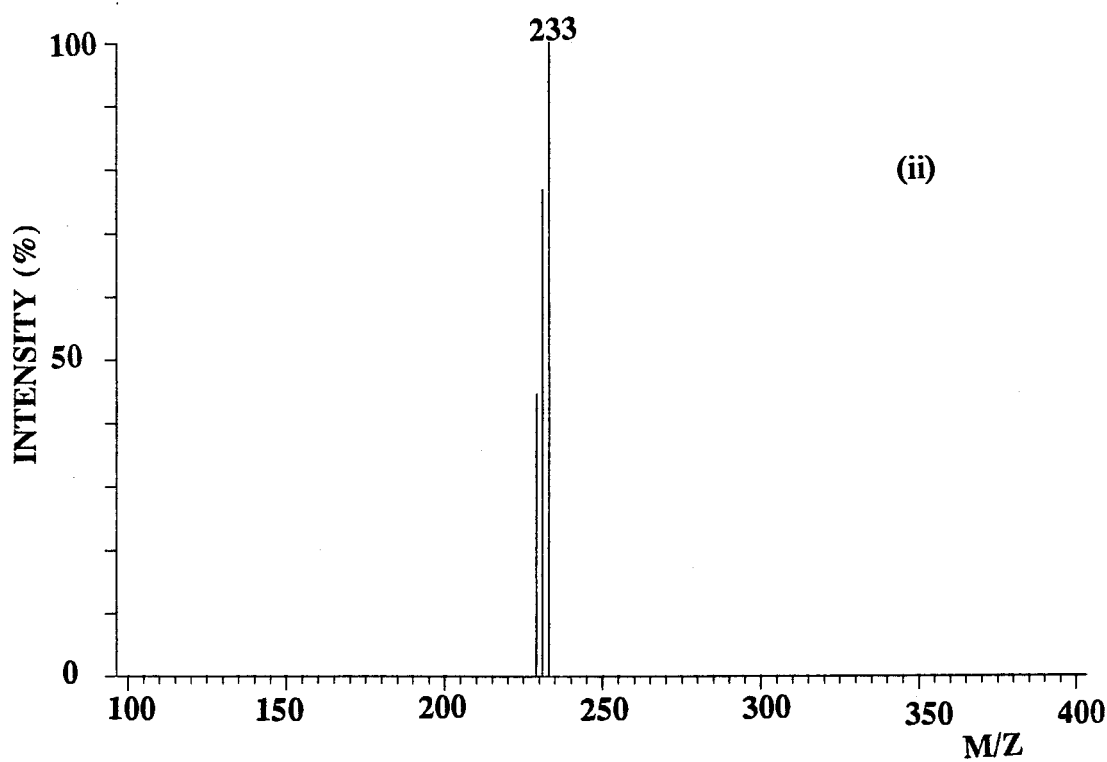
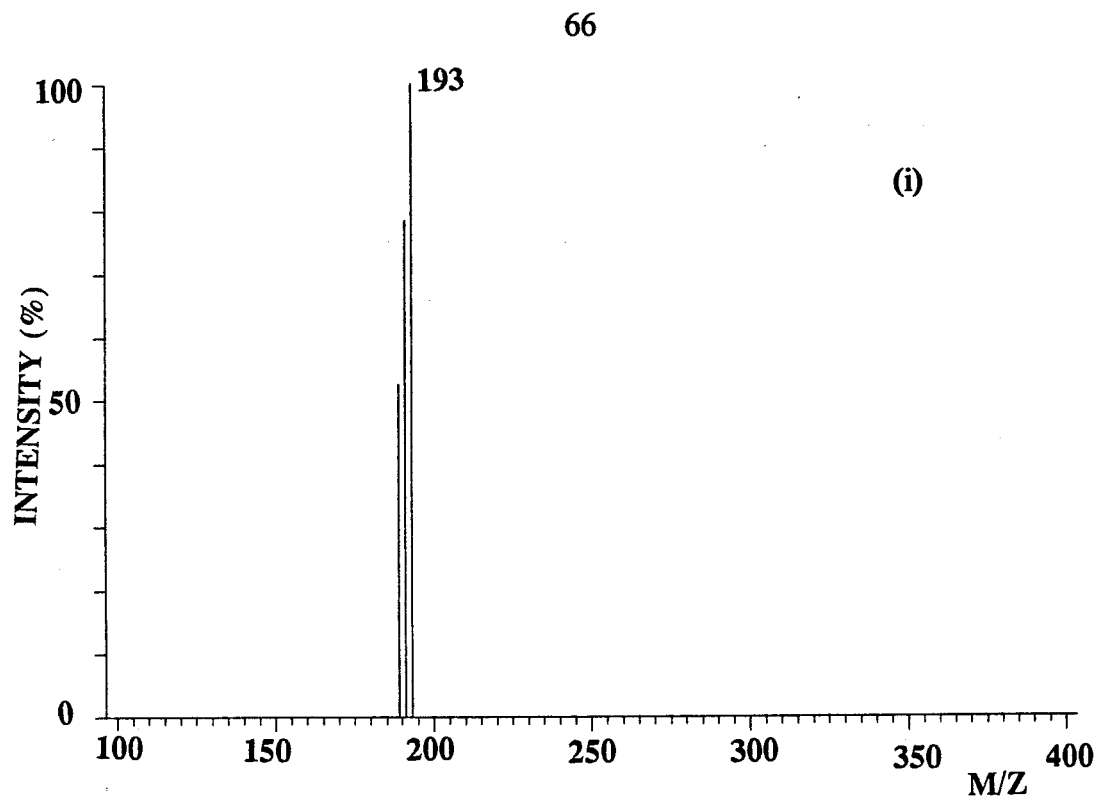


Figure 2.12 Mass spectra of (i) peak C and (ii) peak D in Figure 2.10 above indicating the presence of tributyltin and dicyclohexyltin species respectively.

2.4.7 Organotin concentrations in some marine organisms of British Columbia, Canada.

The marine animals selected for organotin analyses consisted mainly of bivalves molluscs. This was mainly because of their availability in the marine locations sampled. The analysis of marine organisms for organotin compounds was carried out with the following objectives:

- (i) To obtain an indication of the geographical spread of organotin pollution in the coastal areas of British Columbia in terms of dibutyltin, tributyltin, and the cyclohexyltin compounds. The latter were of particular interest because dicyclohexyltin species have been found in surface microlayers of some British Columbian marine waters, and biota¹¹⁷.
- (ii) To study organotin concentrations in particular species of marine animals, over a period of three years.
- (iii) To examine organotin concentrations in different animals from one particular location to see if any particular animal has the ability to accumulate organotin compounds more than the others.

In practice, animal availability varied from location to location thereby making it difficult to obtain data from the same species of animals in all locations sampled.

The map of the locations sampled is shown in Appendix A.

2.4.7.1 Organotin concentrations in oysters.

The organotin concentrations in the Pacific oyster Crassostrea gigas from

some locations in British Columbia, Canada are shown in Table 2.12.

Table 2.12 Organotin concentrations in the oyster Crassostrea gigas from some coastal areas of British Columbia.

Year of collection	Location	ng/g as Sn (Wet weight)		
		$(C_4H_9)_2Sn^{2+}$	$(C_4H_9)_3Sn^+$	$(C_6H_{11})_2Sn^{2+}$
July, 1991	Denman Island ^b	12.5 ± 1.8^a	ND	ND
Sept., 1991	Von Donop Inlet, Cortes Island	17.3 ± 0.3	7.6 ± 0.3	ND
May, 1991	Pendrell Sound	ND	ND	ND

ND = Not detected.

a = Standard error for two separate sample determinations. All other standard errors given are for two replicate injections of one sample.

b = Oysters were purchased.

Oysters in particular have been shown to be very sensitive to tributyltin pollution²⁴. Effects of tributyltin pollution on oysters include shell malformation and retarded growth²². Oysters from Pendrell Sound British Columbia (Table 2.12) showed no organotin pollution. Comparative data on the organotin body burden of oysters from another Canadian location, Fanny Bay, British Columbia has been reported by Stewart and Thompson¹⁶⁴. According to them, the oyster Crassostrea gigas contained tributyltin and monobutyltin concentrations of 52 ng/g (dry wt as Sn) and 4.6 ng/g (dry wt as Sn) respectively. These organotin concentrations translate to approximately 10.4 ng/g (wet wt as Sn) tributyltin species and 0.92 ng/g (wet wt as Sn) monobutyltin species. No dibutyltin species were detected by the authors¹⁶⁴. This shows that Fanny bay is comparable to Von Donop Inlet, British Columbia in tributyltin pollution (Table 2.12). Other organotin data for oysters from other parts of the world are available. Rice et al¹⁶⁵ have reported tributyltin concentrations of 9 ng/g (wet wt as tributyltin cation) or 3.7 ng/g (wet wt as Sn) for oysters from Sarah Creek, and 834 ng/g (wet wt as tributyltin cation) or 341.3 ng/g (wet wt as Sn) for oysters from Kings Creek, Virginia U.S.A.. Tributyltin concentrations of 49.74 - 189 ng/g (wet wt as tributyltin cation) or 20.4 - 77.3 ng/g (wet wt as Sn) have also been reported by Wolniakowski et al¹⁶⁶ for the oyster Crassostrea gigas from Coos Bay Estuary, U.S.A..

A comparison of the butyltin body burden for oysters analyzed in this study (Table 2.12) with the butyltin body burden reported by Rice et al¹⁶⁵ indicates that oysters from Von Donop Inlet, British Columbia, contain higher tributyltin levels

than those from Sarah Creek, Virginia U.S.A., but less tributyltin levels than oysters from Kings Creek, Virginia, U.S.A..

Concentrations expressed in wet weight are not comparable to concentrations expressed in dry weight, unless appropriate conversion factors are applied. An approximate conversion factor applied in this study for oysters is $x \mu\text{g/g}$ dry wt basis = $5x \mu\text{g/g}$ wet wt basis. This conversion factor was arrived at, after freeze-drying known weight of wet oyster samples.

Waldock and Miller¹⁶⁷ have reported tributyltin levels of up to $4.5 \mu\text{g/g}$ dry weight or approximately ($0.37 \mu\text{g/g}$ wet wt as Sn) for some oysters from England. Rapsomanikis and Harrison¹⁶⁸ have also reported tributyltin levels of $0.027 - 1.66 \mu\text{g/g}$ (dry wt as tributyltin cation) or $2.2 - 135.9 \text{ ng/g}$ (wet wt as Sn) and dibutyltin levels of $0.012 - 0.402 \mu\text{g/g}$ (dry weight as dibutyltin cation) or $2.4 - 32.9 \text{ ng/g}$ (wet wt as Sn) for some oysters from England. Other tributyltin levels in oysters have been reported by Stewart and de Mora⁸⁶ for the Mangrove oyster Crassostrea mordax of Fiji. Tributyltin concentrations in the range 626 to 3180 ng/g (dry wt as tributyltin cation) or 51.2 - 260.3 ng/g (wet wt as Sn) were obtained. In New Zealand, tributyltin concentrations in the range $0.033 - 1.38 \mu\text{g/g}$ (dry wt as tributyltin) or $2.7 - 110.5 \text{ ng/g}$ (wet wt as Sn) and $0.049 - 0.467 \mu\text{g/g}$ (dry wt as tributyltin cation) or $4.0 - 38.2 \text{ ng/g}$ (wet wt as Sn) have been reported for the oysters Crassostrea gigas and Saccostrea glomerata respectively, for the Tamaki Estuary of New Zealand¹⁶⁹. Han and Weber⁷⁹ have determined dibutyltin and tributyltin concentrations of 840 and 2200 ng/g (dry wt as Sn) respectively for a French oyster sample. By using a dry

weight/wet weight conversion ratio of about 0.2 as given by these authors⁷⁹, dibutyltin and tributyltin concentrations of 168 and 440 ng/g (wet wt as Sn) respectively were obtained for the French oyster sample.

A visual inspection of the oysters' shells prior to their analysis did not reveal obvious shell malformations. Oysters from the Canadian location Denman Island did not show the presence of tributyltin species, but did show the presence of dibutyltin species which may have originated from the metabolism of tributyltin compounds. The available data in Table 2.12 do not indicate pollution by dicyclohexyltin species.

2.4.8 Spread of organotin compounds in the Canadian environment.

The extent of organotin pollution in British Columbia was monitored by sampling various available marine organisms from different locations in British Columbia. The results obtained are shown in Table 2.13 below. The concentrations and species of organotin compounds detected in any one location should be a reflection of the type of industrial activity going on in that environment. By the very nature of introduction of tributyltin compounds into the environment, areas of high boating or shipping activity should show high tributyltin concentrations. Data in Table 2.13 show the occurrence of tributyltin species in a substantial number of locations sampled. An interesting feature of Table 2.13 is the observation that the highest concentration of dibutyltin species 67.3 and 39.6 ng/g (wet wt as Sn) were found in the Blue mussels Mytilus edulis from Anyox shore, and Kitimat respectively. The highest concentration of tributyltin species (37.3 ng/g wet wt as Sn) was also found

Table 2.13 Organotin concentrations, spread and speciation in some marine locations of British Columbia.

Organism	Location and date of collection	Conc.(ng/g wet wt Sn)		
		$(C_4H_9)_2Sn^{2+}$	$(C_4H_9)_3Sn^+$	$(C_6H_{11})_2Sn^+$
Blue mussel <u>(Mytilus edulis)</u>	Marklane Point, Kitimat (1990)	39.6 ± 0.6	ND	ND
Soft shell Clam <u>(Mya arenaria)</u>	Dundas Island (1990)	ND	19.4 ± 0.7	ND
Shrimp <u>(Pandalus tridens)</u>	Holberg Sound (1991)	ND	ND	ND
Blue mussel <u>(Mytilus edulis)</u>	Wreck Beach, Vancouver (1989)	6.7 ± 0.1	14.4 ± 0.4	3.5 ± 0.1
Bentnose Clam <u>(Macoma nasuta)</u>	Alice Arm (1989)	ND	ND	ND

Table 2.13 continued on next page.

Table 2.13 continued.

Organism	Location & date of collection	(C ₄ H ₉) ₂ Sn ²⁺ (ng/g wet wt as Sn)	(C ₄ H ₉) ₃ Sn ⁺ (ng/g wet wt as Sn)	(C ₆ H ₁₁) ₂ Sn ⁺ (ng/g wet wt as Sn)
Bentnose Clam (<u>Macoma nasuta</u>)	Hilton Point, Kitimat. (1990)	ND	ND	ND
Soft shell Clam (<u>Mya arenaria</u>)	Hastings Arm (1990)	ND	ND	ND
Blue mussel (<u>Mytilus edulis</u>)	Anyox Shore (1990)	67.3 ± 8.6	37.3 ± 15.0	21.3 ± 0.1
Soft shell Clam (<u>Mya arenaria</u>)	Anyox Shore (1989)	1.9 ± 0.2	0.7 ± 0.2	ND
Basket Cockles (<u>Clinocardium nuttallii</u>)	Anyox Slag shore (1989)	ND	7.7 ± 2.8	ND

Table 2.13 contd.

California mussel	Quatsino	ND	9.2 ± 1.5	ND
(<u>Mytilus</u>	Sound			
<u>californianus</u>)	(1990)			

ND= Not detected

in the same Blue mussels from Anyox shore. Blue mussels from Wreck beach, Vancouver, also have moderately high concentrations of tributyltin species (14.4 ng/g wet wt as Sn) when compared to other organisms studied, except the Soft shell clam Mya arenaria from Dundas Island. There appeared to be a tendency for Blue mussels to accumulate relatively higher concentrations of organotin compounds than the other bivalve molluscs studied. The occurrence of dicyclohexyltin species is not widespread. Dicyclohexyltin species were found only in the Blue mussels from Wreck Beach, Vancouver, (Figure 2.13) and Anyox shore. Also interesting, is the absence of dicyclohexyltin species in clams and cockles from the same Anyox location. It seems possible that Blue mussels have greater ability to accumulate dicyclohexyltin compounds than the other bivalves studied. This may indicate the incapability of Blue mussels to effectively metabolize or excrete dicyclohexyltin compounds, thereby suggesting different metabolic pathways between blue mussels and other bivalves with regard to organotin metabolism. If this relation holds true, mussels may become good biological indicators for monitoring cyclohexyltin pollution. An examination of Fig

2.13(a), demonstrates the superiority of mass spectrometric detection over most non-specific detectors. With non-specific detectors, the dicyclohexyltin peak D, could have been discarded as baseline noise.

Apart from the present work, and an earlier report by Cullen *et al*¹¹⁷, no concentrations of dicyclohexyltin species have been reported for mussels in British Columbia. However, tricyclohexyltin concentration of 36 ng/g (dry wt as Sn) has been found for sediments from Esquimalt Harbour, British Columbia¹⁷⁰. Recently, cyclohexyltin species have been reported for environmental samples from St John's harbour, New Foundland, Canada¹⁷¹ and Spain¹⁷². Other butyltin concentrations in the range obtained in this study have been found by Garrett¹⁷³ (Table 2.14) for Blue mussels from Nanoose Bay and Wood Bay, British Columbia, Canada. Stallard *et al*¹²² have reported dibutyltin concentrations in the range 0.087 - 0.169 $\mu\text{g/g}$ (wet wt as dibutyltin cation) and tributyltin concentrations in the range 0.068 - 1.067 $\mu\text{g/g}$ (wet wt as tributyltin cation) for Blue mussels from San Diego bay, U.S.A. (Table 2.14).

Higashiyama *et al*¹⁷⁴ have also reported dibutyltin and tributyltin concentrations in the range 0.04-0.54 $\mu\text{g/g}$, and 0.02-0.24 $\mu\text{g/g}$ (wet wt as organotin cation) respectively for mussels from Tokyo bay, Japan (Table 2.14).

To afford a comparison of the British Columbian mussels with the reported organotin concentrations in Table 2.14, the organotin concentrations for mussels in this study were converted from ng/g (wet wt as Sn), to $\mu\text{g/g}$ (wet wt as organotin cation) in Table 2.15. A comparison of organotin data in Tables 2.14 and 2.15

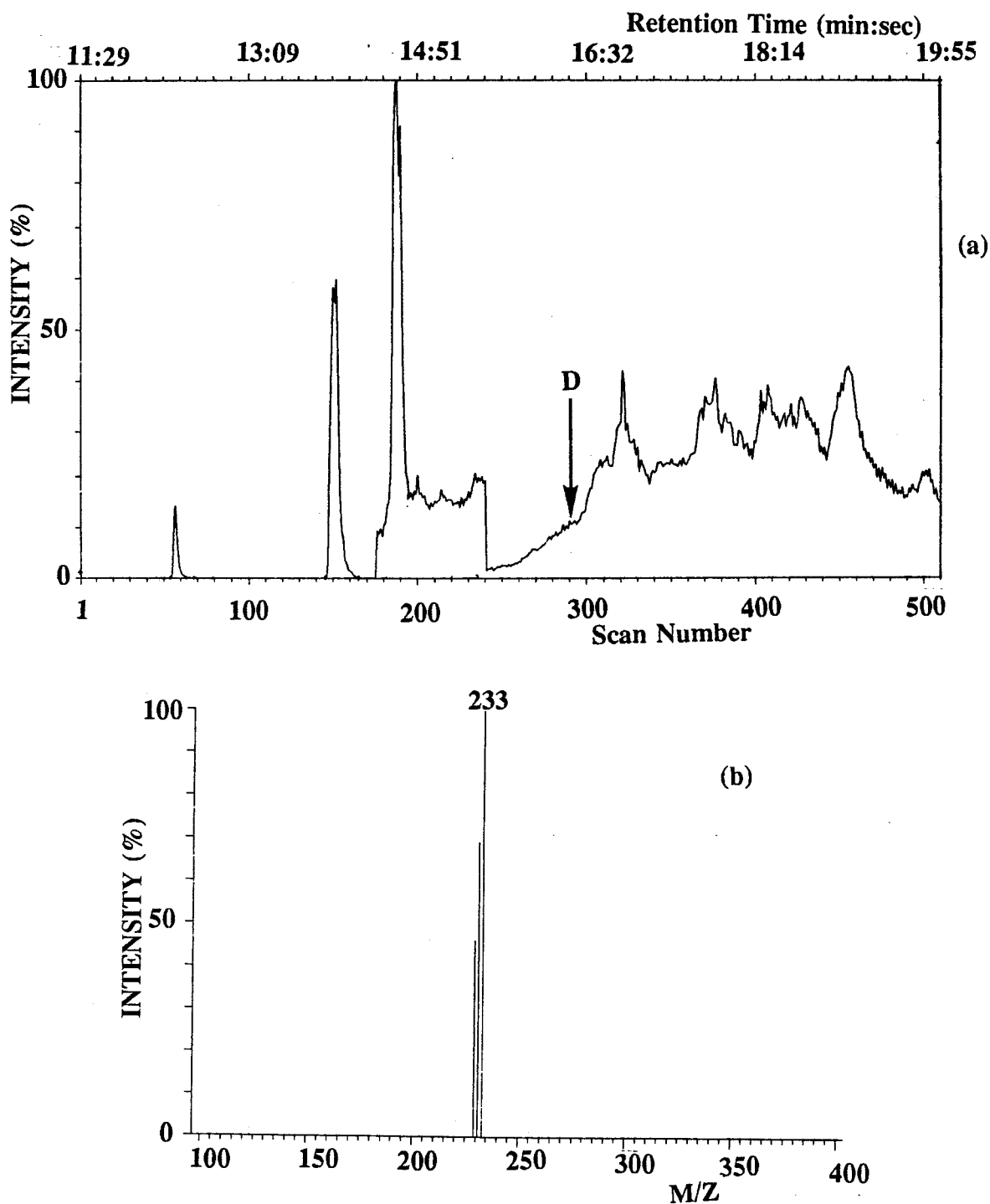


Figure 2.13 (a) Selected ion current chromatogram of extract from Blue mussel *Mytilus edulis* from Wreck Beach, Vancouver. (b) Mass spectra of peak D, revealing the presence of dicyclohexyltin species.

Table 2.14 Some organotin concentrations reported for the Blue mussels Mytilus edulis.

Location	$\mu\text{g/g}$ (wet wt as organotin cation)			Reference
	$(\text{C}_4\text{H}_9)_2\text{Sn}^{2+}$	$(\text{C}_4\text{H}_9)_3\text{Sn}^+$	$(\text{C}_4\text{H}_9)\text{Sn}^{3+}$	
U.S.A				
San Diego Bay	0.169 - 0.087	0.068 - 1.067	0.076 - 0.257	Stallard <u>et al</u> ¹²²
Japan				
Tokyo Bay	0.04 - 0.54	0.02 - 0.24	0.02 - 0.12	Higashiyama <u>et al</u> ¹⁷⁴
Canada				
Nanose Bay	0.002	0.007	0.003	Garret ¹⁷³
Wood Bay	0.02	0.037	0.003	Garret ¹⁷³

indicates that the concentration of tributyltin species found in Anyox, British Columbia is in the range reported by both Stallard et al¹²² and Higashiyama et al¹⁷⁴ for San Diego Bay, U.S.A and Tokyo Bay, Japan respectively. The level of tributyltin species present in Anyox British Columbia is higher than the levels in both Nanose Bay, and Wood Bay British Columbia respectively. The occurrence of dibutyltin

species in Blue mussels from Marklane point, Kitimat and Wreck Beach, Vancouver without a corresponding occurrence of the tributyltin species (Table 2.15) is surprising, and may indicate that for Blue mussels, the excretion of dibutyltin species

Table 2.15 Organotin concentrations in the Blue mussel *Mytilus edulis* converted to $\mu\text{g/g}$ wet wt as organotin cation.

Organism and (Location)	$\mu\text{g/g}$ Wet wt. (as Organotin cation)		
	$(\text{C}_4\text{H}_9)_2\text{Sn}^{2+}$	$(\text{C}_4\text{H}_9)_3\text{Sn}^+$	$(\text{C}_6\text{H}_{11})_2\text{Sn}^+$
Blue mussel (Marklane Point, Kitimat)	0.08	ND	ND
Blue mussel (Wreck beach, Vancouver)	0.01	0.04	0.01
Blue mussel (Anyox shore)	0.13	0.09	0.05

is slower than that of tributyltin species. For soft shell clams, the opposite trend was observed because dibutyltin species were generally not detected (Section 2.4.10, Table 2.18).

2.4.9 Organotin concentrations in various organisms from the same locations.

Marine animals from the same locations were sampled for the presence of organotin compounds with a view to finding their distribution among organisms. The

Table 2.16 Organotin distribution in marine animals from Camano Sound, British Columbia.

Organism	Year of collection	Conc. (ng/g as Sn wet wt)		
		$(C_4H_9)_2Sn^{2+}$	$(C_4H_9)_3Sn^+$	$(C_6H_{11})_2Sn^+$
Butter clam (<u>Saxidomus giganteus</u>)	1989	ND	ND	ND
Basket cockle (<u>Clinocardium nuttallii</u>)	1989	ND	ND	ND
Soft shell clam (<u>Mya arenaria</u>)	1989	ND	7.0 ± 2.6^a	ND

a= Standard error for two determinations, of two replicate injections each.

ND= Not detected.

organotin distribution in organisms from Camano Sound and Tasu Sound is shown in Tables 2.16 and 2.17 respectively. In Camano Sound, no dibutyltin or dicyclohexyltin compounds were detected in the three animals sampled. Only the Soft shell clam Mya arenaria showed the presence of tributyltin species (Table 2.16). The occurrence of tributyltin species in the Soft shell clam, without a corresponding occurrence in the butter clam is surprising, and may indicate different mechanisms of tributyltin detoxification even in different species of the same animal. Of the two animals from Tasu Sound (Table 2.17), the little neck clam showed a much higher concentration of tributyltin species than the Blue mussel. Unfortunately, little neck clams from other locations were not available to study this trend further.

Table 2.17 Organotin distribution in marine animals from Tasu Sound, British Columbia.

	Conc. ng/g as		
	Sn (wet wt.)		
	$(C_4H_9)_2Sn^{2+}$	$(C_4H_9)_3Sn^+$	$(C_6H_{11})_2Sn^{2+}$
Blue mussel	ND	13.2 ± 3.1	ND
<u>(Mya arenaria)</u>			
Native littleneck clam	ND	177.0 ± 11.9	ND
<u>(Protothaca staminea)</u>			

2.4.10 Distribution of organotin compounds in marine animals studied over a period of three years.

The concentration and speciation of organotin compounds in Soft shell clams from Quatsino Sound, British Columbia were monitored for over a period of three years (Table 2.18). An examination of the data in Table 2.18 indicates a very

Table 2.18 Organotin body burden for Soft shell clams *Mya arenaria* from Quatsino Sound, British Columbia studied over a period of three years.

Year of collection	ng/g Sn (wet wt)		
	(\pm) ^a		
	(C ₄ H ₉) ₂ Sn ²⁺	(C ₄ H ₉) ₃ Sn ⁺	(C ₆ H ₁₁) ₂ Sn ²⁺
1989	ND	26.3 \pm 0.6	ND
1990	ND	12.8 \pm 0.4	ND
1991	ND	5.5 \pm 1.8 ^b	ND

a=Standard error for two replicate injections.

b=Standard error for two separate determinations

significant decrease in the concentrations of tributyltin species with time. Such a very significant decrease in tributyltin concentration could only be possible if the input source of tributyltin compounds in this location is decreasing with time. According

to Maguire¹⁵⁵, in 1989 the Canadian Government regulated tributyltin compounds under the Pest Control Products Act (Canada Department of Agriculture 1989). Under this regulation, the permitted daily release rate of tributyltin species is $4\mu\text{g}$ per square centimetre of hull surface. This regulation also prohibits the use of antifouling paints containing tributyltin compounds on vessels less than 25 metres in length. As surmised by Maguire¹⁵⁵, these regulations should minimize the environmental impact of antifouling uses of tributyltin compounds in Canada. The decreasing concentration of tributyltin species with time as shown in Table 2.18 may represent the impact of the Government's regulation on the input of tributyltin compounds into the marine environment. An important trend that is observable from Table 2.18 is the absence of dibutyltin species in the clams. Usually dibutyltin species should co-exist with tributyltin species in organisms because dibutyltin species are metabolites of tributyltin compounds in animals. This trend may indicate that Soft shell clams generally do not metabolize tributyltin species or that dibutyltin species are very quickly excreted from the clams. This observation is in contrast to the trend found for blue mussels (Table 2.15), where all the Blue mussels analyzed contained dibutyltin species. This observation points to different detoxification mechanisms for soft shell clams and blue mussels.

The occurrence of organotin species in some remote British Columbian locations such as Anyox, Hastings Arm, Alice Arm, and Tasu Sound is surprising because of the very low boating and agricultural activity in these locations: perhaps, aerial transport of these compounds needs to be considered.

CHAPTER 3

EFFECT OF TRIBUTYLTIN CHLORIDE, MONOBUTYLTIN TRICHLORIDE AND TRIMETHYLTIN HYDROXIDE ON THE PERMEABILITY OF EGG PHOSPHATIDYLCHOLINE LIPOSOMES.

3.1 INTRODUCTION

This chapter describes the effect of some organotin compounds namely tributyltin chloride, monobutyltin trichloride, and trimethyltin hydroxide on model biological membranes formed by the hydration of egg phosphatidylcholine (EPC) or a mixture of organotin compound and EPC in tris buffer to form liposomes, also known as vesicles. The experiment was originally designed to study the permeation of these organotin compounds through these liposomes. However at the high concentrations of tributyltin chloride and monobutyltin trichloride needed inside the liposomes for their ^1H NMR signals to be observed, the liposomes do not form. Therefore, the approach adopted was to use a molecular probe which is capable of easy permeation through the liposomes, to monitor the effects of low concentrations of organotin compounds on the permeability of these model biological membranes. The compound chosen as a probe was dimethylarsinic acid (DMA). The reasons for choosing DMA as a probe molecule are given below in Section 3.2. In an earlier study by Tosteson and Weith¹⁵⁶ the probe ions tetraphenylboron, and tetraphenylarsonium were used to study the effect of tributyltin chloride on the membrane potential of a phosphatidylethanolamine planar lipid bilayer. A decrease

of about 70 mV in the intrinsic dipole potential of the planar lipid bilayer caused by tributyltin chloride was observed by Tosteson and Weith¹⁵⁶.

The experimental technique employed in the present study was NMR spectroscopy. NMR spectroscopy is well suited for the study of solute or molecular permeation through liposomal membranes, provided the NMR signals of the solute inside and outside the liposomes can be differentiated from each other. The differentiation of the outside and inside NMR signals is usually achieved by the use of spectroscopic shift reagents; these reagents are usually first row transition metal complexes and complexes of the lanthanide elements¹⁷⁵, and are usually added to the sample prior to the NMR experiment. By using NMR spectroscopy the permeation of molecules or solutes can be followed to equilibrium without the intermittent withdrawal of samples from the reaction system. In addition, the technique is capable of providing information on the state of the liposomes, particularly liposome lysis during the experiment, because the NMR signal inside and outside the liposome would collapse into a single peak if the liposome disintegrates or bursts.

3.2 DIMETHYLARSINIC ACID (DMA) AS A PROBE FOR STUDYING THE EFFECT OF ORGANOTIN COMPOUNDS ON THE MEMBRANES OF LIPOSOMES.

The permeation of dimethylarsinic acid (DMA) through EPC liposomes has been studied by Herring *et al*¹⁷⁶. DMA has the following properties which make it suitable as a probe molecule for further studies:

- (i) DMA permeates across EPC liposomes by passive diffusion
- (ii) DMA has good aqueous solubility which enables high concentrations to be trapped in the small aqueous volumes of the liposomes. This in turn makes it easy to observe the NMR signals of DMA in the liposomes. Butyltin compounds do not possess high enough aqueous solubility to enable the NMR signals of trapped butyltin compounds to be detected.
- (iii) The rate of efflux of DMA from EPC liposomes is slow enough to permit its study by NMR spectrometry.
- (iv) The methyl hydrogen atoms of DMA give rise to a simple NMR spectra (singlet) which can be shifted by using spectroscopic shift reagents.

3.3 LIPOSOMES AS MODELS FOR BIOLOGICAL MEMBRANES.

Biological membranes are made up of two major components, phospholipids and proteins¹⁷⁷, and other components such as oligosacchrides¹⁷⁸. The major barrier to membrane permeability is provided by the phospholipid bilayer. The proteins are inserted into the phospholipids which are oriented in the bilayer. An important property of the phospholipids is the possession of hydrophilic and hydrophobic ends (Figure 3.1). When hydrated in aqueous solutions, most phospholipids form closed structures called vesicles or liposomes which possess internal aqueous volumes (intraliposomal compartment) which can be used to trap many compounds (Figure 3.2). The permeability properties of the liposomes are similar to those of biological membranes¹⁷⁹. The advantage of using liposomes over biological membranes for

permeability studies is that experimental results are easier to interpret because proteins and oligosacchrides, which might otherwise complicate permeation processes

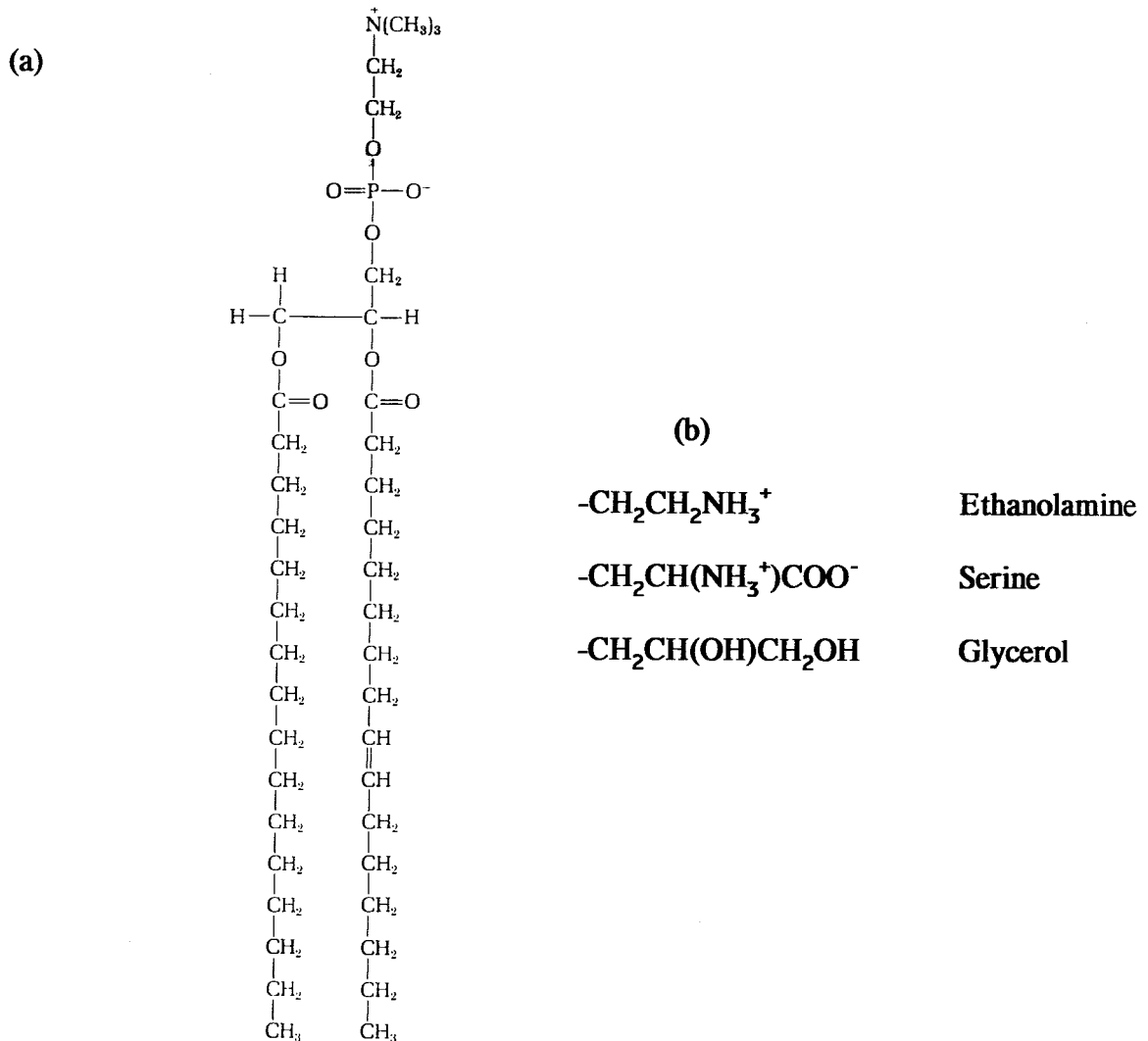


Figure 3.1 (a) Structure of a phospholipid (phosphatidylcholine) and (b) other commonly occurring head groups on the phospholipid.

are absent. Also, the liposomes can easily be prepared in a controlled and reproducible manner.

3.4 TYPES OF LIPOSOMES AND METHODS OF PREPARATION.

Various methods for the preparation of liposomes are available. These methods of preparation have been a subject of reviews by Hope *et al*¹⁸⁰, and Szoka

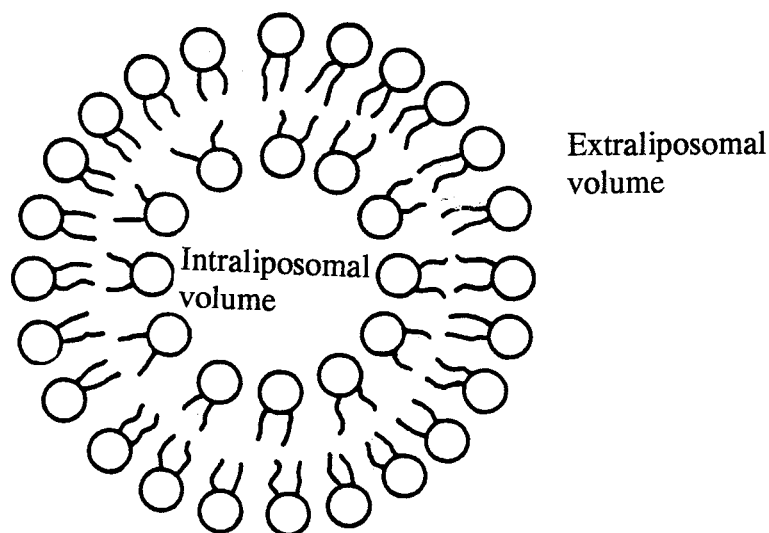


Figure 3.2 Liposome, showing the intraliposomal compartment/volume where molecules of a permeant can be encapsulated.

and Papahadjopoulos¹⁸¹. Three types of liposomes namely multilamellar vesicles (MLVs), small unilamellar vesicles (SUVs), and large unilamellar vesicles (LUVs) have been popularly used and the methods available for the preparation of these

vesicles are given below.

3.4.1 Multilamellar vesicles (MLVs).

Bangham prepared the first vesicles (MLVs)¹⁸² in 1965. His method involved a gentle dispersion of a lipid in buffer. The vesicles that formed were heterogenous in size, and aqueous volumes of the different lamellae were later reported by Gruner *et al*¹⁸³ to be depleted in solutes relative to the buffer in which they are made, and as such, are under osmotic compression. MLVs having uniform solute distribution in the lamellae can be prepared by the methods reported by Gruner *et al*¹⁸³ and Mayer *et al*¹⁸⁴. The methods involve the evaporation of ether from an ether-buffer-lipid mixture, followed by resuspension of the sonicated emulsion in buffer¹⁸³ or the repeated freezing and thawing of the lipid-buffer preparation¹⁸⁴. Another method of MLV formation reported by Kirby and Gregoriadis¹⁸⁵, involved the dehydration of lipids from an aqueous solution by using either freeze-drying or direct vacuum evaporation, followed by controlled rehydration. The major draw back in the use of MLVs for permeation studies is the presence of multilamellae, and the size inhomogeneity of the liposomes.

3.4.2 Small unilamellar vesicles (SUVs).

Early methods employed for the preparation of SUVs were based on the sonication of multilamellar vesicles. According to Johnson¹⁸⁶, the size of the SUVs is dependent on the lipid composition, with the vesicle diameter varying from 204 Å

for egg phosphatidylcholine (EPC) vesicles to 362 Å for EPC vesicles containing 50% cholesterol. Preparation of SUVs can also be accomplished by the French press method of Barenholtz¹⁸⁷. The very small trapped volumes of the SUVs (< 0.2 μL per μmol phospholipid) and vesicle instability are the major draw back to their use in permeation studies.

3.4.3 Large unilamellar vesicles (LUVs).

Large unilamellar vesicles (LUVs) are the liposomes of choice for most permeation experiments, and were the liposomes used in the present study because of their unilamellarity and large trapped volumes. The LUVs can be prepared by the ethanol injection method of Kremer *et al*¹⁸⁸, the reverse phase evaporation method of Szoka and Papahadjopoulos¹⁸⁹, the ether injection method of Deamer and Bangham¹⁹⁰, the detergent dialysis method of Madden¹⁹¹, and the rapid extrusion method of Olson *et al*¹⁹², Hope *et al*¹⁹³ and Meyer *et al*¹⁸⁴.

The ethanol injection, ether injection, and the reverse phase evaporation methods involve the dispersion of lipids in an appropriate organic solvent, and the subsequent injection into a buffer. The organic phase is evaporated off at the time of hydration for the ether injection method, removed under reduced pressure for the reverse phase evaporation method, or is diluted into the buffer for the ethanol injection method. An additional step involving gel permeation chromatography is usually employed to remove organic solvents. The detergent dialysis method involves the detergent induced solubilization of the lipid into micelles and the subsequent

removal of the detergent by dialysis. These methods described above are tedious, and usually entrap residual organic solvents or detergents. The presence of residual solvents in the LUVs is not desirable because it may change the properties of the liposomes.

The entrapment of residual organic solvents can be avoided by rapidly extruding MLVs under low pressure, as reported by Olson *et al*¹⁹². These authors also reported that reverse phase vesicles exhibit greater size homogeneity after low pressure extrusion through a polycarbonate filter. The use of moderate pressure extrusion to produce defined pore sized, unilamellar vesicles from multilamellar vesicles has been reported by Hope *et al*¹⁹³ and Meyer *et al*¹⁸⁴.

3.5 TRANSPORT PROCESSES IN MEMBRANES.

Solute or ionic transport across biological membranes can be described in terms of the following:-

- (i) Simple or passive diffusion
- (ii) Facilitated diffusion
- (iii) Active transport

A brief description of these transport processes is given in the following sections:-

3.5.1 Simple or passive diffusion.

Passive diffusion occurs when a concentration gradient exists across a membrane. The movement of molecules through the membrane is due to thermal

molecular motion¹⁹⁴. The direction of transport is determined by the concentration gradient, and diffusion is in the direction of lower solute concentration, until concentration on each side of the membrane is equalized. Passive diffusion obeys Fick's first law:-

$$J = -D \frac{dC}{dX}$$

where J, is the flux (mol/cm²/s), D, is the diffusion coefficient (cm²/s) , dX is the membrane thickness, and dC/dX is the concentration gradient.

In general, the rate of diffusion is determined by the concentration difference across the membrane, the molecular size of the permeant, the viscosity and width of the membrane, and on temperature. In passive diffusion, it is assumed that lipophilic solutes penetrate the membrane by dissolving in the hydrophobic layer and then diffusing across the bilayer, while hydrophilic solutes pass through aqueous pores on the membrane. This assumption is based on the observation that the rate of permeation is non-saturable, and permeation is not inhibited competitively by analogous compounds of the permeant¹⁹⁵. A detailed description of passive diffusion has been given by Heinz¹⁹⁵.

3.5.2 Facilitated diffusion.

In facilitated diffusion, the transport of the permeant is aided by the presence of another molecule capable of acting as a carrier or capable of forming channels in

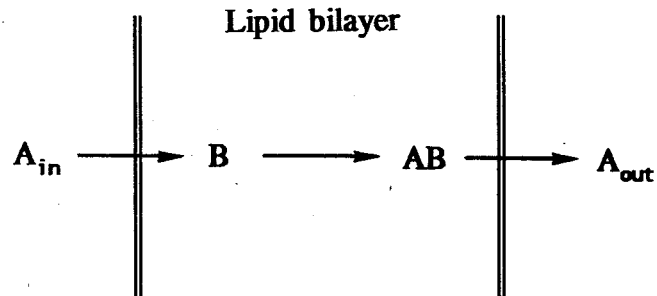
the membrane. The direction of transport is along the concentration gradient and Fick's first law is not obeyed¹⁹⁶. The mechanism of solute transport by facilitated diffusion is described in terms of the following models:-

3.5.2.1 Solute translocation through channels.

In this model, the permeant moves across the membrane via channels. Channels are transient pores formed in the membrane by ionophoric substances. The transient pores appear to oscillate between two conformational states. Channels show specificity, for different permeants, and the specificity shown is not related to the size of the permeant. Channels are subject to competitive inhibition.

3.5.2.2 Translocation through carriers.

The carrier model postulates that a carrier molecule binds specifically to the permeant molecule at one side of the membrane barrier, transports it through the barrier, releasing it at the other side. The carrier molecule is able to move freely within the bilayer without leaving it. In situations where the size of the carrier exceeds the thickness of the lipid bilayer (30-50 Å), it has been suggested that the whole carrier molecule does not move but only a loose chain or part of the carrier swings from one side of the membrane to the other, releasing the bound permeant¹⁹⁵. A detailed description of facilitated diffusion has been presented by Hofer¹⁹⁴, Heinz¹⁹⁵, and Stein¹⁹⁷. A schematic diagram of the various steps involved in facilitated diffusion is shown in Figure 3.3.



A is the permeant

B is the carrier molecule

AB is the carrier-permeant complex

Figure 3.3 Schematic diagram of facilitated diffusion (efflux) mediated by a carrier.

3.5.3 Active transport.

In active transport, a permeant is moved across the membrane by a carrier molecule usually a protein against the permeant's electrochemical potential gradient. The energy required for this process is provided by ATP hydrolysis, or electron flow connected with some redox reactions in the cell¹⁹⁶. A detailed description of active transport has been given by Hofer¹⁹⁴, and Stein¹⁹⁷.

3.6 SOLUTE TRANSPORT ACROSS LIPOSOMAL MEMBRANES.

3.6.1 Transport of solutes across membranes.

When there is a difference in the electrochemical potential of a solute on both sides of a membrane, there will be a net diffusion of molecules of that solute across the membrane. This situation is represented as follows:

$$\Delta \mu = \mu^{out} - \mu^{in} \neq 0$$

where μ the chemical potential of the solute is given by the following,

$$\mu = \mu^* + RT \ln a + ZF\epsilon\Psi + Vp$$

where a , is the activity of the solute, ϵ is the charge on the electron, p is the applied pressure, V is the volume of the solute, μ^* is the chemical potential of the solute in its standard state, Ψ is the electric potential, and F is the Faraday's constant. If the applied pressure and the electric potential are equivalent on both sides of the membrane, any observed chemical potential difference across the membrane is due to unequal activity of the solutes on either side of the membrane.

The net flux of a solute across a membrane has been described by Stein¹⁹⁷, and is given below:

$$J = -D \frac{\partial C}{\partial X} \approx -D \frac{\Delta C}{\Delta X}$$

where J (mol/s/cm²) is the flux, D (cm²/s) is the diffusion coefficient in the

membrane, and ΔX is the membrane thickness.

The ease of permeation through a membrane is described in terms of permeability coefficients. For non-ionic solutes, there is a strong correlation between the permeability coefficient P for the transport of the solute across a lipid bilayer and the hydrophobicity of the solute¹⁹⁸. This observation is known as Overton's rule.

A schematic diagram for the permeation of a non-ionic solute across a liposomal lipid membrane from the intraliposomal compartment to the extraliposomal compartment is shown in Figure 3.4. As the solute permeates, it also partitions between the lipid bilayer and the aqueous phase. An equation that relates the permeability of a solute to its partition coefficient has been derived by Jain¹⁹⁹, and is given below;

$$P = \frac{KD}{\Delta X}$$

where K is the partition coefficient of the solute in the bilayer (Figure 3.4), P (cm/s) is the permeability coefficient, ΔX (cm) is the membrane thickness and D (cm²/s) is the diffusion coefficient of the molecule in the membrane. The kinetics of this permeation process is described by the following rate constants:-

- (i) The rate constant for diffusion to the lipid bilayer k_1 .
- (ii) The rate constant for diffusion in the lipid bilayer k .
- (iii) The rate constant for diffusion away from the lipid bilayer k_2 .

The rate of diffusion in the bilayer is the slowest step and is therefore the rate determining step.

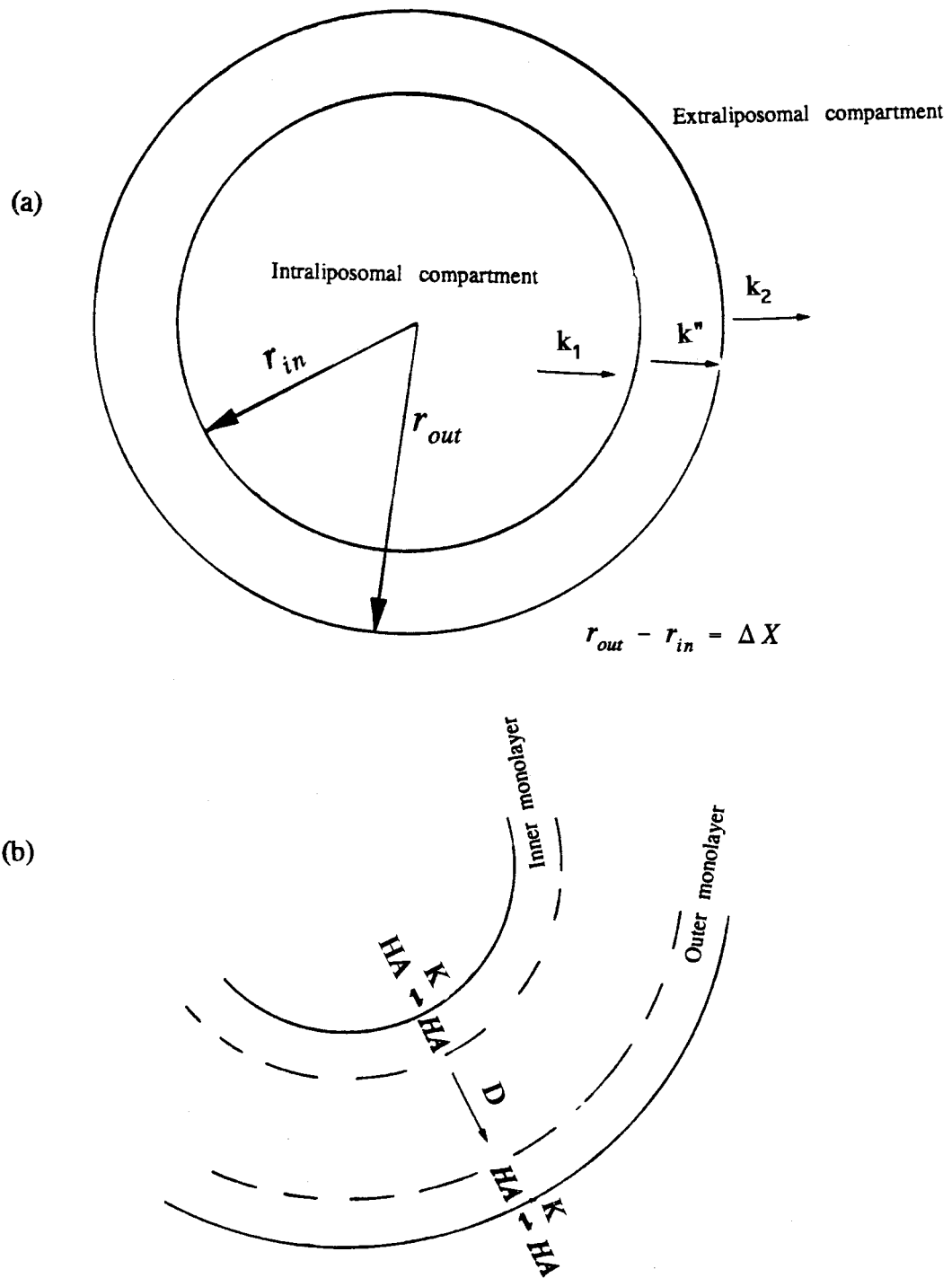


Figure 3.4 Passive diffusion of a permeant HA across a liposomal membrane showing:- (a) the various permeation rate constants and (b) partitioning of the permeant as it diffuses across.

The permeation of non ionic solutes is influenced by such factors as molecular size^{200,201}, and hydrogen bonding capability²⁰². Orbach and Finkelstein²⁰³ have suggested that the effect of molecular size and hydrogen bonding capability is less important than the hydrophobicity of the molecule.

3.6.2 Transport of ions.

In general, the flux of ions across lipid membranes is much lower than the flux of non ionic molecules. The permeability of water and ionic solutes across lipid membranes has been reviewed by Deamer and Bramhall¹⁷⁹.

Attempts to explain the low permeability of ions to lipid membranes were complicated by the observation that anions permeate lipid bilayers easier than cations. According to Hauser *et al*²⁰⁴, at pH 5.5 the first order rate constant for the escape of chloride ions from small unilamellar vesicles was three orders of magnitude higher than the rate constant for sodium ions. Many theories have been put forward to explain this difference in cation and anion permeabilities. According to Persegian²⁰⁵, the major energetic barrier to membrane transport of ionic solutes is the Born energy: defined as the energy of an ion in an environment with a given dielectric constant²⁰⁵.

Flewelling and Hubbel²⁰⁶ have proposed a mechanism to account for the permeability difference across lipid bilayers observed for cations and anions. According to them, the observed permeability differences could be accounted for if other contributions to the Born energy such as image energy, dipole energy, and

neutral energy are considered. Their energy model produced reasonable agreement between the observed and calculated thermodynamic parameters for the translocation of tetraphenylphosphonium cation and tetraphenylboron anion in a lipid bilayer. The image energy arises from the interaction between the charge of an ion in the lipid bilayer and the interfaces. The dipole energy arises from a two dimensional array of point dipole sources located at each membrane surface. This dipole source is believed to originate from the ester linkages of the fatty acid chain of the lipid bilayer. These dipoles give the interior of the bilayer a positive potential of several hundred millivolts. This has the effect of increasing the permeability of anions, and decreasing the permeability of cations. The neutral energy takes into account the non-electrical interactions between a permeant and the membranes. Such non-electrical interactions include hydrophobicity, and steric factors. However, the Born energy considerations are not able to explain the anomalously high permeability of protons and hydroxyl ions when compared to other small monovalent ions.

On the molecular mechanism of solute and ion transport, no general agreement has been reached. No one model has satisfactorily explained the permeation of ionic solutes. For lipophilic solutes, permeation is explained in terms of the solubility-diffusion model, whereby the solute is thought to dissolve in the non-polar region of the bilayer and cross the bilayer by simple diffusion. For hydrophilic solutes, permeation is usually explained in terms of diffusion through aqueous pores in the bilayer, or by permeation directly through the lipid bilayer via transient defects which occur in the bilayer as a result of thermal fluctuations.

3.7 PROPERTIES OF LIPOSOMES CAPABLE OF YIELDING INVESTIGATIVE INFORMATION.

The properties of liposomes that can be used to study the effect of other compounds on the lipid bilayer are its material properties such as permeability, partition coefficient, electrical properties, elastic properties and gel to liquid (L_b - L_d) transitions. The material properties of the lipid bilayer have been described by Gruner²⁰⁷. These material properties are a function of the vesicle composition, and as such, any interaction of a "foreign" compound such as an organotin compound with the vesicle would exert some effects on these properties. This has been found to be true experimentally. Tosteson and Weith¹⁵⁶ have determined that tributyltin chloride affects the internal potential of a phosphatidylethanolamine planar lipid membrane, lowering its dipolar potential by 70 mV.

In the present study, bilayer permeability was the material property of choice to be used for studying the effect of tributyltin chloride, monobutyltin trichloride and trimethyltin hydroxide on the permeability of egg phosphatidylcholine liposomes by using dimethylarsinic acid (DMA) as a permeability probe.

3.8 BUTYLTIN COMPOUNDS: THE NEED FOR THE PRESENT STUDY.

The pioneering work of Selwyn *et al*^{15,208} on the effect of the triorganotin compounds on membranes has shown that the organotin compounds (trimethyltin, triethyltin, tripropyltin, tributyltin and triphenyltin species) partition into the membranes of mitochondria, liposomes, erythrocytes, and chloroplasts, and mediate

chloride-hydroxide transport across the membrane. Motais et al¹⁷ found that tripropyltin chloride is able to act as carrier and mediate chloride-chloride and chloride-hydroxide exchanges in red blood cells.

Although the ability of the triorganotin cations to act as carriers for Cl^- and OH^- in the membrane has been established, the effect of the organotin compounds on the other properties of the membrane has received very little attention. Heywood et al²⁰⁹ have provided evidence that tributyltin cation associates with the phosphate head groups at the surface of liposomes. Such interactions are expected to modify the membrane properties of the liposomes. Alteration of membrane properties by tributyltin compounds is suspected to be responsible for the in vitro inhibition of intracellular Ca^{2+} mobilization reported by Arakawa et al¹⁵⁷.

Tosteson and Weith¹⁶ have reported that the tributyltin cation preferentially transports Cl^- over NO_3^- across a planar lipid bilayer. In the environment, the toxicity of other pollutants may be enhanced, if tributyltin cation preferentially mediates their diffusion across biomembranes.

Hence, the present study aims to investigate the effect of organotin compounds on the permeability of biomembranes, and any possible transport mediating ability of the organotin cation on a probe permeant; dimethylarsinic acid which is also an environmentally occurring compound.

3.9 THEORETICAL DESCRIPTION OF THE DIFFUSION EXPERIMENT APPLICABLE TO NMR SPECTROMETRY.

3.9.1 Passive diffusion

During the efflux experiments, as the DMA diffuses out of the vesicles, the intensity of the DMA peak inside the liposomes decreases, while the intensity of the DMA peak outside the liposomes increases. A mathematical description for the first order efflux of DMA from egg phosphatidylcholine liposomes by passive diffusion has been derived by Herring *et al*¹⁷⁶, and has also been given by Nelson²¹⁰. The mathematical equation describing the exponential decay of the DMA peak integral to equilibrium value is given below.

$$I_{in}^t = I_{in}^{eq} + (I_{in}^0 - I_{in}^{eq}) \exp\{- (1 + f)kt\} \quad [3.0]$$

I_{in}^t , I_{in}^{eq} , I_{in}^0 are the integrals of the DMA peak inside the liposome at time t , equilibrium, and zero time respectively. Zero time refers to time before spectral acquisition; f , is the volume ratio of the intraliposomal compartment to the extraliposomal compartment (i.e, $f = V_{in}/V_{out}$); k is the observed rate constant for DMA efflux from the liposome and t , is the efflux time in seconds.

3.9.2 Facilitated diffusion.

Another transport mechanism which was considered because some of the experimental data obtained in the present study did not fit equation [3.0], is

facilitated diffusion. In facilitated diffusion, the diffusing molecule enters into some form of reversible chemical association or complexation with a carrier molecule which transports it across the membrane.

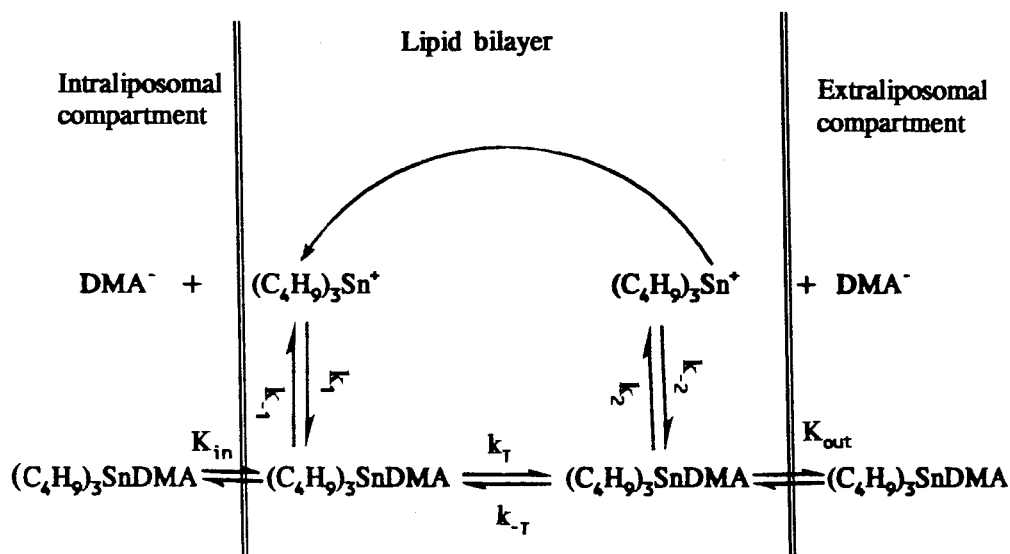
In solution at pH 7.4, the probe molecule dimethylarsinic acid (DMA) exists as two chemical species²¹⁰: the undissociated dimethylarsinic acid (DMAH), and the anionic species DMA^- . Both species are capable of passive diffusion in the membrane, but only DMA^- is likely to be transported by triorganotin cation during facilitated diffusion. Therefore, in this study, DMA refers to a mixture of DMAH and DMA^- present in solution.

A proposed schematic diagram of tributyltin cation acting as a carrier is shown in Figure 3.5. In this scheme, DMA^- diffuses into the lipid bilayer where it associates with the tributyltin cation to form a tributyltin-DMA complex which is mobile within the lipid bilayer. At the interface of the liposome and the extraliposomal compartment, the tributyltin-DMA complex dissociates to liberate the DMA^- into the extraliposomal compartment.

A theoretical treatment for facilitated diffusion based on Hxhe adsorption equilibria of Langmuir²¹¹ has been described by Widdas²¹² to account for the placental diffusion of glucose, and by Hall and Baker²¹³.

The theoretical treatment by Widdas²¹² is further developed below for trialkyltin cation mediated transport of DMA^- across a liposomal membrane.

- (a) DMA^- can associate with the tributyltin cation which is the carrier to form a tributyltin-DMA complex.



$k_1 = k_{-2}$ is the formation rate constant for $(C_4H_9)_3SnDMA$.

$k_{-1} = k_2$ is the dissociation rate constant for $(C_4H_9)_3SnDMA$.

$\phi = k_2/k_{-2}$ is the equilibrium dissociation constant for $(C_4H_9)_3SnDMA$.

$\beta = k_1/k_{-1}$ is the equilibrium formation constant for $(C_4H_9)_3SnDMA$.

β/ϕ is the ratio of equilibrium formation constant to equilibrium dissociation constant of the carrier-permeant complex.

K_{in} is the partition coefficient of the carrier-permeant complex in the interface between the intraliposomal compartment and the bilayer.

K_{out} is the partition coefficient of the carrier-permeant complex in the interface between the extraliposomal compartment and the bilayer.

k_+ and k_{-+} are the transfer rate constants of $(C_4H_9)_3SnDMA$ to the extraliposomal and intraliposomal compartments respectively.

Figure 3.5 Proposed mechanism of tributyltin mediated efflux of dimethylarsinate (DMA^-) from a liposome and the equilibria of the carrier-permeant interactions.

- (b) The tributyltin-DMA complex travels through the membrane and upon reaching the other surface dissociates and liberates the DMA⁻ into the adjacent medium. The free organotin cation returns to its original position may be, with a different anion in solution to start a new permeation cycle.
- (c) The carriers are in equilibrium with the substrate at the interfaces.
- (d) The carriers pass backwards and forwards across the liposomal membrane.
- (e) The rate of transfer of the carrier-substrate complex is much smaller than the rate of formation and dissociation of the complex, and is the rate limiting step.
- (f) The net rate of transfer is proportional to the difference in the fraction of saturated carriers on both liposomal membrane interfaces.

According to Langmuir²¹¹, the adsorption equilibrium at any interface can be expressed as:-

$$\theta = \frac{\beta C}{\beta C + \phi} = \frac{\frac{\beta}{\phi} C}{\frac{\beta}{\phi} C + 1} \quad [3.1]$$

where θ is the fraction of tributyltin saturated with DMA⁻. C , is the concentration of DMA⁻ in solution at the interface, ϕ is the dissociation constant of the carrier-permeant complex, and β is the formation constant of the carrier-permeant complex. According to Widdas²¹², equation [3.1] assumes the form of the expression of concentration of enzyme combined with substrate in Michaelis-Menten's equation²¹⁴ for enzyme kinetics (Appendix C). Therefore, Widdas²¹² considered ϕ , analogous to the Michaelis-Menten's constant. Also, Hall and Baker²¹³ considered the dissociation

constant of the carrier-permeant complex as a Michaelis-Menton's constant.

The rate of disappearance of the tributyltin-DMA complex at the interface between the lipid bilayer and the intraliposomal compartment (mi), is given by the expression:-

$$\frac{\partial n_{mi}}{\partial t} = -k_T \theta_{mi} + k_{-T} \theta_{mo} \quad [3.2]$$

where n_{mi} , refers to the number of moles of DMA⁻ in the interface between the bilayer and the intraliposomal compartment. θ_{mi} , and θ_{mo} refer to fraction of carriers saturated with DMA⁻ at the inside and outside interfaces of the liposome respectively, and k_T and k_{-T} are the transfer rate constants of the tributyltin-DMA complex towards the outside and inside interfaces of the liposome respectively.

Substituting equation [3.1] into equation [3.2], the rate of disappearance of the carrier-permeant complex at the inner interface (mi) becomes:-

$$\frac{\partial n_{mi}}{\partial t} = -k_T \left\{ \frac{\frac{\beta}{\phi} C_{mi}}{\frac{\beta}{\phi} C_{mi} + 1} \right\} + k_{-T} \left\{ \frac{\frac{\beta}{\phi} C_{mo}}{\frac{\beta}{\phi} C_{mo} + 1} \right\} \quad [3.3]$$

If the concentrations C_{mi} and C_{mo} are small such that $(\beta/\phi)C \ll 1$, equation [3.3] becomes :-

$$\frac{\partial n_{mi}}{\partial t} = \frac{\beta}{\phi} (-k_T C_{mi} + k_{-T} C_{mo}) \quad [3.4]$$

β/ϕ is the ratio of formation constant to dissociation constant for the tributyltin-

DMA complex.

Re-writing equation [3.4] in terms of moles of carrier-permeant complex:-

$$\frac{\partial n_{mi}}{\partial t} = \frac{\beta}{\phi} \left\{ -k_T \left(\frac{n_{mi}}{V_{mi}} \right) + k_{-T} \left(\frac{n_{mo}}{V_{mo}} \right) \right\} \quad [3.5]$$

where V_{mi} and V_{mo} refer to the volumes of the inner and outer interfaces of the liposomes respectively, n_{mi} and n_{mo} refer to the moles of carrier-permeant complex in the inner and outer interfaces respectively.

$$K_{in} = \frac{C_{mi}}{C_{in}} = \frac{n_{mi} V_{in}}{n_{in} V_{mi}} \quad [3.6]$$

Where K_{in} is the partition coefficient of the carrier-permeant complex in the inside interface between the liposome and the intraliposomal compartment.

Therefore,

$$n_{mi} = \frac{K_{in} V_{mi}}{V_{in}} n_{in} \quad [3.7]$$

Also,

$$K_{out} = \frac{C_{mo}}{C_{out}} = \frac{n_{mo} V_{out}}{n_{out} V_{mo}}$$

Therefore,

$$n_{mo} = \frac{K_{out} V_{mo}}{V_{out}} n_{out} \quad [3.8]$$

Substituting equation [3.7] and [3.8] into equation [3.5], and simplifying the resulting equation, the rate of disappearance of the carrier-permeant complex at the inner interface (rate of decrease of the DMA⁻ NMR signal inside the liposome) becomes:-

$$\frac{\partial n_{in}}{\partial t} = \frac{V_{in}}{K_{in} V_{mi}} \frac{\beta}{\phi} \left\{ -k_T K_{in} \frac{n_{in}}{V_{in}} + k_{-T} K_{out} \frac{n_{out}}{V_{out}} \right\} \quad [3.9]$$

If $k_T = k_{-T} = k$, $K_{in} = K_{out}$, and $V_{mi} \ll V_{in}$, equation [3.9] becomes:-

$$\frac{\partial n_{in}}{\partial t} = V_{in} k \frac{\beta}{\phi} \left\{ -\frac{n_{in}}{V_{in}} + \frac{n_{out}}{V_{out}} \right\} \quad [3.10]$$

N , the total number of moles of DMA⁻ in both the intraliposomal and extraliposomal volumes, and the outer and inner interfaces is given by the equation:-

$$N = n_{in} + n_{out} + n_{mi} + n_{mo}$$

But, n_{mi} and n_{mo} are very small when compared to n_{in} and n_{out} because of the very small volumes of the inner and outer liposomal interfaces. Therefore,

$$n_{out} = N - n_{in} \quad [3.11]$$

Substituting equation [3.11] into equation [3.10] and simplifying,

$$\frac{\partial n_{in}}{\partial t} - V_{in} k \frac{\beta}{\phi} \left\{ -\frac{n_{in}}{V_{in}} + \frac{(N - n_{in})}{V_{out}} \right\} \quad [3.12]$$

Simplifying equation [3.12],

$$\frac{\partial n_{in}}{\partial t} - V_{in} k \frac{\beta}{\phi} \left\{ -n_{in} \left(\frac{1}{V_{in}} + \frac{1}{V_{out}} \right) + \frac{N}{V_{out}} \right\} \quad [3.13]$$

Let,

$$V' = \frac{1}{V_{in}} + \frac{1}{V_{out}} \quad [3.14]$$

Substituting equation [3.14] into equation [3.13],

$$\frac{\partial n_{in}}{\partial t} - V_{in} k \frac{\beta}{\phi} \left(-n_{in} V' + \frac{N}{V_{out}} \right) \quad [3.15]$$

Re-arranging equation [3.15] and integrating,

$$\int_{n_{in}^0}^{n_{in}^t} \frac{\partial n_{in}}{\left(n_{in} V' - \frac{N}{V_{out}} \right)} - V_{in} k \frac{\beta}{\phi} \int_0^t \partial t \quad [3.16]$$

$$-\frac{1}{V'} \ln \left(n_{in} V' - \frac{N}{V_{out}} \right) \Big|_{n_{in}^0}^{n_{in}^t} - V_{in} k \frac{\beta}{\phi} t \quad [3.17]$$

$$\ln \left\{ \frac{n_{in}^t V' - \frac{N}{V_{out}}}{n_{in}^0 V' - \frac{N}{V_{out}}} \right\} = -V' V_{in} \frac{\beta}{\phi} kt \quad [3.18]$$

Re-arranging equation [3.18],

$$\frac{1}{n_{in}^0 V' - \frac{N}{V_{out}}} \left(n_{in}^t V' - \frac{N}{V_{out}} \right) = \exp - \left\{ V' V_{in} k \frac{\beta}{\phi} t \right\} \quad [3.19]$$

Let V' also be:-

$$V' = \frac{1+f}{V_{in}} \quad [3.20]$$

Where f is the volume ratio of the intraliposomal to the extraliposomal volumes

$$(f = V_{in}/V_{out})$$

Substituting equation [3.20] into equation [3.19] and re-arranging the resulting equation,

$$n_{in}^t \left(\frac{1+f}{V_{in}} \right) - \frac{N}{V_{out}} = \left(n_{in}^0 \left(\frac{1+f}{V_{in}} \right) - \frac{N}{V_{out}} \right) \exp - \left\{ \left(\frac{1+f}{V_{in}} \right) V_{in} k \frac{\beta}{\phi} t \right\} \quad [3.21]$$

At equilibrium,

$$t \rightarrow \infty, n_{in}^t = n_{in}^{eq}$$

$$\left(n_{in}^0 \left(\frac{1+f}{V_{in}} \right) - \frac{N}{V_{out}} \right) \exp - \left\{ \left(\frac{1+f}{V_{in}} \right) V_{in} k t \right\} \rightarrow 0 \quad [3.22]$$

Therefore the expression for N in equation [3.21] becomes,

$$N = n_{in}^{eq} \left(\frac{1+f}{V_{in}} \right) V_{out} \quad [3.23]$$

Substituting equation [3.23] into equation [3.21] and simplifying,

$$n_{in}^t - n_{in}^{eq} = (n_{in}^0 - n_{in}^{eq}) \exp - \left\{ (1+f) \frac{\beta}{\phi} kt \right\} \quad [3.24]$$

Re-arranging equation [3.24],

$$n_{in}^t = n_{in}^{eq} + (n_{in}^0 - n_{in}^{eq}) \exp - \left\{ (1+f) \frac{\beta}{\phi} kt \right\} \quad [3.25]$$

The peak area of the proton resonance in ^1H NMR is directly related to the number of particles, therefore equation [3.25] can be re-written in terms of the integral of the methyl resonance of the DMA $^-$:-

$$I_{in}^t = I_{in}^{eq} + (I_{in}^0 - I_{in}^{eq}) \exp - \left\{ (1+f) \frac{\beta}{\phi} kt \right\} \quad [3.26]$$

When there is no facilitated diffusion, there is no β or ϕ therefore, equation [3.26] reduces to equation [3.0] for passive diffusion previously derived by Herring et al¹⁷⁶. Equation [3.26] predicts the exponential decay of the DMA $^-$ resonance inside the liposome with time, and shows that facilitated diffusion is controlled by the ratio of the formation constant to the dissociation constant β/ϕ for the carrier-permeant complex.

3.10 EXPERIMENTAL

3.10.1 Instrumentation

3.10.1.1 Nuclear magnetic resonance spectrometry (NMR).

A Bruker AM400 NMR spectrometer was used to obtain all NMR spectra. NMR facilities were provided by Professor F.G. Herring. The spectrometer was operated in the water suppression mode. The 5mm NMR tubes used for all the experiments were obtained from Norell Inc., Landisville, New Jersey, U.S.A.. The operating parameters that were used for spectral acquisition and water suppression are given in Appendix B.

3.10.1.2 Lipid extruder and membrane filters.

The lipid extruder used to produce unilamellar vesicles (liposomes) was provided by Professor F.G. Herring, and was purchased from Lipex Biomembranes Inc., Vancouver, Canada. The 200 nm pore-sized polycarbonate filters used with the extruder were purchased from Costar Corporation, Cambridge, Massachusetts, U.S.A..

3.10.1.3 UV-Visible spectrophotometry.

A Shimadzu 600 spectrometer was used for all phosphorus assays. All measurements were taken at 815 nm.

3.10.2 Chemicals and reagents.

Tributyltin chloride was purchased from Ventron (Alfa Inorganics) Beverly, Massachusetts, U.S.A.. Monobutyltin trichloride and deuteriated 3-(trimethylsilyl) propionic acid sodium salt 2,2,3,3-d₄ (TSP) were procured from Aldrich Chemical Company, Milwaukee, U.S.A.. Dimethylarsinic acid (DMA) was obtained from Fisher Scientific Company, Fairlawn, New Jersey, U.S.A.. Tris(hydroxymethyl)aminomethane hydrochloride (tris buffer) and α -D(+)-glucose were purchased from Sigma Chemical Company, U.S.A.. Egg phosphatidylcholine (EPC) was procured from Avanti Polar Lipids, Birmingham, Alabama, U.S.A.. Solutions of the tris buffer were prepared by dissolving appropriate amounts in de-ionized water and adjusting the pH to 7.4 with sodium hydroxide. All solvents used for lipid extraction were Spectrograde. A stock solution of DMA (25 mg/mL) was prepared in tris buffer (300 mM), and its pH was adjusted to 7.4 with sodium hydroxide solution. The organotin compounds were freshly dissolved in tris buffer (40 mM), and their pH was adjusted to 7.4 with sodium hydroxide solution if necessary.

3.10.3 Preparation of large unilamellar vesicles (LUVs) from egg phosphatidylcholine (EPC) and the encapsulation of dimethylarsinic acid.

A stock solution of EPC was prepared by dissolving EPC (1 g) in chloroform (10 mL). This stock solution was stored in the freezer until needed. The stock solution (2 mL) was pipetted into a test-tube, and the solvent was evaporated off by using a gentle flow of nitrogen gas, and then the resulting paste was dried for 3

hours on a vacuum line. Multilamellar vesicles (MLVs) were then prepared by adding 300 mM tris buffer (1 mL) containing dimethylarsinic acid (25 mg/mL) at a pH of 7.4. The suspension was vortex mixed for 5 minutes, and then subjected to five freeze-thaw cycles, according to the method of Meyer *et al*¹⁸⁴. The sample was dipped in liquid nitrogen for about 2 minutes and thawed in a water bath (30 °C). The freeze-thawed vesicles were then forced by using pressure from a nitrogen tank (200-500 psi), to pass through two stacked 200 nm pore sized polycarbonate filters in an extruder, to afford large unilamellar vesicles (LUVs). The LUVs were divided into two portions of about 0.4 mL, to allow duplication of each DMA efflux experiment. For the DMA efflux experiments, the LUVs (0.4 mL) were applied onto a Sephadex G-50 gel permeation column (1.5 cm i.d x 4 cm), pre-equilibrated in tris buffer (40 mM, pH 7.4). Elution was achieved by the use of further 40 mM tris buffer (pH=7.4). Upon the application of the LUVs onto the gel permeation column, timing was initiated. Only about the first 1 mL of the eluted LUVs were collected. An aliquot of the eluted LUVs (400 μ L) was pipetted into the NMR tube which already contained the following: α -D(+)-glucose (28 mg), manganese sulfate (40 μ L of 30 mM), TSP (25 μ L of 40 mM), and tris buffer (135 μ L 40 mM, pH 7.4). The use of glucose was to control the osmotic pressure on the liposomes. The amount of glucose added was calculated to approximately balance the osmotic pressure acting on the liposomes.

The time course for the efflux of DMA from the EPC LUVs was followed by acquiring NMR spectra at appropriate time intervals, until equilibrium was reached.

The operating parameters that were used for spectral acquisition and water suppression are given in Appendix B.

The following experiments were performed on the liposomes in which DMA had been encapsulated:-

- (i) Efflux of encapsulated DMA from the liposome in the absence of any organotin compound.
- (ii) Efflux of encapsulated DMA from the liposome, with organotin compound (trimethyltin hydroxide or tributyltin chloride or monobutyltin trichloride) added in the extraliposomal compartment.

3.10.4 Preparation of butyltin-EPC LUVs and the encapsulation of DMA.

The stock EPC solution (2 mL) in chloroform was pipetted into a test tube. Also, aliquots of tributyltin chloride or monobutyltin trichloride (0.5, 1.5 or 5 $\mu\text{g}/\text{mL}$) in chloroform (1 mL) were pipetted into the same test-tube, and vortex mixed. The chloroform was evaporated off, and the butyltin-EPC mixture dried on a vacuum line for 3 hours. DMA (1 mL of 25 mg/mL solution) in tris buffer (300 mM, pH 7.4) was added to the dried butyltin-EPC mixture and vortex-mixed for about 5 minutes, to achieve the encapsulation of DMA in the butyltin-EPC multilamellar vesicles (MLVs) that were formed. The butyltin-EPC MLVs were forced to pass through two stacked 200 nm pore sized polycarbonate filters in the extruder, as described in Section 3.10.3 to produce large unilamellar vesicles (LUVs). The butyltin compounds possess highly hydrophobic butyl groups which

favour their incorporation into the lipid bilayer. However there will be some residual organotin compounds in the intraliposomal compartment. Butyltin-EPC liposomes of the following composition were prepared:-

- (a) 0.5 μ g tributyltin chloride : 0.2g EPC (TBT-EPC A)
- (b) 1.5 μ g tributyltin chloride : 0.2g EPC (TBT-EPC B)
- (c) 5.0 μ g tributyltin chloride : 0.2g EPC (TBT-EPC C)
- (d) 0.5 μ g monobutyltin trichloride : 0.2g EPC (MBT-EPC A)
- (e) 1.5 μ g monobutyltin trichloride : 0.2g EPC (MBT-EPC B)

The butyltin-EPC LUVs were divided into two portions of about 0.4 mL each, to permit the duplication of each DMA efflux experiment. A portion of the butyltin-EPC liposomes (0.4 mL) was added onto a Sephadex G-50 gel permeation column (1.5 cm i.d \times 3.0 cm) and eluted as described in Section 3.10.3. The first fraction (about 0.7 mL) of the eluted butyltin-EPC was collected. An aliquot of the eluted butyltin-EPC liposomes (400 μ L) was quickly pipetted into the NMR tube which already contained glucose (28 mg), aqueous manganese sulfate solution (40 μ L of 30 mM solution), TSP (25 μ L of 40 mM solution) and tris buffer (135 μ L of 40 mM solution, pH 7.4). When the presence of butyltin chloride was desired in the extraliposomal compartment, 135 μ L of 16.7 μ M solution in tris buffer of the same butyltin chloride used to form the liposome was added. The DMA efflux experiment monitored by using the NMR spectrometer was conducted, as described in section 3.10.3 above.

The following experiments were performed on the butyltin-EPC liposomes:-

- (i) Efflux of encapsulated DMA from the butyltin-EPC liposomes with no butyltin chloride added into the extraliposomal compartment.
- (ii) Efflux of DMA from the butyltin-EPC liposomes with tributyltin chloride or monobutyltin trichloride added into the extraliposomal compartment.

3.10.5 The NMR water suppression and spectral acquisition conditions for DMA efflux from EPC and butyltin-EPC liposomes.

The Bruker AM400 NMR spectrometer was operated in the water suppression mode, which made it possible to obtain the NMR spectra of samples prepared in aqueous buffers. The water signal suppression was achieved by applying a narrow presaturation pulse at the frequency of the water signal, followed by a broadband excitation pulse which was applied at the frequency of the DMA resonance, while the water signal was still saturated.

The time course for the efflux of DMA from the LUVs was followed by spectral acquisition at various time intervals. At each time interval, 48 scans were collected and averaged. The free induction decays were acquired by using a pulse width of 6 milliseconds, and Fourier transformed with a line broadening of 10 Hz. The spectrometer has variable temperature capability, which was used in some experiments.

The micro-program used to operate the NMR spectrometer in the water suppression mode with automated spectral acquisition is given in Appendix B.

3.10.6 Determination of phospholipid concentrations by phosphorus assay.

3.10.6.1 Extraction of phospholipid from liposomes prior to phosphorus determination.

Prior to determining the phosphorus concentration of the liposomes, the phospholipid (EPC) was separated from DMA by extraction into chloroform because arsenic interferes with the subsequent phosphorus determination.

The extraction was carried out according to the following procedure. The LUVs (0.5 mL) were diluted to 1 mL with deionized water. Methanol (2.2 mL) and chloroform (1 mL) were added to the vesicles, and the mixture was vortex-mixed. Deionized water (1 mL) and chloroform (1 mL) were further added into the mixture, causing it to separate into two phases. The top phase contained methanol, water, and DMA. The bottom phase contained chloroform and the lipid.

3.10.6.2 Lipid concentration determination.

Lipid concentrations of the vesicles were then determined by analyzing their phosphorus content as previously described by Fiske and Subbarow²¹⁵, and Bottcher *et al*²¹⁶. Lipid phosphorus was converted to phosphomolybdic acid which was subsequently reduced by the Fiske-Subbarow reagent to a blue compound which can be measured colorimetrically. The procedure is as follows. Aliquots (25 μ L) of the chloroform extract of the vesicles were dispensed into test tubes and the chloroform was gently evaporated off with a stream of nitrogen gas. Perchloric acid (7.25 mL)

was placed into each of the test tubes which was then covered with a marble ball, and placed in a metal test tube-holding block which was heated (180°C - 200°C, 1.5 hours). The test tubes were cooled, and 7.0 mL ammonium molybdate reagent (0.22 % w/v ammonium molybdate in 2% H₂SO₄ w/v) and 0.6 mL Fiske-Subbarow reagent (30g NaHSO₃, 1g Na₂SO₃ and 0.5g bis 1-amino-2-naphthol-4-sulphonic acid in 200 mL water) were added into each of the test tubes. The contents of each test tube were vortex-mixed, heated for 15 minutes in a boiling water bath, cooled, and their absorbances measured at 815 nm. The samples were standardized against known concentrations of NaH₂PO₄ which had undergone similar chemical treatment as the samples. Each assay was carried out in duplicate, and the average phosphorus concentration determined. The phospholipid concentration was then calculated from the relationship that 1 mole of EPC contains 1 mole of phosphorus.

3.10.7 Processing of the NMR spectra.

For each experiment involving the efflux of encapsulated DMA from the liposomes, 25-30 data points collected over 11-17 hours were processed. Each data point, represents an average of 48 scans. The accumulated free induction decays (FID) were Fourier transformed with a line broadening of 10 Hz to produce the NMR spectra (Figure 3.6). In Figure 3.6, peak A (sharp singlet) is assigned to the DMA inside the liposome. Peak B (broad singlet) is assigned to DMA that has diffused out of the liposomes: the peak has been broadened and shifted by the manganese sulfate, a spectroscopic shift/broadening reagent added to the NMR tube

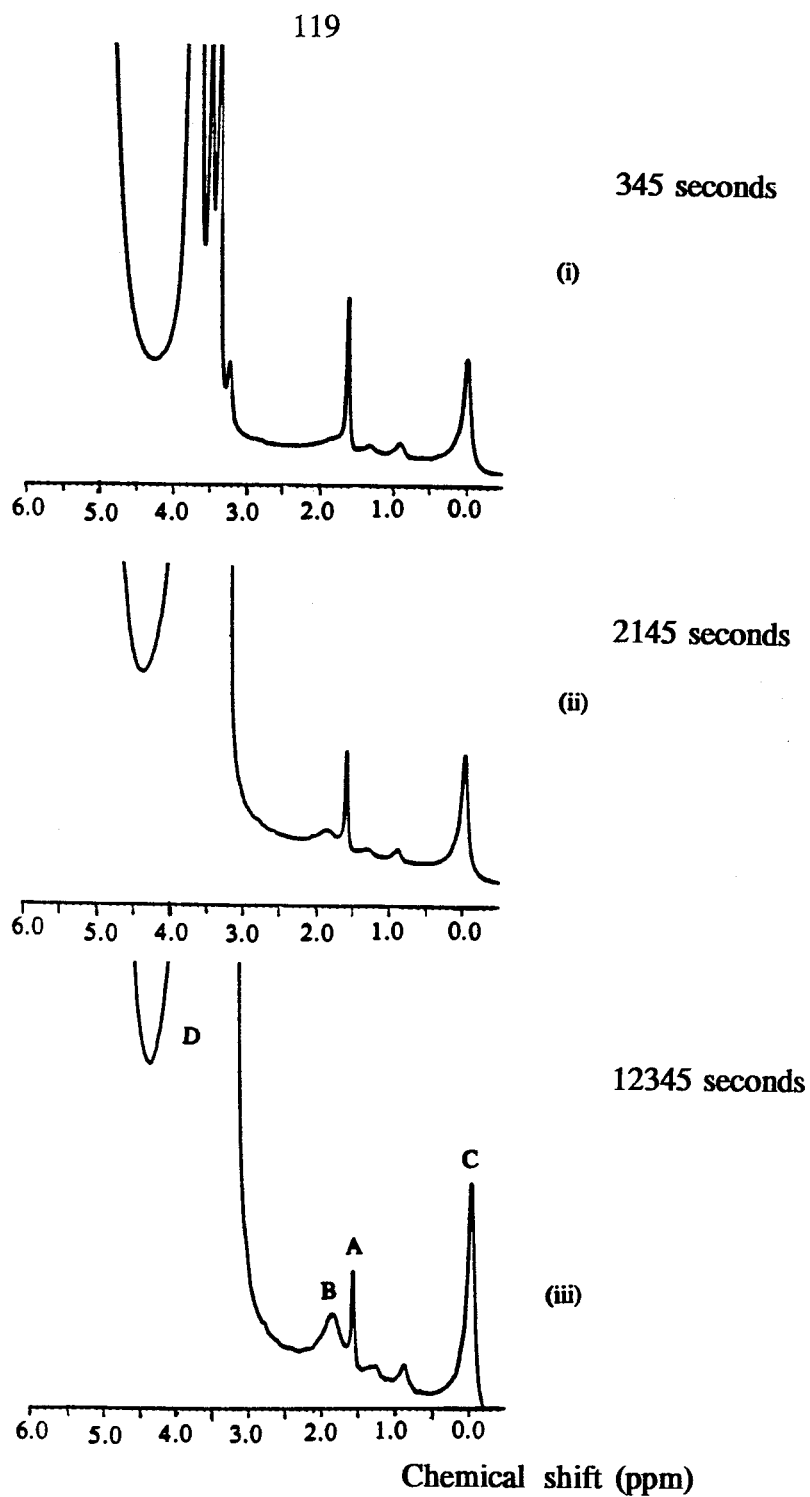


Figure 3.6 ^1H NMR spectra of DMA as it diffuses out of EPC liposomes. Peaks A and B are due to DMA inside and outside the liposomes respectively. Peak D is due to tris buffer. All peaks are referenced to TSP (peak C).

contents at the beginning of the experiment. Peak D ($\delta=2.4-4.5$) is assigned to tris buffer. All peaks were referenced to TSP (peak C). As the experiment progresses, the peak due to the DMA inside the liposome decreases while the peak due to the DMA outside the liposome increases (Figure 3.6, i, ii, iii). Either of the peaks can be used to monitor DMA efflux from the liposomes. However, it was convenient to monitor the decrease of the peak due to DMA remaining in the liposome because the peak area was easier to obtain by integration. The peak due to tris buffer was used as an internal standard to nullify the effects of fluctuations in the instrument's operating parameters. The peak area ratios of DMA inside the liposome to the tris buffer were calculated and plotted as a function of time to describe the efflux behaviour of the DMA molecules.

Each data point is a combined signal from the methyl resonance of the two species of DMA namely; DMAH and DMA⁻ present in solution.

3.10.8 Analysis and treatment of data.

3.10.8.1 Determination of rate constants and mode of permeation.

The experimental data for every efflux of DMA from EPC or butyltin chloride-EPC liposomes were analyzed for passive or facilitated diffusion by using equations [3.0] or [3.26] respectively.

$$I_{in}^t = I_{in}^{eq} + (I_{in}^0 - I_{in}^{eq}) \exp\{- (1 + f)kt\}$$

[3.0]

$$I_{in}^t = I_{in}^{eq} + (I_{in}^0 - I_{in}^{eq}) \exp - \left\{ (1 + f) \frac{\beta}{\phi} kt \right\} \quad [3.26]$$

A plot of $\ln(I_{in}^t - I_{in}^{eq})$ versus time gives a straight line with slope $-(1+f)k$ (Figure 3.7) for passive diffusion, or $-(1+f)(\beta/\phi)k$ for facilitated diffusion, where f is the ratio of the internal volume to the external volume. At equilibrium, the ratio of the peak integrals of the DMA signal inside the liposome to the signal outside the liposome corresponds to f . Therefore,

$$f = \frac{V_{in}}{V_{out}} = \frac{I_{in}^{eq}}{I_{out}^{eq}} \quad [3.27]$$

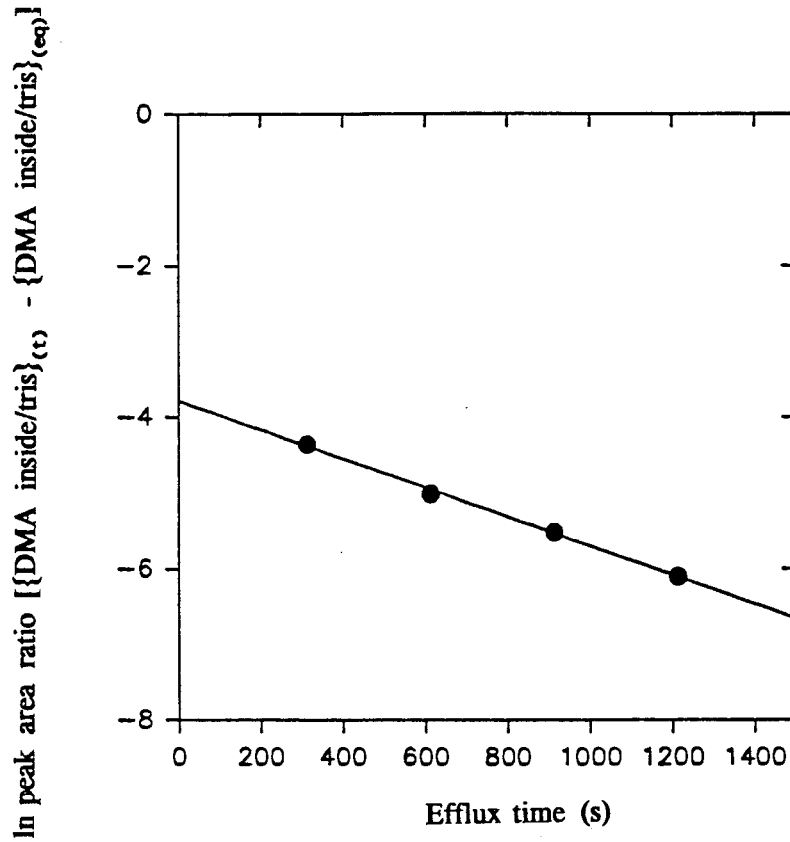


Figure 3.7 Log plot for the efflux of DMA from EPC liposomes.

where I_{in}^{eq} and I_{out}^{eq} are the peak integrals (area) due to DMA inside and outside the liposomes at equilibrium respectively, β/ϕ is the ratio of the formation constant to the dissociation constant of the carrier-permeant complex (see Figure 3.5). A method for estimating the ratio β/ϕ , and k is described in Section 3.11.1. The total volume of reagents in the NMR tube for each experiment was 0.6 mL.

Therefore,

$$V_{in} + V_{out} = 0.6 \text{ mL} \quad [3.28]$$

A combination of equations [3.27] and [3.28] allows V_{in} and V_{out} to be calculated. Hence f in equation [3.27] is determined, and k is calculated.

From a plot of equation [3.0], the intercept $\ln(I_{in}^o - I_{in}^{eq})$ is obtained. I_{in}^{eq} is estimated from the peak integral of DMA inside the liposome at equilibrium. Then, I_{in}^o is calculated. Equation [3.0] was fitted onto the experimental data points by an iterative procedure until convergence was obtained. This was done by using a commercially available mathematical software Sigmaplot 5.0 (Jandel Scientific). The calculated values of I_{in}^{eq} , f , and k were kept constant while I_{in}^o was permitted to vary by about ± 0.005 units about the calculated value. A good fit of equation [3.0] onto the experimental data points indicates efflux by passive diffusion, provided the magnitude of the efflux rate constants is in the range expected for passive diffusion. This provision is necessary because in some situations (discussed in Section 3.11.1), equation [3.0] can also fit data for facilitated diffusion.

If the experimental data points did not fit equation [3.0], they were analyzed for facilitated diffusion by using equation [3.26].

At a pH of 7.4, which was the case for all experiments described in this chapter, Herring *et al*¹⁷⁶ have determined that the major species of DMA

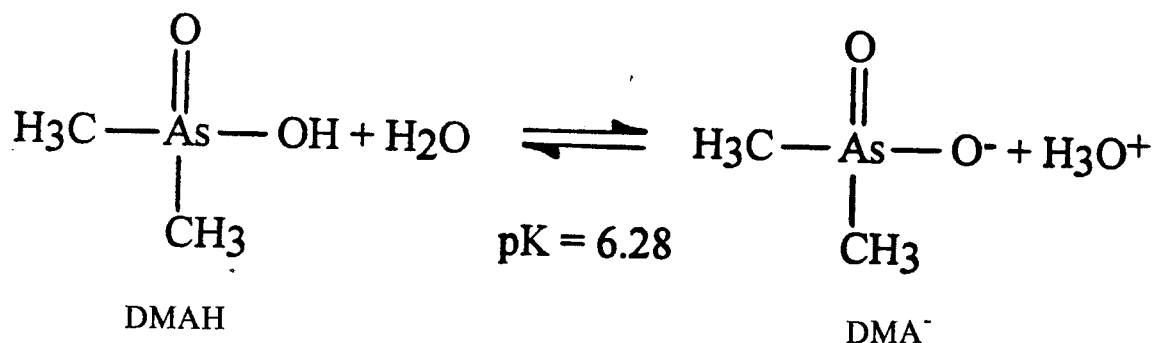


Figure 3.8 Chemical species of dimethylarsinic acid (DMA) present at pH 7.4 (pH at which all experiments reported in this thesis were conducted).

permeating by passive diffusion is the undissociated acid represented as DMAH (Figure 3.8). The passive diffusion of the anionic species DMA⁻ is very slow.

As the NMR signal obtained is composed of methyl resonances from both DMAH and DMA⁻, the calculated values for the efflux rate constant k , and the permeation coefficient P , were corrected for the permeating species according to the equations²¹⁰ below:-

$$k = \alpha k' \quad [3.29]$$

$$P = \alpha P' \quad [3.30]$$

where α is the fraction of DMAH in solution, and is given by the relationship¹⁷⁶ $\alpha = [\text{H}^+] / (K_a + [\text{H}^+])$ for a monoprotic weak acid. For DMAH¹⁷⁶, α is 0.0593 at pH

7.4. K_a is the dissociation constant. k' , and P' are the corrected values for the permeating species DMAH. Fraction of DMA^- in solution is $1-\alpha$, and has a value of 0.9407.

3.10.8.2 Determination of permeability coefficients.

The permeability coefficients were calculated according to equation 3.31

$$P = \frac{k \times V_{in} / \mu\text{mol.lipid}}{A} \quad [3.31]$$

where k (/s) is the efflux rate constant, V is the trap volume of the liposome per μmol of phospholipid, A is area per μmol phospholipid, and has been calculated²¹⁰ to be $1.81 \times 10^3 \text{ cm}^2/\mu\text{mol}$ phospholipid.

The lipid concentration (μmol phospholipid) was determined by phosphorus assay as described in Section 3.10.6.2.

3.11 RESULTS AND DISCUSSION.

3.11.1 The use of DMA as a probe in permeability studies of EPC liposomes, in the absence and presence of organotin compounds in the extraliposomal aqueous compartment.

To observe the effect of organotin compounds on the permeability properties of the liposomes, experiments were carried out by monitoring the efflux of encapsulated dimethylarsinic acid (DMA) from liposomes in the presence and absence of the organotin compounds added into the extraliposomal compartment. At pH 7.4, two species of DMA namely DMAH and DMA⁻ are present in solution. The ¹H NMR spectra obtained are due to the combined proton resonances of the two species, therefore the graphs presented in this chapter describe the efflux of DMA, while the tables of data are for DMAH or DMA⁻ efflux. Under conditions of passive diffusion, DMAH is the major species permeating out of the liposomes. The permeation of DMA⁻ by passive diffusion is very slow²¹⁰, and is not treated in the present study, except in situations where it permeates by facilitated diffusion.

The time course for the efflux of DMA in the absence of any organotin compound at 24°C is shown in Figure 3.9. This efflux behaviour conforms to a first order passive diffusion as demonstrated by fitting a curve through the data points by using equation [3.0]. Previously, Herring *et al*¹⁷⁶ had reported that DMA efflux from EPC liposomes is by passive diffusion. The fit of the data points around the curved portion of their graph is also similar to that shown in Figure 3.9. The rate constants

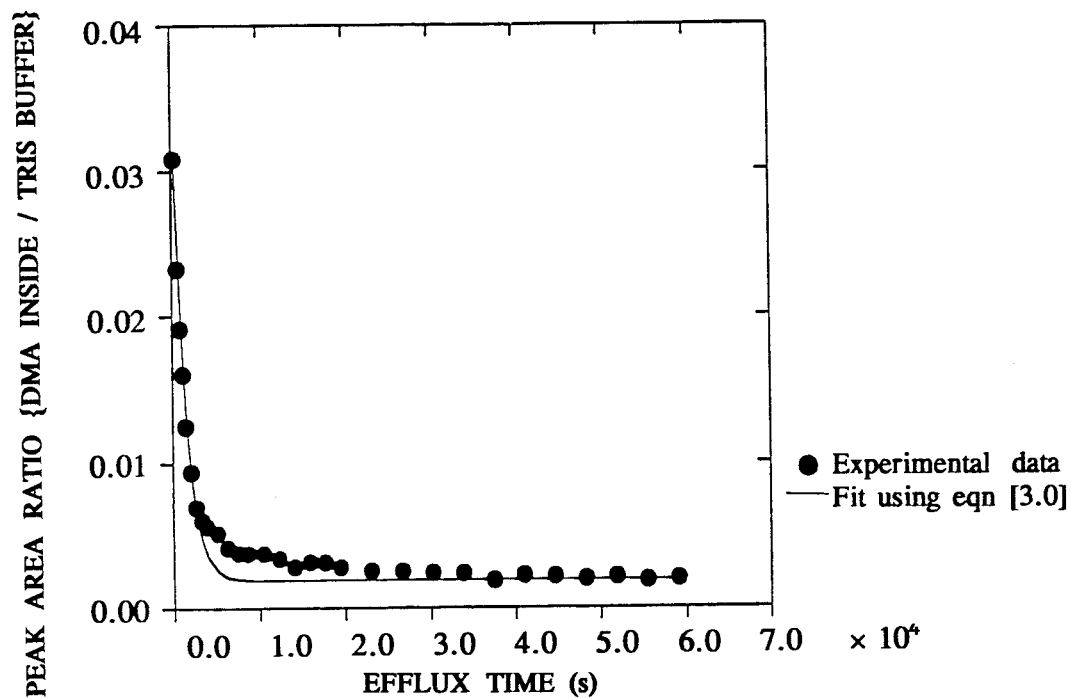


Figure 3.9 Efflux of DMA from EPC liposomes (organotin compounds are absent in the extraliposomal compartment).

Table 3.1 Efflux data for the diffusion of DMAH from EPC liposomes in the absence of organotin compounds

Parameters	Value ^a	Data from ref 213
$t'_{1/2}$ (s)	62 ± 2	
k' (/s)	$(1.1 \pm 0.04) \times 10^{-2}$	$(0.97 \pm 0.15) \times 10^{-2}$
P' (cm /s)	$(1.7 \pm 0.2) \times 10^{-8}$	

^a $a = t'_{1/2}$, k' , and P' have been corrected for the major permeating specie DMAH.

permeation half-life and permeability coefficient for the efflux of DMAH in the absence of the organotin compounds are shown in Table 3.1. Also, data for DMAH efflux from EPC liposomes in HEPES buffer obtained by Nelson²¹⁰ are shown in Table 3.1, and are in close agreement with those obtained in this study. This indicates that tris buffer used in this study, or HEPES buffer do not introduce any significant effect in the efflux rate constants.

The time course for DMA efflux in the presence of tributyltin chloride and monobutyltin trichloride is shown in Figures 3.10 and 3.11 respectively.

The permeability data for DMAH efflux in the presence of tributyltin chloride in the extraliposomal aqueous compartment are shown in Table 3.2.

A comparison of the efflux data of DMAH from EPC liposomes in the absence of any organotin compound (Table 3.1), and its efflux data in the presence

Table 3.2 Effect of 33.2 μ M tributyltin chloride on the efflux of DMAH from EPC liposomes.

Parameter	Value
$t'_{1/2}$ (if diffusion is passive)	25 ± 1
k' (/s) (if diffusion is passive)	$(2.8 \pm 0.1) \times 10^{-2}$
P' (cm/s) (if diffusion is passive)	$(4.9 \pm 1.0) \times 10^{-8}$

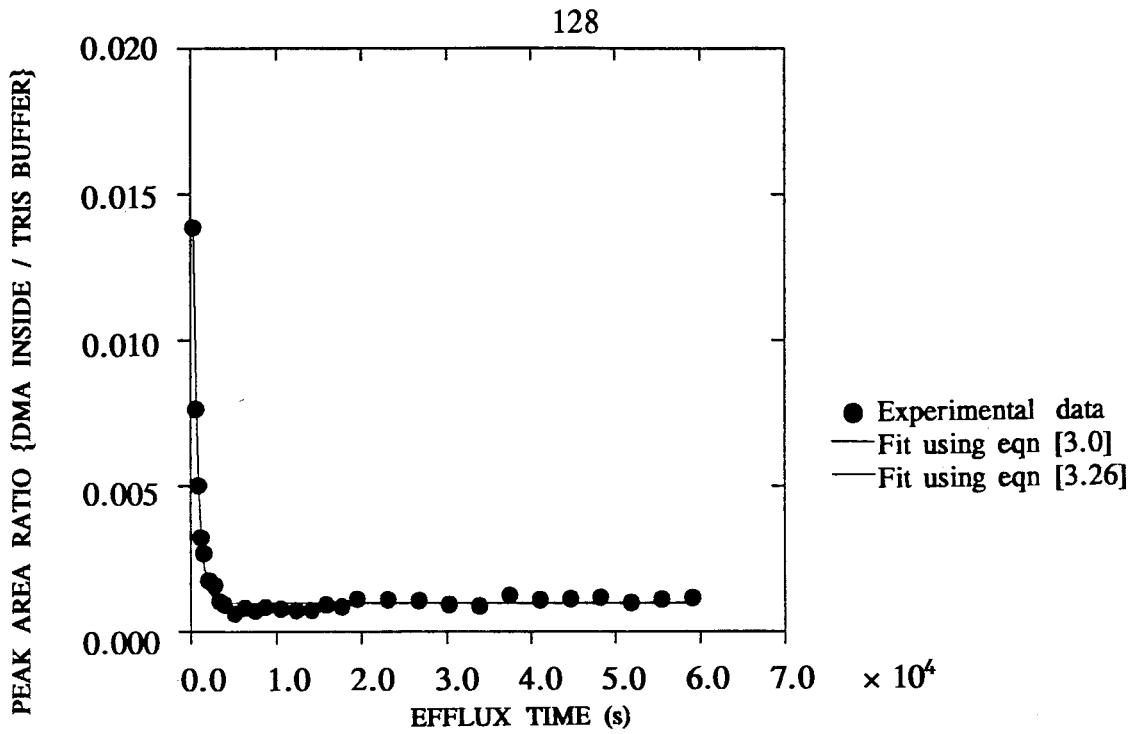


Figure 3.10 Time course for the efflux of DMA from EPC liposomes (tributyltin chloride present in the extraliposomal compartment).

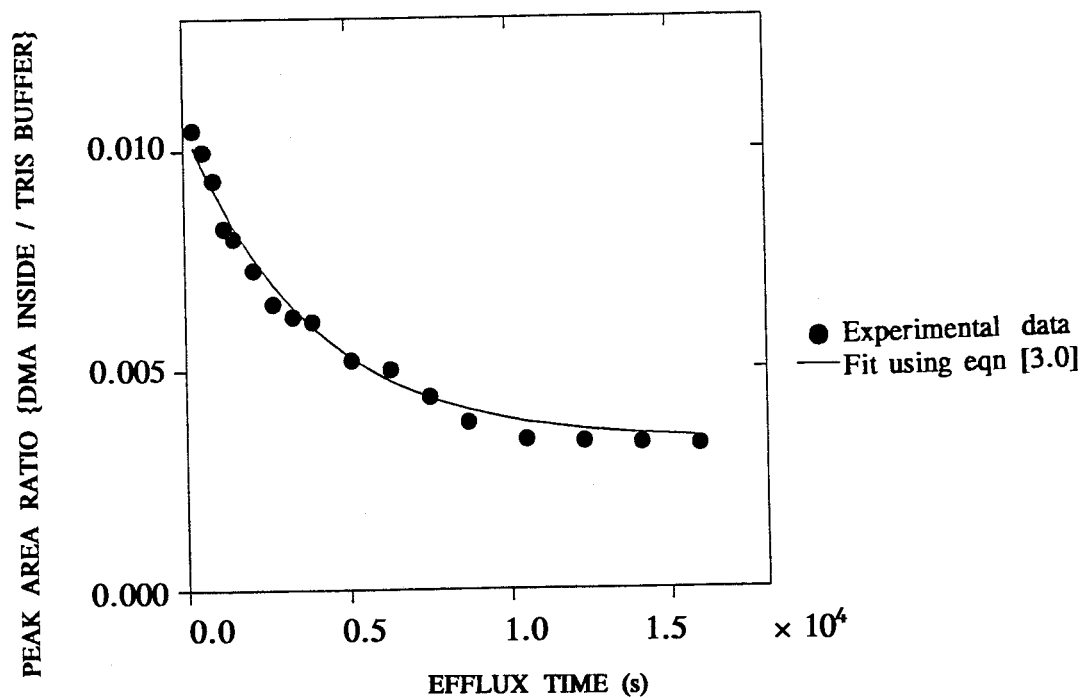


Figure 3.11 Time course for the efflux of DMA from EPC liposomes (monobutyltin trichloride present in the extraliposomal compartment).

of tributyltin chloride (Table 3.2) shows that in the presence of tributyltin chloride, the permeation half-life $t'_{1/2}$ of DMAH efflux becomes about 2.5 times smaller than in its absence, indicating increased rate of permeation. The permeability coefficient is also about 2.9 times greater than in the absence of tributyltin chloride. The efflux rate constant k' also increased by more than twice. This increased permeability of DMAH observed in the presence of tributyltin chloride suggests that some properties of the EPC liposomes have been changed by the tributyltin chloride. According to Heywood *et al*²⁰⁹, the tributyltin cation causes membrane disruption and rupture (lysis) of EPC liposomes. Such rupture or pore formation in the liposomal bilayer would result in increased permeability to permeants.

The increased permeability of the EPC liposomes to dimethylarsinic acid in the presence of tributyltin chloride could also arise if the tributyltin cation acted as a carrier, and mediated the transport of DMA⁻ by facilitated diffusion. The ability of the tributyltin cation to facilitate the diffusion of Cl⁻ and OH⁻ has been reported by Selwyn^{15,208} and Tosteson¹⁶.

The equations [3.0] for passive diffusion and [3.26] for facilitated diffusion,

$$I_{in}^t = I_{in}^{eq} + (I_{in}^0 - I_{in}^{eq}) \exp - \{(1+f)kt\} \quad [3.0]$$

$$I_{in}^t = I_{in}^{eq} + (I_{in}^0 - I_{in}^{eq}) \exp - \left\{ (1+f) \frac{\beta}{\phi} kt \right\} \quad [3.26]$$

used in this study for fitting curves onto the observed experimental data, are not capable of distinguishing between situations where there is a 100% passive diffusion

or 100% facilitated diffusion, unless the magnitudes of the expected rate constants are known. This is because when there is 100% passive diffusion or facilitated diffusion, a plot of $\ln(I_{in}^t - I_{in}^{eq})$ versus t , gives a straight line with slope $(1+f)k$ for passive diffusion or $(1+f)(\beta/\phi)k$ for facilitated diffusion. Each of the constants β/ϕ and k for facilitated diffusion cannot be calculated separately, instead they are incorporated into each other as one parameter. The combined value of $(\beta/\phi)k$ of equation [3.26] is equivalent to k of equation [3.0]. Under this condition, any curve generated by using either equation [3.0] or [3.26] should fit the experimental data (Figure 3.10).

A method for obtaining the value of the constant β/ϕ when efflux takes place by a mixture of passive diffusion and facilitated diffusion is described later in this section.

The time course for the efflux of DMA in the presence of monobutyltin trichloride is shown in Figure 3.11 above. The efflux of DMAH is by passive diffusion, but the rate of efflux has become slower (Table 3.3). The values of the rate constant and permeability coefficient shown in Table 3.3 are smaller than their values when no organotin compound was present (Table 3.1). The permeation half-life of DMAH is about 3 times larger, indicating retarded permeation. Also, the permeability coefficient is decreased by about a factor of 4.3.

The effect of externally added monobutyltin trichloride on the EPC liposomes is to decrease their permeability. A probable mechanism for this behavior is that monobutyltin trichloride permeates into the lipid bilayer and causes a decrease in the

membrane fluidity. Any compound capable of decreasing membrane fluidity such as cholesterol²¹⁷ and α -tocopherol²¹⁸ would decrease permeability. Such decrease in the membrane fluidity caused by dibutyltin dichloride has been observed on phosphatidylinositol 4-monophosphate and phosphatidylinositol 4,5-diphosphate

Table 3.3 Effect of 33.2 μM monobutyltin trichloride on the efflux of DMAH from EPC liposomes.

Parameters	Value
$t'_{1/2}$ (s)	188 ± 6
k' (/s)	$(3.7 \pm 0.1) \times 10^{-3}$
P' (cm/s)	$(4.0 \pm 1.2) \times 10^{-9}$

vesicles^{219,220}. Unfortunately, apart from the present study, there are no other reports of the interaction of monobutyltin trichloride with liposomal membranes. However, from the data presented in Tables 3.2 and 3.3, it seems that the monobutyltin species, unlike the tributyltin species, neither have the capability to induce membrane disruption nor act as carrier. Hence, the retarded permeation of DMAH.

Monobutyltin is a degradation product of tributyltin in the environment and the scheme is tributyltin \rightarrow dibutyltin \rightarrow monobutyltin \rightarrow inorganic tin. These products are progressively less toxic to life perhaps because debutylation leads to products less capable of causing membrane disruption.

The efflux of DMA across EPC liposomes in the presence of trimethyltin hydroxide ($32.3 \mu\text{M}$) in the extraliposomal compartment was also studied. Analysis of this permeation behaviour by plotting $\ln(I_{in}^t - I_{in}^{eq})$ against t , of equation [3.0] or [3.26] gave two straight lines of different slopes (Figure 3.12, slopes A and C). This behaviour is not predicted by equation [3.0], if permeation is by passive diffusion.

$$I_{in}^t = I_{in}^{eq} + (I_{in}^0 - I_{in}^{eq}) \exp - \{(1 + f)kt\} \quad [3.0]$$

$$I_{in}^t = I_{in}^{eq} + (I_{in}^0 - I_{in}^{eq}) \exp - \left\{ (1 + f) \frac{\beta}{\phi} kt \right\} \quad [3.26]$$

If slope A (Figure 3.12) is considered a region of facilitated diffusion, the parameter $(\beta/\phi)k$ of equation [3.26] is calculated. When the value of $(\beta/\phi)k$ was used in equation [3.26] to fit the experimental data, only the data points from the early and very late parts of the efflux experiment fitted (Figure 3.13 solid curve). Data obtained at intermediate efflux times did not fit.

If slope C (Figure 3.12) is considered a region of passive diffusion, the efflux rate constant k , for DMAH is calculated. When k was used in equation [3.0] to fit the experimental data, there was a close fit for data obtained at intermediate and late parts of the efflux (Figure 3.13 broken line). Towards equilibrium, equations [3.0] and [3.26] gave a close fit. A possible explanation for this phenomenon is that slope A (Figure 3.12) is a region dominated by facilitated diffusion of DMA⁻ mediated by trimethyltin cation, while slope C is a region dominated by passive

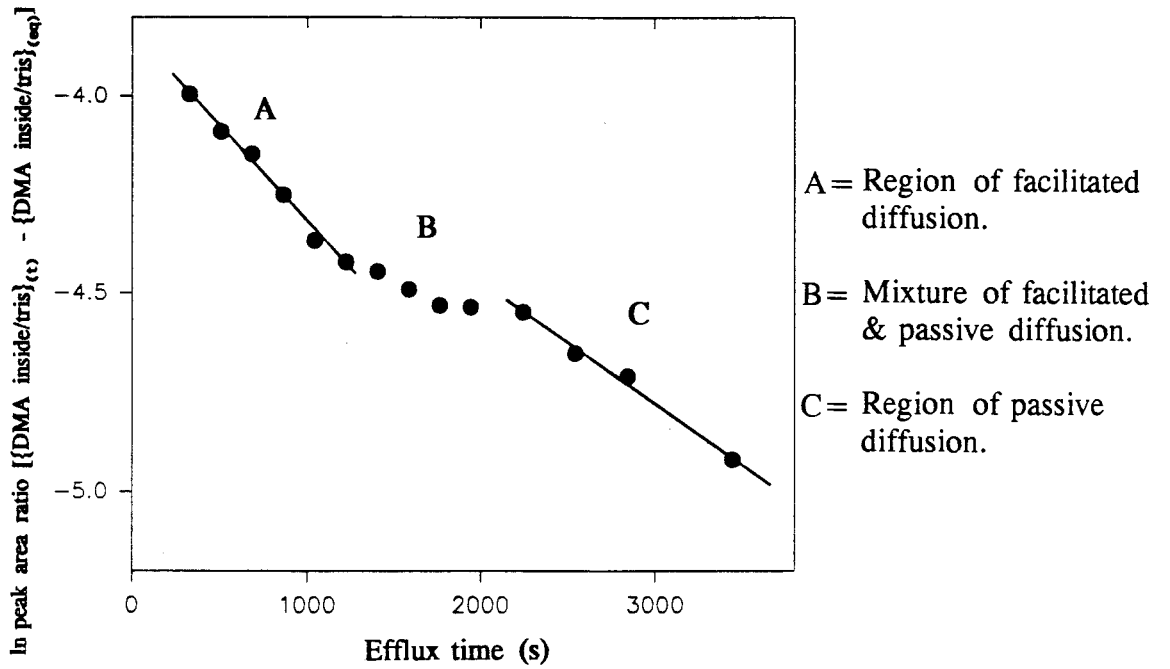


Figure 3.12 Log plot of DMA efflux from EPC liposomes (33.2 μ M trimethyltin hydroxide present in extraliposomal volume).

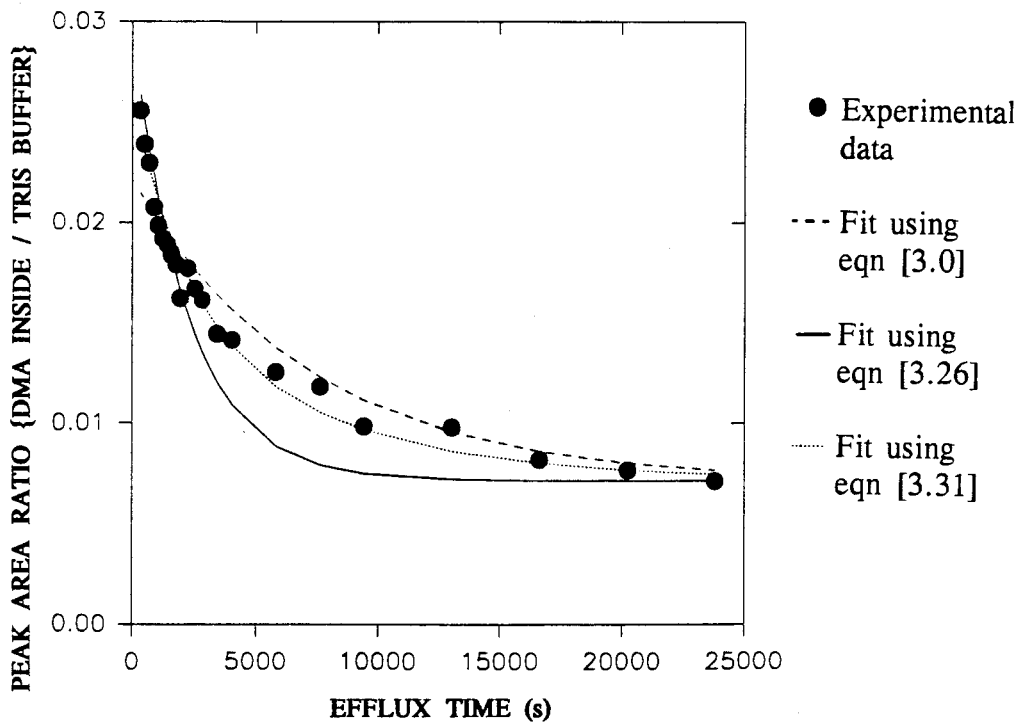


Figure 3.13 Time course for DMA efflux from EPC liposomes (33.2 μ M trimethyltin hydroxide present in extraliposomal volume).

diffusion of DMAH and DMA⁻. The passive diffusion of DMA⁻ is very slow²¹⁰. Slope B (Figure 3.12) is a region dominated by a mixture of facilitated and passive diffusion. Thus, facilitated diffusion sets in at the early part of the efflux, and gradually gives way to passive diffusion as the efflux progresses. Assuming that the DMA⁻ is the major species permeating by facilitated diffusion while DMAH is the major species permeating by passive diffusion, the rate constant obtained from slope C (Figure 3.12) should be divided by 0.9407; the fraction of DMA⁻ (1- α) present at pH 7.4 (Section 3.10.8.1), to obtain the rate constant k' for the passive efflux of DMA⁻. Then, the parameter β/ϕ for facilitated diffusion of DMA⁻ can be calculated from slope A (Figure 3.12) by using the rate constant k' (for passive diffusion of DMA⁻) calculated from slope C.

The calculated parameters k' (DMA⁻), k (DMAH), β/ϕ , and I_{in}^0 are substituted into equation [3.31] which is a combination of equations [3.0] and [3.26], modified by introducing the parameters M and N . Equation 3.31 was fitted onto the experimental data by keeping every other parameter except M and N constant (Figure 3.13, dotted line).

$$I_{in}^t = M(I_{in}^{eq} + (I_{in}^0 - I_{in}^{eq})\exp\{-((1+f)kt)\}) + N\left(I_{in}^{eq} + (I_{in}^0 - I_{in}^{eq})\exp\left\{-\left(1+f\right)\frac{\beta}{\phi}kt\right\}\right) \quad [3.31]$$

(M is the percentage contribution of passive diffusion to efflux, while N is the percentage contribution of facilitated diffusion to efflux). The efflux parameters for this experiment are shown in Table 3.4.

Similar increased flux of chloride ions across liposomal membranes, mediated by trimethyltin cation as carrier has been reported by Selwyn¹⁵.

Table 3.4 Data for the efflux of DMA from EPC liposomes in the presence of 33.2 μM trimethyltin hydroxide.

Parameter	Value
k' DMAH (/s)	$(2.5 \pm 0.5) \times 10^{-3}$
k' DMA ⁻ (/s)	$(1.6 \pm 0.3) \times 10^{-4}$
β/ϕ (experimental) ^a	2.5 ± 0.5
β/ϕ (curve fit) ^b	2.2 ± 1.0
N (% facilitated diffusion) ^b	66 ± 21
M (% passive diffusion) ^b	35 ± 21

a= Calculated from experimental data

b=obtained from the curve fitting result.

3.11.2 Effect of organotin concentration on the efflux of DMA

The effect of tributyltin chloride concentration on the efflux of DMAH across EPC liposomes is shown in Table 3.5. As the concentration of tributyltin chloride in the extraliposomal compartment is increased from 0 to 8.3 μM , there is an initial decrease in the efflux rate constant and the permeability coefficient, followed by an

increase as the tributyltin concentration is raised from 8.3 to 33.2 μM . The values for the efflux half-life $t'_{1/2}$ also change in accordance with the changes in the permeability coefficients and the efflux rate constants, by becoming smaller as the permeability of the liposome increases.

The increase in the permeability coefficients, efflux rate constants, and the decrease in the efflux half-lives indicates that either the liposomal membrane has become more permeable to DMAH or that the tributyltin cation is facilitating the efflux of DMA^- .

The effect of tributyltin chloride on the permeation of DMAH is concentration dependent. A plot of efflux rate constant versus tributyltin chloride

Table 3.5 Effect of tributyltin chloride concentration on DMAH efflux^a

Conc. (μM)	P' (cm/s) $\times 10^{-8}$	$t'_{1/2}$ (s)	k' (/s) $\times 10^{-2}$
0.0	(1.7 \pm 0.2)	62 \pm 2	(1.1 \pm 0.04)
8.3	(1.3 \pm 0.1)	85 \pm 11	(0.8 \pm 0.1)
16.7	(1.6 \pm 0.1)	45 \pm 0.4	(1.5 \pm 0.02)
33.2	(4.9 \pm 1.0)	25 \pm 1	(2.8 \pm 0.1)

^a—It could not be determined if increased efflux was by passive or facilitated diffusion.

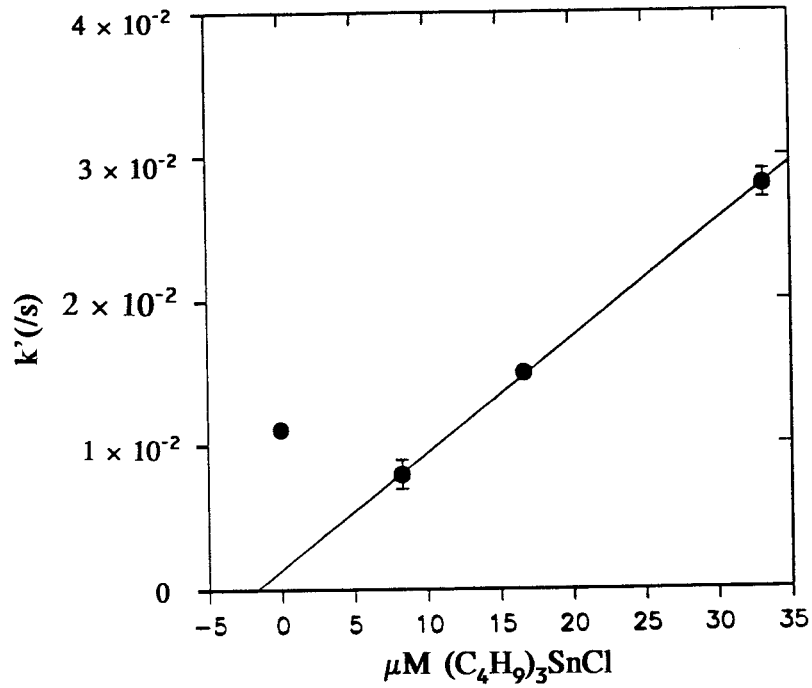


Figure 3.14 Effect of tributyltin chloride concentration on the permeability of EPC liposomes (tributyltin chloride was added into the extraliposomal compartment).

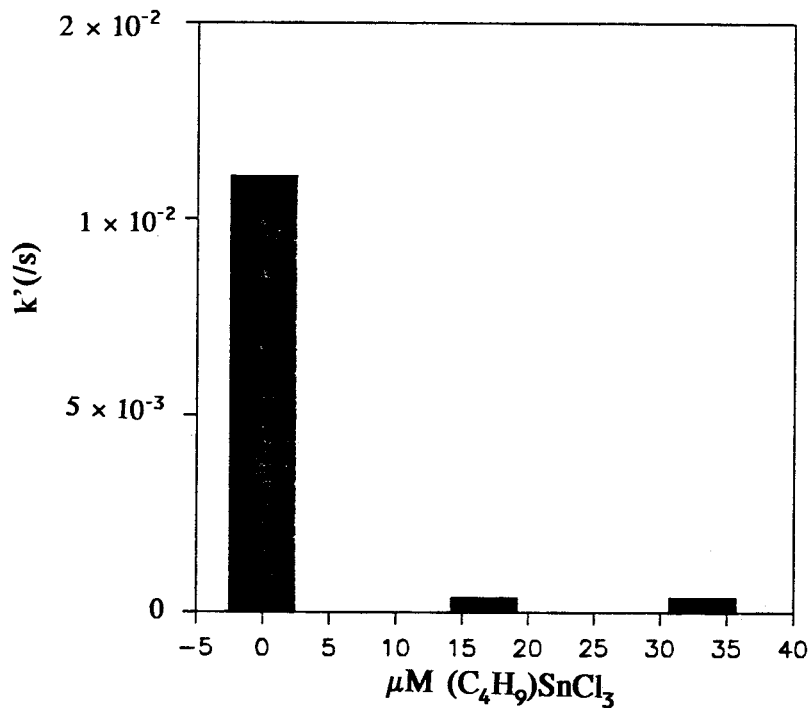


Figure 3.15 Effect of monobutyltin trichloride on the permeability of EPC liposomes (monobutyltin trichloride was added in the extraliposomal compartment).

concentration shows a linear relationship (Figure 3.14) described by the equation $Y=8.01 \times 10^{-4} X + 1.46 \times 10^{-3}$, and a regression coefficient of 0.9990. The data point corresponding to zero concentration of tributyltin chloride does not fall on the regression line. This is probably because tributyltin chloride modified the properties of the liposomes. Therefore, the data obtained at zero tributyltin chloride concentration, and the other data points effectively belong to different types of liposomes. Alternatively, non-linearity could also result if different modes of transport of DMA exist between the liposomes which are in contact with tributyltin chloride, and those not in contact with it.

Table 3.6 Effect of monobutyltin trichloride concentration on the efflux of DMAH.

Conc (μM)	P' (cm/s) $\times 10^{-9}$	$t'_{1/2}$ (s)	k' (/s) $\times 10^{-4}$
0	(17.3 \pm 0.2)	64 \pm 0.5	(111.0 \pm 0.04)
16.7	(2.8 \pm 0.4)	188 \pm 6	(3.7 \pm 0.1)
33.2	(2.8 \pm 0.1)	188 \pm 6	(3.7 \pm 0.1)

The effect of monobutyltin trichloride concentration on the permeation of DMA across EPC liposomes is shown graphically in Figure 3.15, while the permeability data are shown in Table 3.6. As the concentration of monobutyltin

trichloride is increased from 0 to 16.7 μM , there is a large decrease in the permeability coefficients and the rate constants. The permeation half-life increased by about thirty fold, indicating a very retarded permeability of the liposomal bilayer. No further change in the permeation parameters was observed as the concentration of monobutyltin trichloride was further increased.

3.11.3 Efflux of DMA from tributyltin chloride-EPC liposomes (with tributyltin chloride absent in the extraliposomal compartment).

The efflux of DMA from liposomes composed of a mixture of tributyltin chloride (TBT) and egg phosphatidylcholine (EPC) was studied to establish the permeability properties of these model membranes. In these experiments no tributyltin chloride was added to the extraliposomal compartment. The liposomes were prepared as described in Section 3.10.4 and are designated as TBT-EPC liposomes. The composition of the different TBT-EPC liposomes that were studied is as follows:

- (a) TBT-EPC A (0.5 μg tributyltin chloride : 0.2 g EPC)
- (b) TBT-EPC B (1.5 μg tributyltin chloride : 0.2 g EPC)
- (c) TBT-EPC C (5.0 μg tributyltin chloride : 0.2 g EPC)

The permeability properties of these liposomes were studied by measuring the efflux of encapsulated DMA from these liposomes. As an example, the efflux of DMA from TBT-EPC C liposomes is described. Analysis of this efflux experiment by plotting $\ln(I_{in}^t - I_{in}^{eq})$ of equations [3.0] or [3.26] as described in Section 3.11.1

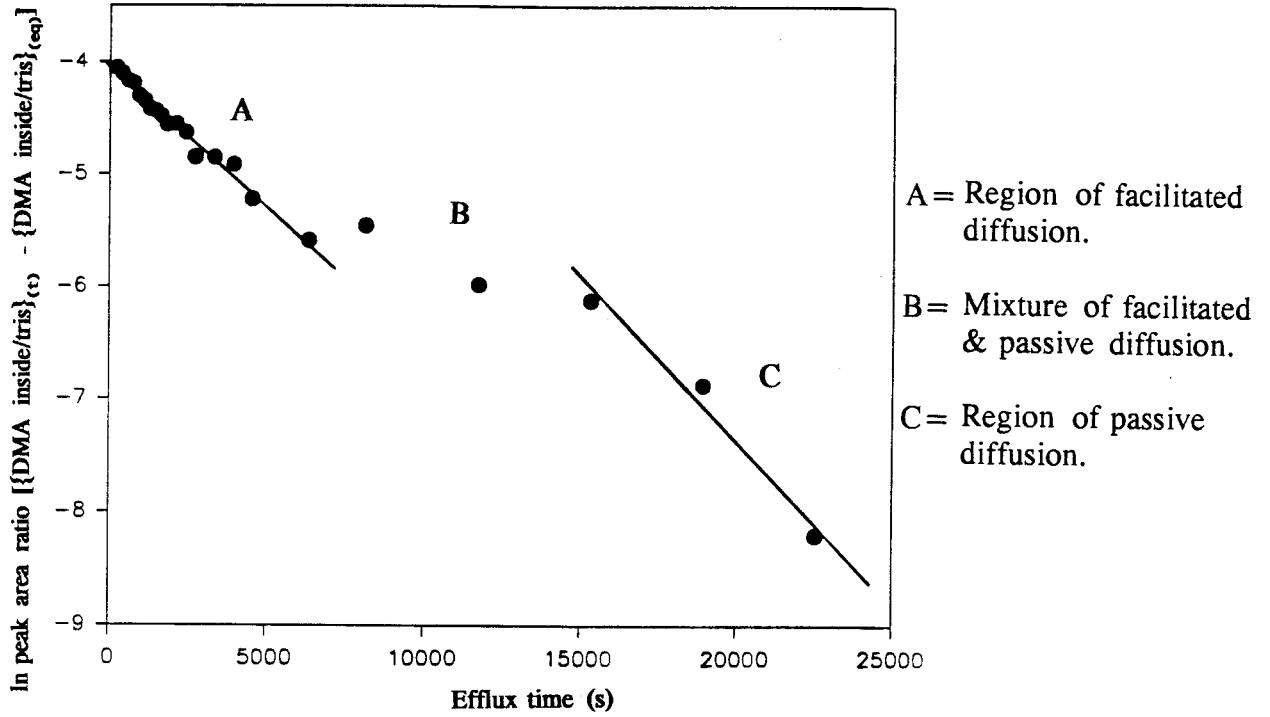


Figure 3.16 Log plot of DMA efflux from TBT-EPC C liposomes.

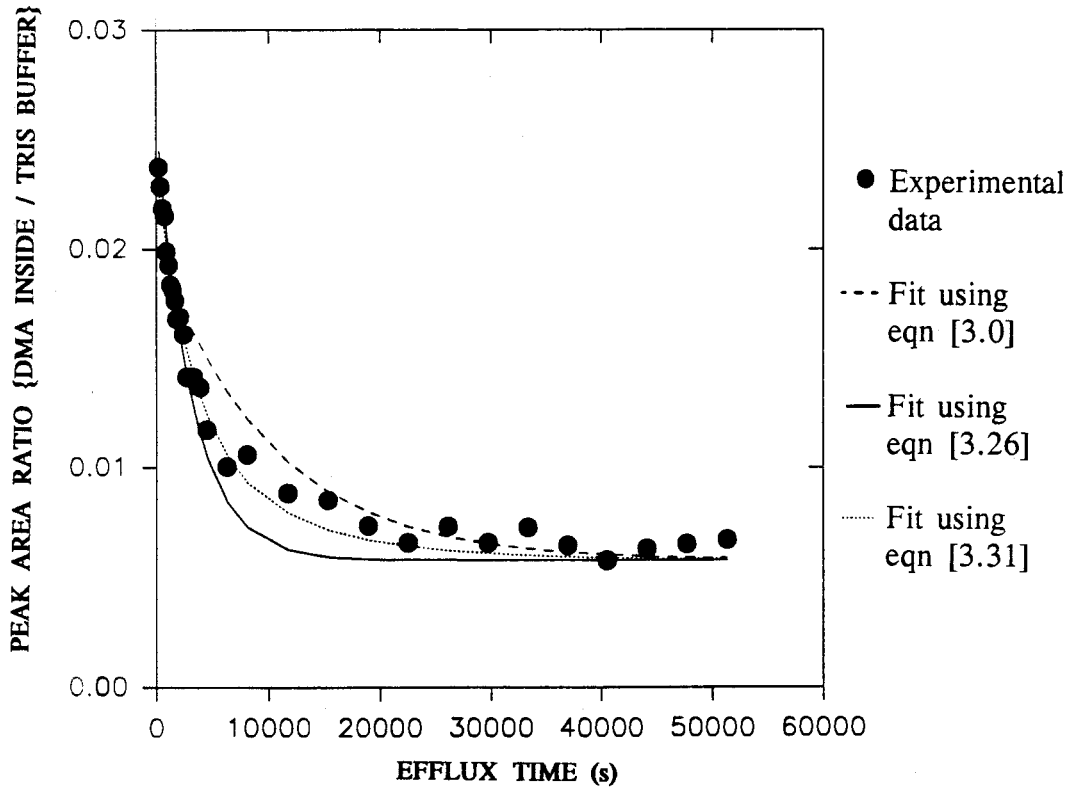


Figure 3.17 Time course for DMA efflux from TBT-EPC C liposomes.

shows two lines with different slopes (Figure 3.16), which indicates that the efflux of DMA from TBT-EPC C is by a mixture of passive diffusion and facilitated diffusion. Facilitated diffusion is the major mode of DMA⁻ transport at the early stages of the efflux (Figure 3.17 solid line), while passive diffusion of DMAH dominates at the later stages (Figure 3.17 broken line). At intermediate times, a mixture of facilitated diffusion and passive diffusion dominate the efflux. The observed efflux behavior is therefore better described by fitting equation [3.31] (a combination of equations [3.0] and [3.26], Section 3.11.1) onto the experimental data (Figure 3.17, dotted line).

Table 3.7 Diffusion parameters for the efflux of DMA from tributyltin-EPC liposomes by a mixture of passive and facilitated diffusion^a.

Liposome	k' (DMA ⁻) $\times 10^{-4}$ (/s)	k' (DMAH) $\times 10^{-3}$ (/s)	β/ϕ	% facilitated diffusion	% passive diffusion
TBT-EPC A	2.0	3.1	2.2	66	34
TBT-EPC B	1.4	2.2	1.8	58	42
TBT-EPC C	1.1	1.8	2.2	54	46

^a=Tributyltin chloride was not added into the extraliposomal compartment.

Mean value $\beta/\phi = 2.1 \pm 0.2$

The efflux of DMA from TBT-EPC A and TBT-EPC B, can also be accounted for by a mixture of facilitated diffusion and passive diffusion. The diffusion constants, and the percentage contributions of facilitated and passive diffusion to permeation are shown in Table 3.7.

As the concentration of tributyltin chloride in the liposome is increased, facilitated diffusion decreases, while passive diffusion increases (Figure 3.18).

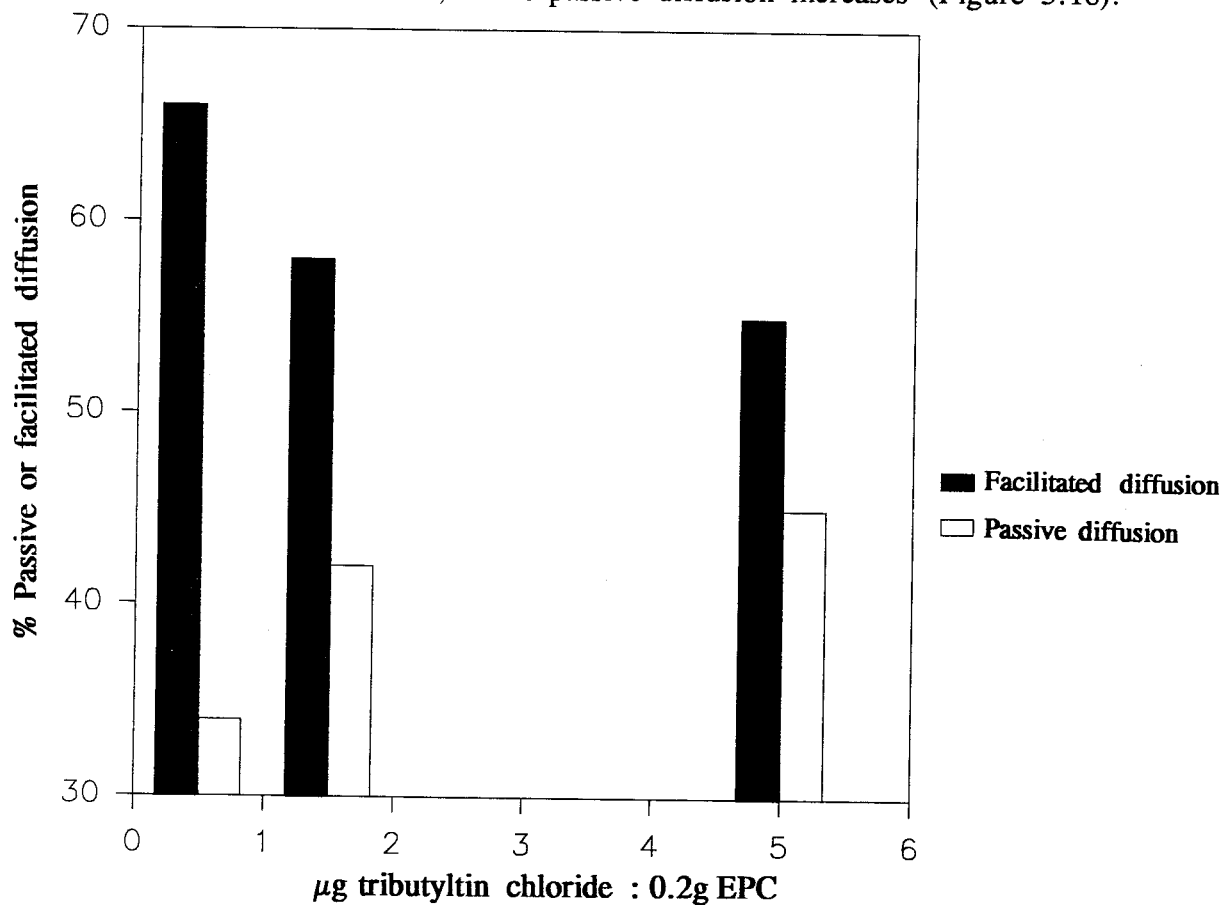


Figure 3.18 Contribution of passive and facilitated diffusion to the efflux of DMA from TBT-EPC liposomes of different tributyltin chloride composition.

When tributyltin chloride ($16.7 \mu\text{M}$) was added into the extraliposomal compartment of TBT-EPC B liposomes, the plot of $\ln(I_{in}^t - I_{in}^{eq})$ versus t , for DMA efflux of either equation [3.0] or equation [3.26] gave one straight line of uniform slope (Figure 3.19).

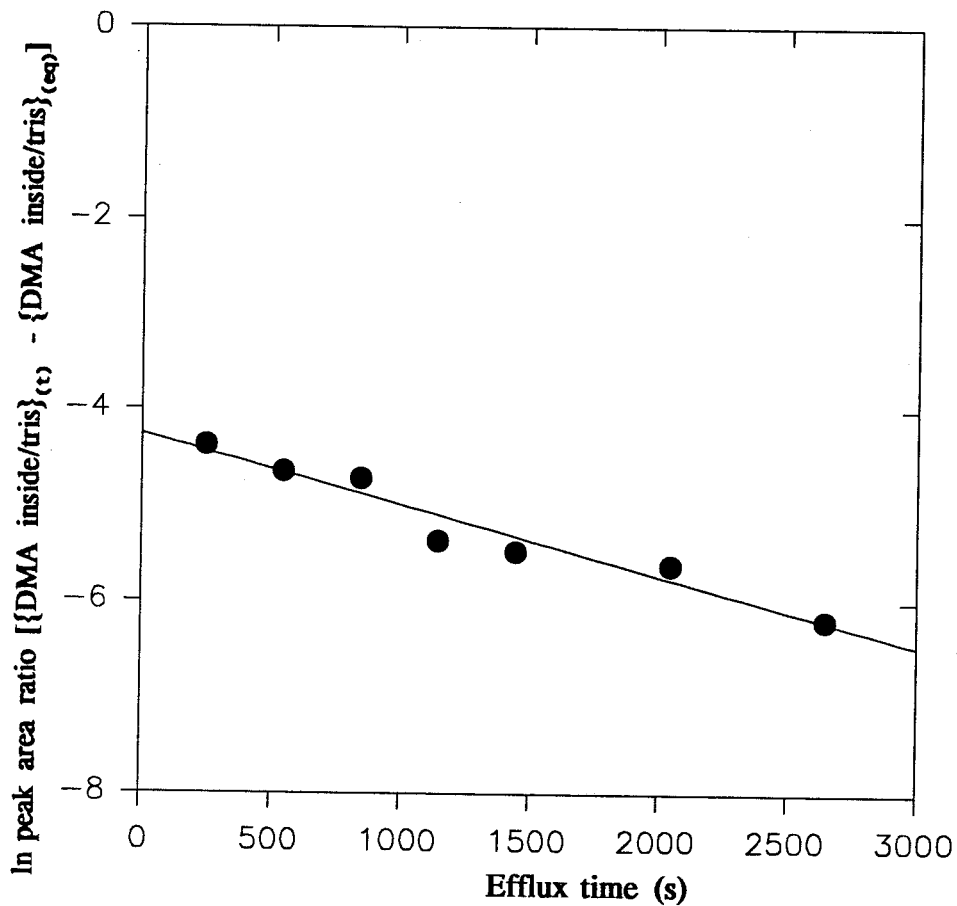


Figure 3.19 Log plot for efflux of DMA from TBT-EPC B liposomes when $16.7 \mu\text{M}$ tributyltin chloride is present in the extraliposomal compartment.

Thus, it seems that when tributyltin chloride is added into the extraliposomal compartment, dissociation of the tributyltin-DMA complex at the interface between the bilayer and the extraliposomal compartment is no longer favourable. The equilibrium for dissociation is shifted to the left thereby suppressing the release of the complexed DMA^- . If the tributyltin-DMA complex does not dissociate at the interface of the extraliposomal compartment, there will be no more free tributyltin cations to sustain the facilitated transfer of DMA^- , therefore the facilitated diffusion of DMA^- ceases. Under these conditions, the passive diffusion of DMAH dominates.

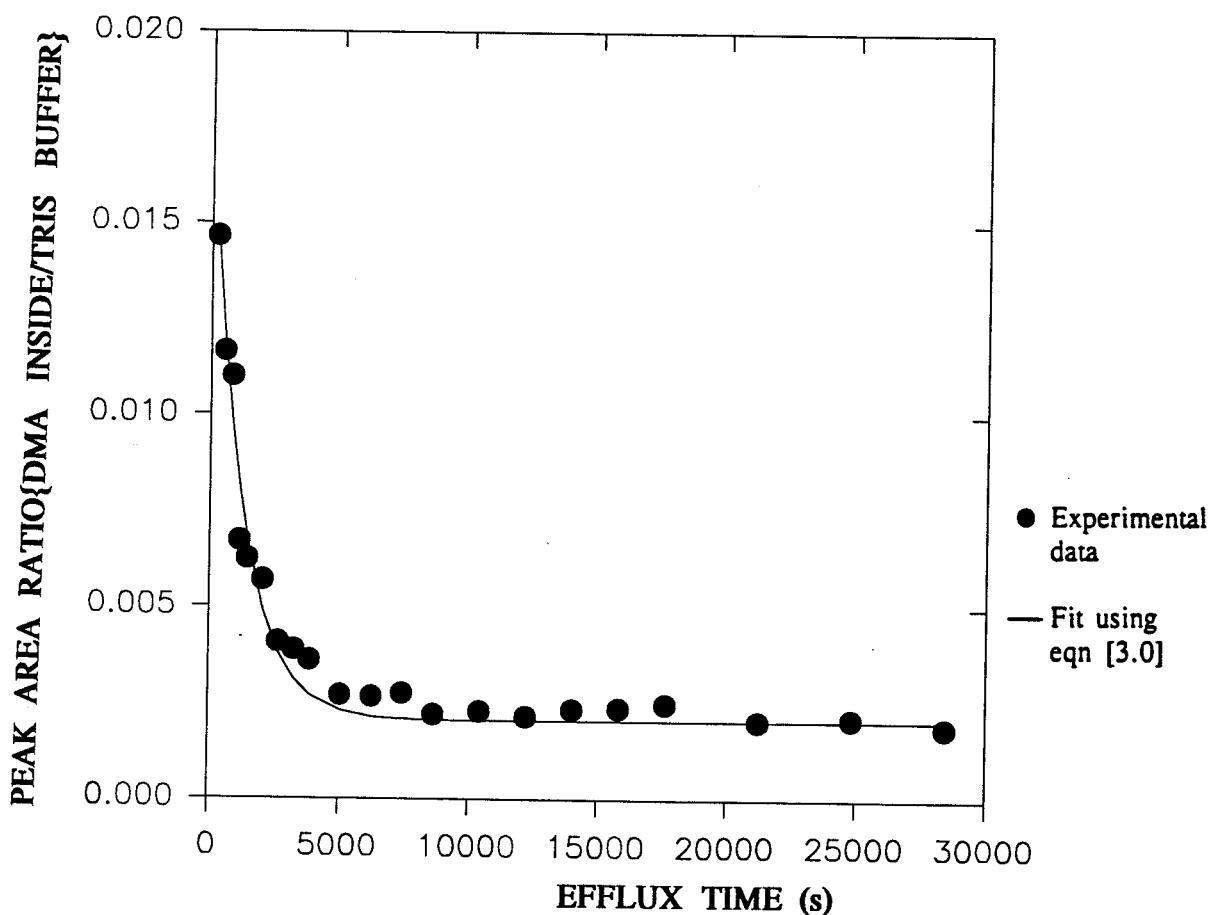


Figure 3.20 Time course for efflux of DMA from TBT-EPC B liposomes when $16.7 \mu\text{M}$ tributyltin chloride is present in the extraliposomal compartment.

The time course for the efflux of DMA from TBT-EPC B liposome in the presence of tributyltin chloride ($16.7 \mu\text{M}$) added into the extraliposomal compartment is shown in Figure 3.20. The efflux behavior is described by equation [3.0] for passive diffusion.

The parameters for this efflux are shown in Table 3.8. The rate constant for the efflux of DMAH from TBT-EPC B in the presence of externally added tributyltin chloride is 1.8×10^{-2} /s (Table 3.8), while in the absence of externally added tributyltin chloride, it is 2.2×10^{-3} /s (Table 3.7). The observed difference in the two situations is attributed to the unequal concentrations of tributyltin chloride involved in the experiments.

Table 3.8 Parameters for the efflux of DMAH from TBT-EPC B liposomes in the presence of externally added tributyltin chloride ($16 \mu\text{M}$).

Parameter	Value
k'	$(1.8 \pm 0.1) \times 10^{-2}$ (/s)
p'	$(2.8 \pm 0.5) \times 10^{-8}$ (cm/s)

3.11.4 Efflux of DMA from monobutyltin trichloride-EPC liposomes.

Monobutyltin trichloride-EPC liposomes designated MBT-EPC liposomes prepared as described in Section 3.10.4 were used to study the permeation of DMA.

MBT-EPC liposomes having the following compositions were studied:-

- (a) MBT-EPC A (0.5 μg monobutyltin trichloride : 0.2 g EPC)
- (b) MBT-EPC B (1.5 μg monobutyltin trichloride : 0.2 g EPC)

The efflux of DMA from MBT-EPC B with no monobutyltin trichloride in the extraliposomal aqueous compartment was studied. The time course for this efflux is shown in Figure 3.22. Analysis of the experimental data points by plotting $\ln(I_{in}^t - I_{in}^{eq})$ versus t , of either equation [3.0] or equation [3.26] gave only a straight line of uniform slope (Figure 3.21). This indicates that only one mode of diffusion is involved. The efflux parameters for DMAH, assuming passive diffusion is shown in Table 3.9.

The efflux of DMA from MBT-EPC B in the presence of externally added monobutyltin trichloride (16.7 μM) was studied. Also, only one mode of DMA efflux was found. The efflux parameters for DMAH, assuming passive diffusion is shown in Table 3.10.

It seemed reasonable to consider the efflux of DMAH from MBT-EPC liposomes to be by passive diffusion either in the presence or absence of monobutyltin trichloride in the extraliposomal compartment, because a comparison of the efflux parameters in Tables 3.9 and 3.10, with the efflux parameters for an "EPC only" liposome (Table 3.1), shows that the permeability coefficient for the MBT-EPC liposomes either in the presence or absence of externally added monobutyltin trichloride is the same as the permeability coefficient for the efflux of

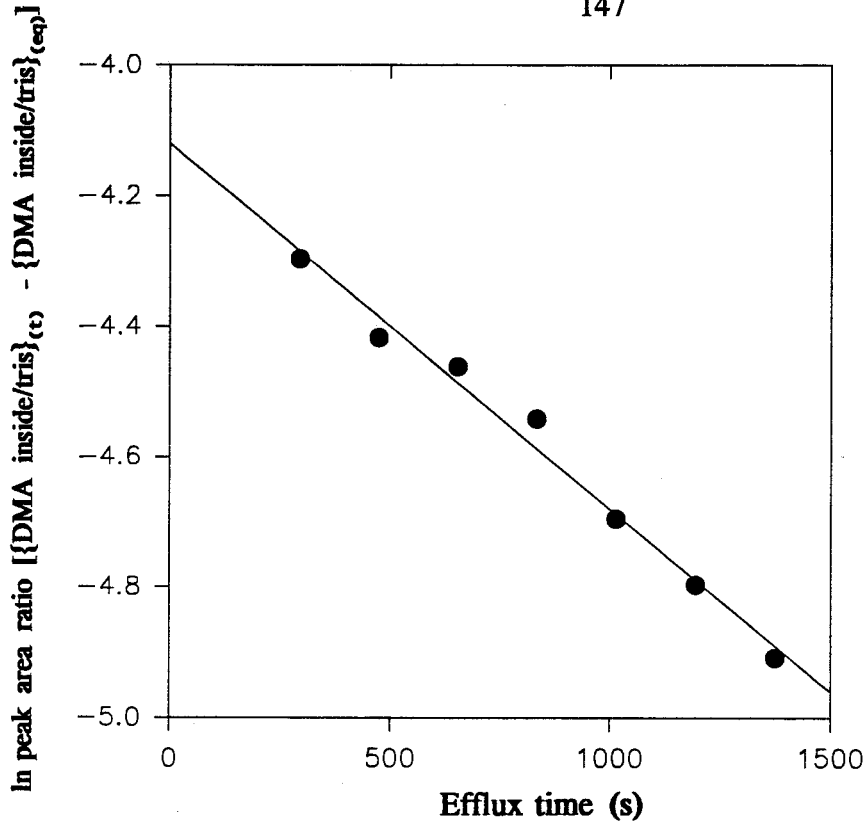


Figure 3.21 Log plot of DMA efflux from MBT-EPC B liposomes.

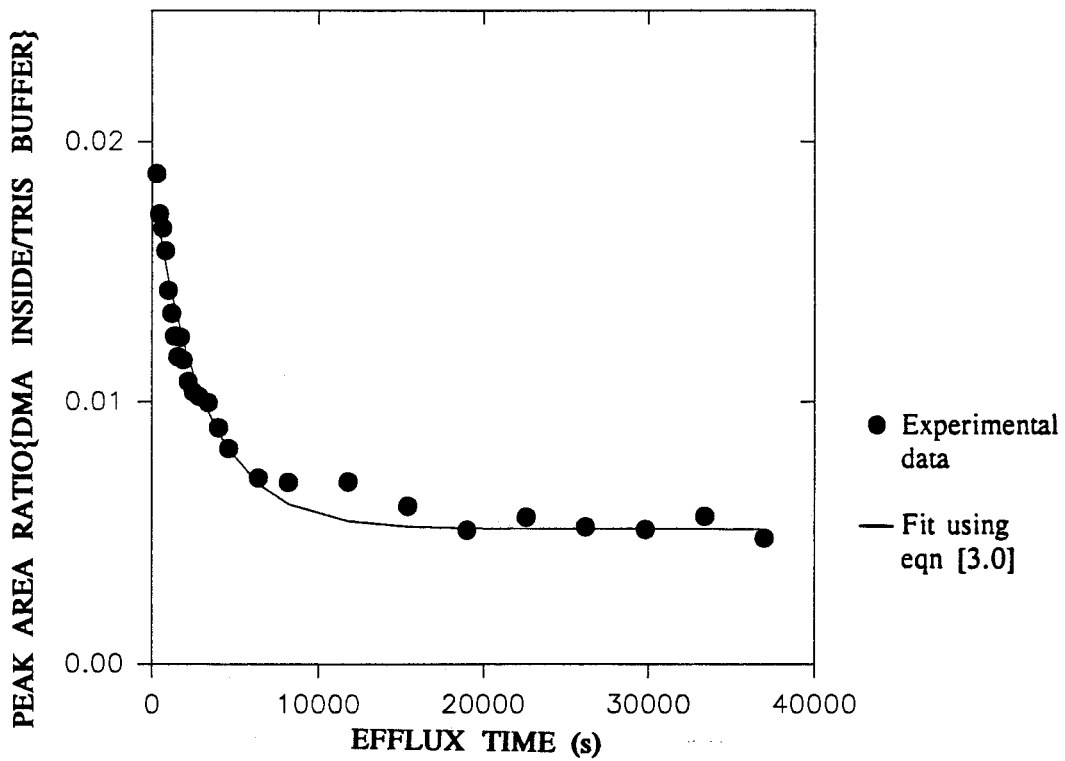


Figure 3.22 Time course for DMA efflux from MBT-EPC B liposomes.

Table 3.9 Permeability data for efflux of DMAH from MBT-EPC B (1.5 μ g butyltin trichloride: 2 g EPC) liposomes (with monobutyltin trichloride absent in the extraliposomal compartment).

Parameter	Value
$k'(/s)$	$(8.3 \pm 0.4) \times 10^{-3}$
$t'_{1/2} (s)$	84 ± 4
$P'(\text{cm}/s)$	$(1.7 \pm 0.1) \times 10^{-8}$

Table 3.10 Permeability data for efflux of DMAH from MBT-EPC B (1.5 μ g monobutyltin trichloride: 0.2g EPC) liposomes with monobutyltin trichloride present in the extraliposomal compartment.

Parameter	Value
$k'(/s)$	$(9.1 \pm 0.5) \times 10^{-3}$
$t'_{1/2} (s)$	76 ± 4
$P'(\text{cm}/s)$	$(1.7 \pm 0.1) \times 10^{-8}$

DMAH from "EPC only" liposomes. The efflux rate constants in Tables 3.1, 3.9 and 3.10, are close. Therefore, monobutyltin trichloride does not have the ability to act as carrier for DMA⁻.

It seems that the incorporation of monobutyltin trichloride into the lipid bilayer of EPC liposomes has no effect on its membrane permeability, but the membrane permeability is greatly retarded if the monobutyltin trichloride is added externally into the extraliposomal compartment (Section 3.11.1, Table 3.3).

3.11.5 Effect of the butyltin chloride concentrations of the liposome on permeability properties of TBT-EPC and MBT-EPC liposomes.

The experiments reported in this section were conducted with tributyltin chloride ($16.7 \mu\text{M}$) added into the extraliposomal compartment of TBT-EPC liposomes because under these conditions, passive diffusion of DMA is induced.

Monobutyltin trichloride ($16.7 \mu\text{M}$) was also spiked into the extraliposomal compartment of MBT-EPC liposomes to maintain similar experimental conditions with the MBT-EPC liposomes.

The efflux of encapsulated DMA from butyltin-EPC liposomes was monitored at 24°C . Studies were conducted by using TBT-EPC A, TBT-EPC B, MBT-EPC A, and MBT-EPC B liposomes.

The permeability data for the efflux of DMAH from TBT-EPC liposomes are shown in Table 3.11. As the tributyltin chloride concentration of the liposome is increased on going from TBT-EPC A to TBT-EPC B, the permeability of the liposomes to DMAH also increases by about a factor of 1.6 (Table 3.11).

The permeability data for MBT-EPC liposomes (with monobutyltin chloride present in the extraliposomal volume) are shown in Table 3.12. The permeability

coefficients, permeation half-lives, and rate constants show very little variation with increase in the monobutyltin trichloride composition of the liposome.

Table 3.11 Effect of tributyltin chloride concentration of TBT-EPC liposomes on permeability (tributyltin chloride solution was also added to the extraliposomal volume).

Liposome	P' (cm/s) $\times 10^{-8}$	$t'_{1/2}$ (s)	k'(/s) $\times 10^{-2}$
TBT-EPC A	(1.7 \pm 0.2)	57 \pm 4	(1.1 \pm 0.1)
TBT-EPC B	(2.8 \pm 0.5)	39 \pm 1	(1.8 \pm 0.1)

Table 3.12 Effect of monobutyltin trichloride concentration of MBT-EPC liposomes on permeability (monobutyltin trichloride was also added to the extraliposomal volume).

Liposome	P' (cm/s) $\times 10^{-9}$	$t'_{1/2}$ (s)	k'(/s) $\times 10^{-3}$
MBT-EPC A	(4.9 \pm 0.8)	195 \pm 7	(3.6 \pm 0.1)
MBT-EPC B	(4.4 \pm 0.3)	218 \pm 19	(3.2 \pm 0.2)

3.11.6 Effect of temperature on the permeability of organotin-EPC liposomes.

The effect of temperature on the permeability of TBT-EPC A and TBT-EPC B liposomes is shown in Tables 3.13 and 3.14 respectively, while the effect of

Table 3.13 Effect of temperature on the permeability properties of TBT-EPC A liposomes.

Temperature °C	P' (cm/s) × 10 ⁻⁸	k' (/s) × 10 ⁻²
24	(1.7 ± 0.2)	(1.2 ± 0.1)
28	(3.1 ± 0.2)	(2.3 ± 0.1)
32	(3.4 ± 1.0)	(4.7 ± 0.1)

Table 3.14 Effect of temperature on the permeability properties of TBT-EPC B (1.5 µg tributyltin chloride : 0.2g EPC) liposomes.

Temperature °C	P' (cm/s) × 10 ⁻⁸	k' (/s) × 10 ⁻²
24	(2.8 ± 0.5)	(1.8 ± 0.1)
28	(4.0 ± 0.03)	(3.5 ± 0.06)
32	(4.9 ± 0.5)	(5.4 ± 1.3)

Table 3.15 Effect of temperature on the permeability properties of MBT-EPC A (0.5 μ g butyltin trichloride : 0.2 g EPC) liposomes.

Temperature (°C)	P' (cm/s) $\times 10^{-9}$	k' (/s) $\times 10^{-3}$
24	(4.9 \pm 0.8)	(3.6 \pm 0.1)
28	(11.9 \pm 1.0)	(7.0 \pm 0.1)
32	(15.1 \pm 1.2)	(14.9 \pm 0.6)

Table 3.16 Effect of temperature on the permeability properties of MBT-EPC B (1.5 μ g monobutyltin trichloride : 0.2g EPC) liposomes.

Temperature (°C)	P'(cm/s) $\times 10^{-9}$	k' (/s) $\times 10^{-2}$
24	(4.4 \pm 0.4)	(5.4 \pm 1.3)
28	(8.7 \pm 0.1)	(7.6 \pm 1.1)
32	(15.8 \pm 1.0)	(1.1 \pm 0.1)

temperature on MBT-EPC A and MBT-EPC B liposomes is shown in Figures 3.15 and 3.16 respectively.

As the temperature is increased, the permeability of both TBT-EPC and

MBT-EPC liposomes to DMAH also increases. Generally, permeation rates increase with increase in temperature. This is due to either increased partitioning of the permeant into the lipophilic bilayer or the increased ease of diffusion through the liposomal bilayer as temperature increases.

3.11.7 Activation energies for the permeation of butyltin chloride-EPC liposomes.

The activation energies for the efflux of DMAH from liposomes of various butyltin chloride/EPC compositions were determined by using the Arrhenius equation:-

$$P = Ae^{-Ea/RT}$$

or

$$\ln P = -\frac{Ea}{RT} + \ln A$$

A plot of $\ln P$ against $1/T$ gives a straight line from which the activation energy can be calculated (Figures 3.23 and 3.24 for TBT-EPC and MBT-EPC liposomes respectively). The activation energies are shown in Table 3.17 for tributyltin chloride-EPC liposomes and Table 3.18 for monobutyltin trichloride-EPC liposomes.

For the TBT-EPC liposomes, the activation energy for the permeation of DMAH decreases with increasing tributyltin chloride concentration in the liposome. When compared to the activation energy for the efflux of DMAH from an "EPC only" liposome (86 ± 20 kJ/mol)²¹⁰, tributyltin chloride reduced the activation energy required for DMAH efflux.

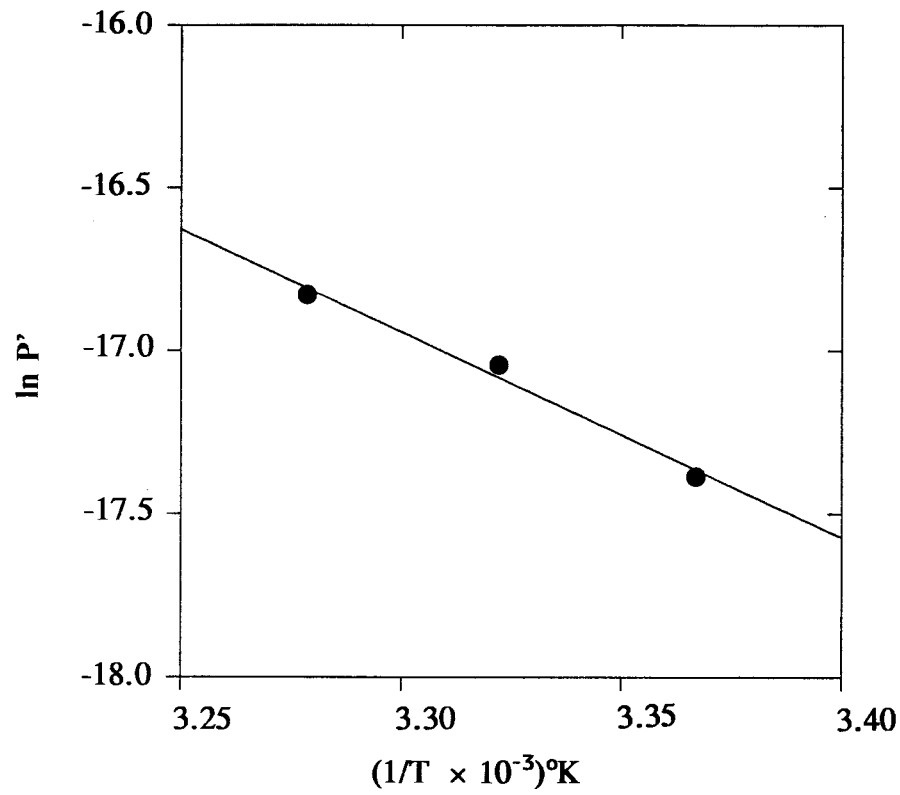


Figure 3.23 Arrhenius plot for DMAH efflux from TBT-EPC B liposomes.

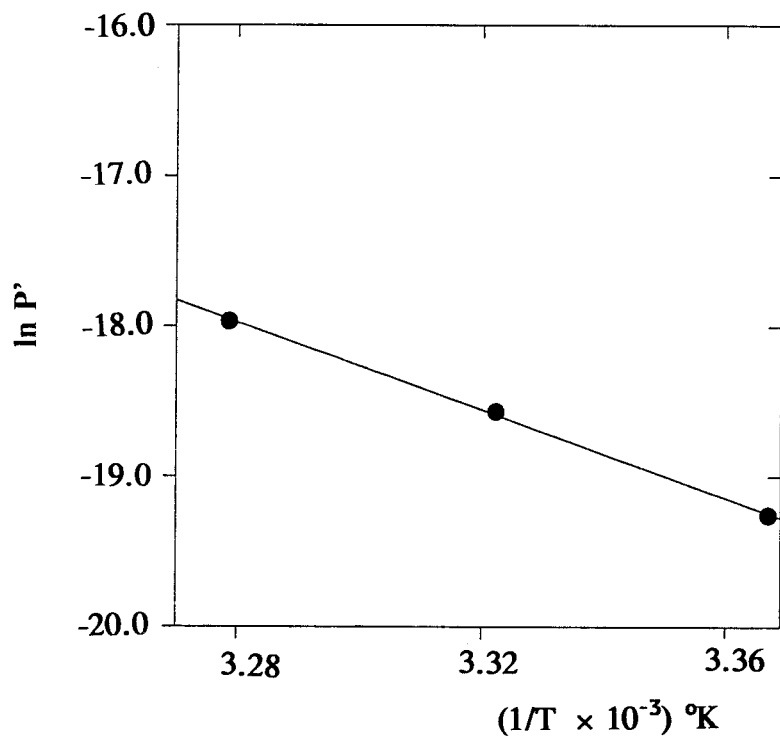


Figure 3.24 Arrhenius plot for DMAH efflux from MBT-EPC B liposomes.

Table 3.17 Effect of tributyltin chloride content of liposome on the activation energy for efflux of DMAH from TBT-EPC liposomes.

Liposome	Activation energy (kJ/mol)
TBT-EPC A	64.4
TBT-EPC B	52.3

Table 3.18 Effect of monobutyltin trichloride content of liposome on the activation energy for efflux of DMAH from MBT-EPC liposomes.

Liposome	Activation energy (kJ/mol)
MBT-EPC A	106.8
MBT-EPC B	121.5

Cohen²²¹, has described the activation energy for a permeant to comprise the following:-

- (i) adsorption of the solute at the lipid membrane/water interphase
- (ii) dehydration of the solute
- (iii) diffusion through the hydrocarbon chain (lipid bilayer)

Thus the activation energy for permeation of a solute should increase as its ability to form hydrogen bonds increases. This is simply related to the number of hydrogen bonds the permeant has to break before it diffuses across the hydrophobic hydrocarbon chains of the lipid bilayer. If the permeating probe molecule dimethylarsinic acid (DMAH) is kept constant, the contribution of the dehydration step to the activation energy should be constant for both TBT-EPC and MBT-EPC liposomes. Therefore, the observed difference in activation energies for the two types of liposomes must be due to either the effect of the organotin compounds on the adsorption of DMAH at the lipid/water interphase, or the effect on diffusion through the liposomal lipid bilayer. The low activation energy observed for the permeation of DMAH across tributyltin chloride-EPC liposomes (Table 3.17) supports the argument that tributyltin chloride modified the liposomal membrane.

For the MBT-EPC liposomes, the activation energy for the permeation of DMAH increases as the concentration of monobutyltin trichloride in the liposomes increases (Table 3.18). This observation indicates that it became more difficult for the DMAH molecules to diffuse across the lipid bilayer and is further evidence that the monobutyltin cation is neither capable of inducing pore formation on the liposomes nor able to act as a carrier for DMAH.

The pre-exponential factors of the Arrhenius equation are shown in Tables 3.19 and 3.20 for TBT-EPC and MBT-EPC liposomes respectively. According to Cohen²²¹, and De Gier *et al*²⁰², the pre-exponential factor is related to the molar

Table 3.19 Arrhenius pre-exponential factor for TBT-EPC liposomes

Liposome	Pre-exponential factor (/s) $\times 10^{-8}$
TBT-EPC A	(2.8 \pm 0.5)
TBT-EPC B	(4.0 \pm 0.4)

Table 3.20 Arrhenius pre-exponential factor for monobutyltin MBT-EPC.

Liposome	Pre-exponential factor (/s) $\times 10^{-8}$
MBT-EPC A	(1.1 \pm 0.3)
MBT-EPC B	(1.0 \pm 0.4)

entropy change of the permeation process by the equation:-

$$\ln A = \text{constant} + \frac{\Delta S}{R}$$

where A is the pre-exponential function, ΔS is the molar entropy change and R is the molar gas constant.

The values of the pre-exponential factors obtained for the TBT-EPC and MBT-EPC liposomes are different from each other, but are fairly constant for each

type of liposome. Therefore it seems that entropy for the permeation process is different for both the TBT-EPC and MBT-EPC liposomes, but remains constant for each type of liposome irrespective of the butyltin chloride concentration of the liposome. The slight variation in the values of the pre-exponential factors shown in Table 3.19 for the TBT-EPC liposomes may be attributed to experimental errors.

The observed differences in the values of activation energies and pre-exponential factors for the TBT-EPC and MBT-EPC liposomes may indicate that these butyltin chlorides act on the model membrane by different mechanisms.

Cohen²²¹ has shown that the magnitude of the activation energy is related to the physical state of the hydrocarbon chains in the lipid bilayer. Thus, as the amount of cholesterol content of the vesicle is increased, the activation energy for its permeation also increases²²¹.

The results of the present study and those of Cohen²²¹ demonstrate that the composition of the liposomes contributes very significantly to the magnitude of activation energy. This is contrary to the report by De Gier *et al*²⁰² that activation energy is solely determined by the capability of the permeating molecules to be involved in hydrogen bonding.

3.11.8 Relevance of this NMR study to the environmental toxicity of butyltin compounds.

A number of chemical reactions of the trialkyltin compounds with other organic molecules of biological relevance have been reported^{219,222}. Trialkyltin

compounds derange mitochondrial function by discharging a hydroxyl-chloride gradient across the membranes, and by inhibiting ATP synthesis¹⁸. They also cause swelling and disruption of the mitochondrial membranes¹⁸, and the rupture of human red blood cells²²³.

Dialkyltin compounds react with enzymes possessing thiol groups¹⁸. The biochemical effect of this is an interference with α -keto acid oxidation¹⁸, while the mono-organotin compounds do not show any significant toxicity.

The effect of butyltin compounds on membranes has not been extensively studied. Early studies by Selwyn *et al*^{15,208}, Tosteson and Weith¹⁶, Motais *et al*¹⁷ show that tributyltin chloride and trimethyltin chloride can mediate chloride-hydroxide exchange across mitochondrial membrane and model cell membranes, while tripropyltin chloride mediates chloride-chloride exchange across mitochondrial membranes. The present study clearly shows that tributyltin chloride and monobutyltin trichloride exert different and opposite effects on the model cell membranes. Tributyltin chloride makes the model membranes more permeable while monobutyltin trichloride makes them less leaky. Since monobutyltin trichloride is by far less toxic than tributyltin chloride, the observed decrease in membrane permeability is likely a phenomenon that leads to reduced toxicity.

The present study concludes that tributyltin and trimethyltin cations are able to function as mobile carriers for dimethylarsinate while monobutyltin cation lacks this ability.

CHAPTER 4**HYDRIDE GENERATION METHODS OF ATOMIC ABSORPTION
SPECTROPHOTOMETRY FOR TOTAL TIN DETERMINATION.****4.1 INTRODUCTION.**

With the advent of organotin pollution in the marine environment, many workers in the field of environmental analysis have devoted their energies to the detection and quantitation of the more toxic organotin species. The determination of the total tin content in marine samples has been largely neglected. Consequently another objective of the present study was to provide information on the total tin content of some marine animals in British Columbia, Canada.

Determination of total tin content in environmental samples is usually accomplished by the use of atomic absorption spectrophotometry (AAS). Methods of sample preparation, prior to total tin determination, usually involve the extraction of the tin compounds into organic solvents by the use of complexing agents, or the digestion of the samples with mineral acids, to convert the various forms of tin to inorganic tin. The total tin content of the digested sample or the organic extract can then be determined either directly by the use of conventional flame AAS^{224,225,226} and graphite furnace atomic absorption spectrophotometry (GFAAS), or by conversion to volatile derivatives such as inorganic tin hydride which can be analyzed by hydride generation-atomic absorption spectrophotometry (HG-AAS)^{227,228} or hydride generation-graphite furnace atomic absorption spectrophotometry (HG-

GFAAS)²²⁹. The HG-GFAAS method has also been used in the analysis of the following elements; bismuth²³⁰, antimony²³¹ and selenium²³².

Conversion of tin compounds in environmental samples to inorganic tin hydride is usually preferred over direct determination, because the analyte is removed from the matrix of the digested sample, thereby minimizing matrix interferences during the HG-AAS or HG-GFAAS analysis.

In this study, two methods of hydride generation atomic absorption spectrophotometry were optimized and used for total tin determination in marine animals: one based on continuous hydride generation atomic absorption spectrophotometry (HG-AAS) and the other on batch hydride generation-graphite furnace atomic absorption spectrophotometry (HG-GFAAS).

The continuous hydride generation method (HG-AAS) utilizes the hydride generator previously reported by Cullen and Dodd²³³ (Fig 4.1), for use in the determination of arsenic. Atomization of tin compounds was achieved inside a quartz cell, which was heated by the air-acetylene flame of the atomic absorption spectrophotometer.

The batch hydride generation method (HG-GFAAS) involved the in situ generation of tin hydride which was then trapped, or adsorbed onto a graphite furnace tube according to the method of Sturgeon et al²²⁹. The graphite furnace tube served as a preconcentration device and also enabled high atomization temperatures to be reached.

The overall reaction for the production of tin(IV) hydride (stannane) is given

below;



4.2 EXPERIMENTAL.

4.2.1 Instrumentation.

4.2.1.1 Continuous hydride generation atomic absorption spectrophotometry (HG-AAS).

The continuous hydride generator employed in this study was a home built glass apparatus described previously by Cullen and Dodd²³³ (Fig 4.1) for arsenic determination. The operation of this hydride generator is similar to the type reported by Vijan and Chan²²⁷ and Subramanian²²⁸ for total tin determination. The hydride generator consisted of a 20 turn reaction glass coil (A, in Figure 4.1) connected to a gas-liquid separator (B, in Figure 4.1) by Teflon[®] tubing. Reagents were pumped into the glass reaction coil by means of a peristaltic pump (Gilson, Middleton Wisconsin, U.S.A.). The generated tin hydride was carried by a flow of nitrogen via a Teflon[®] tubing, into an open-ended T-shaped quartz cell which was heated by the air-acetylene flame of the atomic absorption spectrophotometer. The light from the tin hollow cathode lamp, and the deuterium background corrector were aligned to pass through the T-shaped quartz cell positioned in the optical path of the atomic absorption spectrophotometer. The atomic absorption spectrophotometer is a Varian 1275 model, operated at a slit width of 1 nm. Argon was used as the internal

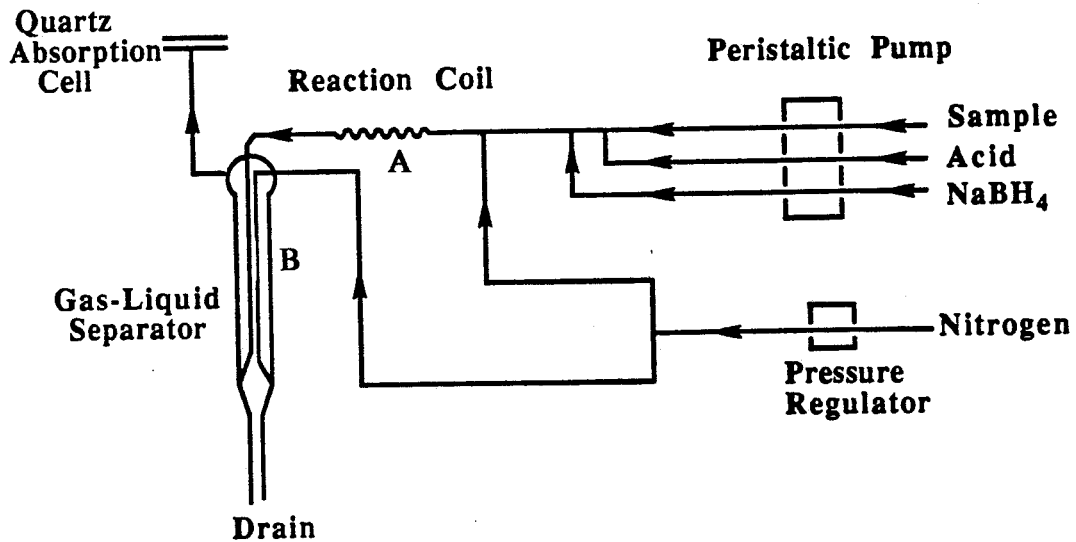


Figure 4.1 Schematic diagram of the apparatus used for the HG-AAS method reported by Cullen and Dodd²³³.

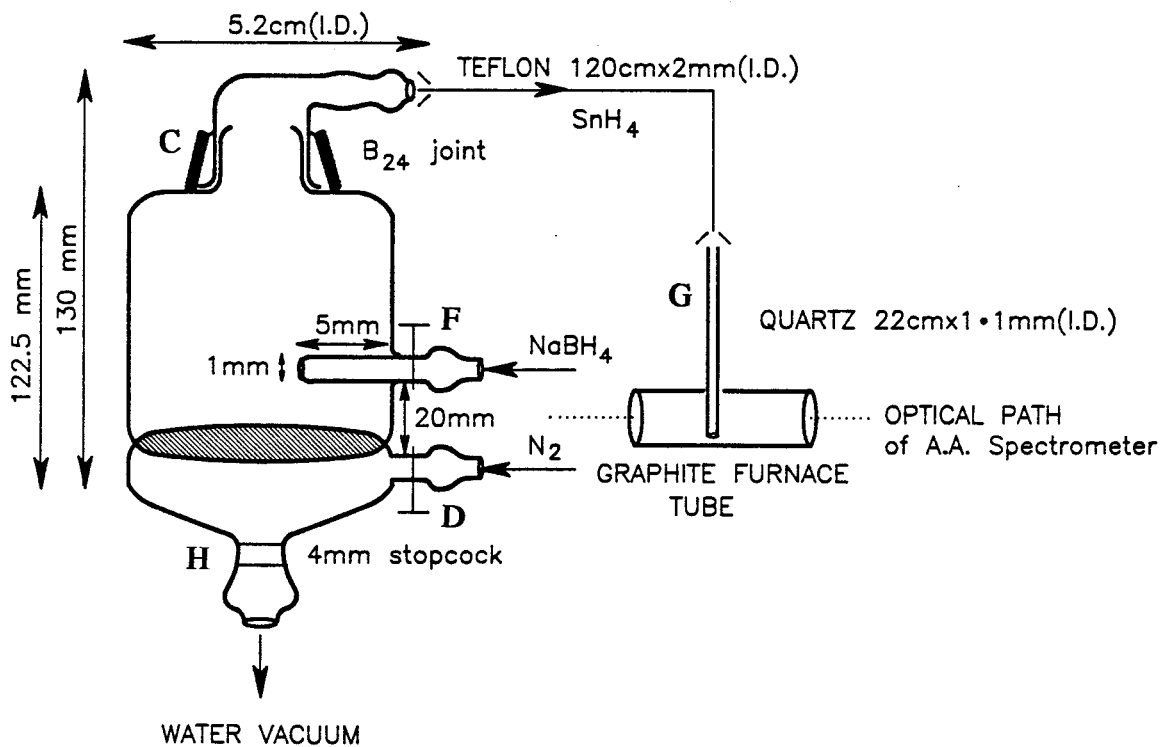


Figure 4.2 Schematic diagram of the hydride generator used for HG-GFAAS.

purge gas. The tin hollow cathode lamp was purchased from Hamamatsu Photonics of Japan. Analyses were carried out at the 224.6 nm spectral line.

4.2.1.2 Batch hydride generation-graphite furnace atomic absorption spectrophotometry (HG-GFAAS).

The batch hydride generator used for the HG-GFAAS is a glass apparatus shown in Figure 4.2, and was modelled to be slightly different from the design reported by Sturgeon *et al*²³⁴ for arsenic and selenium determination, and later for total tin determination²²⁹. The lower portion of the batch hydride generator was constructed of a 25 mL Buchner funnel (Corning Glass Works, Corning, U.S.A) with medium porous glass frit (pore size 10-15 μm). This hydride generator was designed to accommodate larger volumes of reagents than the one reported by Sturgeon *et al*²³⁴, and the larger surface area of the glass frit should enable easier mixing of the reagents, and purging of the generated tin hydride out of the batch hydride generator. The tin hydride produced in the hydride generator was swept by an upward flow of nitrogen via a Teflon[®] tubing to a narrow quartz tube of inner diameter 1.1 mm, which was inserted into the heated graphite tube of the graphite furnace atomizer, aligned in the optical path of the atomic absorption spectrophotometer. The graphite furnace tubes were pre-used Varian Techtron[®] graphite tubes, which were pre-coated with either sodium tungstate or palladium modifiers. When no pre-used tubes were available, fresh graphite tubes whose pyrolytic coatings had been roughened by using an abrasive (sandpaper), were coated

with solutions of these modifiers, and used. Sturgeon *et al*²³⁵ have reported that pre-used graphite tubes are more efficient in trapping the tin hydride than fresh graphite tubes. The orifice on the wall of the graphite furnace tube was widened to a diameter of 2.3 mm to allow the insertion of the quartz tube. The graphite furnace atomizer was a Varian GTA-95 instrument connected to a Varian 1275 atomic absorption spectrophotometer. The spectral line and slit width used are as described in Section 4.2.1.1.

4.2.2 Materials and reagents.

The following chemicals; sodium tungstate dihydrate (Analar grade), L-cysteine, sodium borohydride (Assured grade), potassium hydroxide (Aristar grade) hydrochloric acid (Analytical grade) were purchased from BDH Chemicals Ltd, Poole, England. Palladium powder was procured from Ventron Chemical Company, Danvers, Massachusetts, U.S.A.. Tin metal was obtained from Mallinckrodt Chemical Works, St Louis, Missouri, U.S.A.. Tort 1 (lobster hepatopancreas) standard reference material was obtained from the National Research Council, Canada. Hydrofluoric acid (doubly distilled in quartz) was obtained from Sea Star Chemicals, Victoria, Canada.

4.2.3 Methodology for the hydride generation atomic absorption spectrophotometry.

4.2.3.1 Continuous hydride generation method (HG-AAS).

The reagents were pumped by means of a peristaltic pump into the reaction coil (A in Figure 4.1), where mixing of the reagents and the production of the tin hydride occurred. A flow of nitrogen gas ensured the purging of the generated tin hydride into the gas-liquid separator (B in Figure 4.1) which was further purged by nitrogen gas. The tin hydride was swept into the heated T-shaped quartz cell where atomization occurred. The absorbance reading was recorded after it became stable. All analyses by the HG-AAS method were carried out in triplicate.

4.2.3.2 Batch hydride generation-graphite furnace method (HG-GFAAS).

The batch hydride generator and the hydride transfer lines were silanized by using a 10% (v/v) triethylsilane solution in toluene as follows:- with all the transfer lines connected, and all taps closed except stopcock H at the bottom of the hydride generator, the quartz tube G was immersed in a solution of 10% triethylsilane in toluene with the water vacuum turned on. The triethylsilane solution was drawn into the hydride generator, and the spent solution was then pumped out via stopcock H. The hydride generator was then dried with a gentle flow of nitrogen, admitted through tap D, over a period of about fifteen minutes. This procedure minimized the adsorption of the tin hydride on the walls of the hydride generator.

During the analysis, measured amounts of hydrochloric acid and the sample

were each pipetted onto the porous glass frit via a B24 joint at the top of the hydride generator, while an upward flow of nitrogen was maintained through tap D

Table 4.1 Graphite furnace atomization program for tin determination by (HG-GFAAS).

Step	Temperature °C	Time (s)	Gas flow (L/min)
1	700	19	3.0
2	700	40	3.0
3	700	40	3.0
4	700	40	3.0
5	700	40	3.0
6	700	4.0	3.0
7	2700	4.0	0.0 *
8	2700	2.0	0.0 *
9	2700	1.0	3.0

* = When absorbance measurement was taken.

Steps 1-6 represent trapping and drying conditions.

Steps 7-8 represent atomization conditions.

Step 9 is clean up.

(Figure 4.2). Measured amounts of sodium borohydride solution were delivered into the hydride generator by means of a peristaltic pump via tap F. The tin hydride produced in the hydride generator was swept by an upward flow of nitrogen admitted through tap D, to a narrow quartz tube of inner diameter 1.1 mm, which was inserted into the heated graphite tube of the graphite furnace atomizer, and trapped by using the furnace program shown in Table 4.1.

A gentle flow of argon maintained an inert atmosphere inside the graphite furnace tube, except during the atomization step when the argon flow was stopped. After the tin hydride had been trapped in the graphite furnace tube, the nitrogen flow into the quartz tube was stopped, and the quartz tube was manually removed from the graphite furnace tube which was then quickly heated to 2700 °C, to atomize the analyte. After each determination, the solution remaining in the hydride generator was pumped out, by using the water vacuum.

4.2.4 Preparation of matrix modifiers and standard tin solutions.

4.2.4.1 Preparation of palladium modifier.

The palladium modifier solutions (2-10 % w/v) used to treat the graphite tubes were prepared by dissolving palladium metal in 1 mL of a warm mixture of concentrated hydrochloric acid and nitric acid (1:5 v/v), and diluting with 2 % ascorbic acid solution in a 5 mL volumetric flask.

4.2.4.2 Preparation of sodium tungstate modifier.

Solutions of the sodium tungstate modifier (2 - 10 % w/v) were prepared by dissolving sodium tungstate dihydrate in de-ionized water.

4.2.4.3 Preparation of standard tin solutions.

Stock standard solutions were typically prepared by dissolving tin metal shot in 2 mL of a warm mixture of concentrated HCl and HNO₃ (1:1), and then diluting the resulting solution to 50 mL in a volumetric flask. Working standard solutions were prepared by diluting appropriate amounts of the stock solution in 0.5 M aqueous HCl solution. The working standard solutions used for quantitation were prepared in 0.5 M HCl solutions containing 2% L-cysteine.

4.2.5 Optimum concentration of reagents used in the continuous hydride generation method (HG-AAS).

The generation of tin hydride is pH dependent¹¹³. The optimum pH and reagent concentrations were established as follows:- various concentrations of sodium borohydride in the range 0.5 - 2.5% (w/v) were prepared in aqueous potassium hydroxide solution (0.2% w/v). A standard tin solution in 0.5 M HCl, and different concentrations of hydrochloric acid in the range 0.1 - 1.0 M were each prepared in different volumetric flasks. When required, these reagents were pumped into the reaction coil of the continuous hydride generator by using the parameters shown in Table 4.2.

At a fixed concentration of hydrochloric acid, standard tin solution, and varying concentrations of sodium borohydride, simultaneously pumped into the reaction coil, the absorbance of the tin hydride produced was measured by the atomic absorption spectrophotometer. The absorbance measured was taken to be an indication of the yield of tin hydride. The reagent concentrations giving the highest absorbance of tin hydride were then used for the determination of total tin.

Table 4.2 Operating conditions for the continuous hydride generation atomic absorption spectrophotometry (HG-AAS).

Flow rate	Sample	4.4 mL/min
Flow rate	HCL	4.4 mL/min
Flow rate	NaBH ₄	4.4 mL/min
Purging gas flow rate		0.6 L/min

4.2.6 Use of L-cysteine to remove interferences.

During the atomic absorption analyses of the marine animal samples, it was observed that the absorbance signal started to decrease as the analysis progressed, until it finally disappeared. This phenomenon was more noticeable when digested environmental samples were introduced either into the batch or continuous hydride generators. Such behavior had previously been encountered by other workers including Brindle and Le²³⁶, Beach and Shrader¹¹³, Le et al²³⁷, and Quevauviller et

al¹¹². To eliminate this interference they added either L-cystine²³⁶ or L-cysteine^{113,237} to the reaction mixture prior to hydride generation. Consequently, in the present work a study was carried out to find the optimum concentration of L-cysteine needed to prevent the disappearance of the tin absorbance.

4.2.6.1 Optimum concentration of L-cysteine required to remove interferences.

Standard tin solutions (0.2 $\mu\text{g}/\text{mL}$) containing 0.5 - 3.0 $\mu\text{g}/\text{mL}$ L-cysteine were prepared in 0.5 M hydrochloric acid. The absorbance corresponding to the tin hydride produced from the reaction between the standard tin solutions and sodium borohydride were measured by using HG-AAS.

For the batch hydride generation method, no optimization was carried out, but the use of the optimum concentration of L-cysteine obtained for the continuous hydride generator was sufficient to prevent the disappearance of the tin absorbance.

4.2.7 Optimum conditions for the batch hydride generation-graphite furnace atomic absorption spectrophotometry (HG-GFAAS).

The batch hydride generation method was optimized for concentration and volume of reagents, trapping temperature, and trapping time of the tin hydride in the graphite furnace tubes coated with 8% sodium tungstate modifier solution.

4.2.7.1 Optimization of reagent concentrations for HG-GFAAS.

A standard tin solution (1 mL of 12 ng/mL tin solution), prepared in 0.5 M hydrochloric acid, was added into the batch hydride generator, and then reacted with various volumes of 0.2 M hydrochloric acid solution, and 2 % (w/v) sodium borohydride in 0.2 % potassium hydroxide solution. The absorbance of the generated tin hydride was measured, and taken to be an indication of the yield of tin hydride. The results obtained for this optimization are discussed in Section 4.4.4.1.

4.2.7.2 Optimization of trapping temperatures and trapping time for tin hydride in the graphite furnace tube.

With the optimum volumes of reagents established, the trapping temperature for the generated tin hydride in the graphite furnace was varied, and the atomic absorbance of tin hydride measured. The experiment was repeated at other trapping temperatures.

After the optimum trapping temperature had been established, the effect of the trapping time on the absorbance was also studied, by varying the trapping time of the tin hydride at a constant trapping temperature and reagent concentrations. The results obtained in this study are discussed in Section 4.4.4.3 and 4.4.4.4.

4.2.8 Treated graphite furnace tubes:- coating the graphite furnace tubes with solutions of sodium tungstate and palladium modifiers.

The method used in this study for the treatment of graphite furnace tubes with

matrix modifiers, is similar to the procedure described by Fritzsche *et al*²³⁸. Pre-used graphite furnace tubes were soaked for 26 hours in aqueous sodium tungstate solution (2 -10% w/v) or in a solution of palladium (2 - 10% w/v) in 2 % aqueous citric acid. The preparation of the palladium and sodium tungstate modifiers is described in Section 4.2.5. The soaked graphite furnace tubes were dried in an oven at 125 - 129 °C for 4.5 hours. Prior to use, they were cleaned once by raising the temperature of the graphite furnace to 3000 °C, and then conditioned by running the graphite furnace program (shown in Table 4.1) four consecutive times.

4.2.8.1 Optimum modifier treatment of graphite furnace tubes.

A standard tin solution was used to produce tin hydride which was trapped in the graphite furnace tubes treated with varying concentrations of sodium tungstate (2 - 10 % w/v) or palladium modifier (2 - 10 % w/v) solutions. The preparation of the sodium tungstate and palladium modifiers is described in Section 4.2.4.

A plot of absorbance versus modifier concentration (Section 4.4.4.5) revealed the optimum modifier concentration required to coat the graphite furnace tubes.

4.2.8.2 Calibration curves for the HG-GFAAS method.

Tin standards (2 - 14 ng/mL) in 0.5 M HCl containing L-cysteine (2% w/v) were introduced into the batch hydride generator, and reacted with 0.2 M HCl (5 mL), and 4 mL of 2 % sodium borohydride solution containing 0.2 % KOH, to produce tin hydride which was trapped on sodium tungstate-treated graphite tubes.

The measured absorbances were plotted as a function of the concentrations of the standard tin solutions, to obtain a calibration curve.

4.3 Sample digestion and preparation.

Freeze dried oysters or the standard reference lobster hepatopancrease, Tort 1 (about 2.00 g) and 2% aqueous potassium hydroxide (20 mL) were placed in a 500 mL round bottom flask fitted with an air cooled reflux condenser previously described by Dodd²³⁹ (Appendix D), and refluxed for 1h 45 min. The contents of the round bottom flask were cooled, and concentrated sulphuric acid (4 mL of 12 M) and concentrated nitric acid 30 mL of 15 M) were added to the round bottom flask, and further refluxed until all solution had gone into the reflux condenser, and the residue in the round bottom flask has charred. Heating was stopped, and after a few minutes, when the solution in the reflux condenser had dripped back into the round bottom flask, refluxing was resumed until the solution became clear and colorless, or very light yellow. The round bottom flask was cooled, and de-ionized water(10-20 mL) was added through the reflux condenser. Reflux was then continued until the solution turned colorless. The solution was cooled and then transferred to a 250 mL glass beaker where the solution was evaporated down to about 10 mL, by using a hot plate. The solution was transferred to another 250 mL beaker made of Nalgene®, followed by the addition of 1 mL hydrofluoric acid. The solution was further evaporated on the hot plate to about 5 mL. Concentrated hydrochloric acid, and de-ionized water (50 mL) were added to the Nalgene® beaker, and further heated until

the volume of the solution has reduced to about 30 mL. The solution was cooled, transferred to a 50 mL volumetric flask containing L-cysteine, and made up to the mark with 0.5 M hydrochloric acid solution to form the digested sample in 2% w/v L-cysteine solution.

A blank solution containing all the reagents used for sample digestion was also digested, by following the same digestion procedure described for the sample.

4.4 RESULTS AND DISCUSSION.

4.4.1 Optimum concentrations of sodium borohydride and hydrochloric acid necessary for the production of stannane in the continuous hydride generator.

The effect of the concentrations of hydrochloric acid and sodium borohydride on the generation of tin hydride, as monitored by measuring the absorbance of the generated hydride, is shown in Figure 4.3. The error bars on all the graphs in this Chapter are the standard errors for three replicate determinations. At all the sodium borohydride concentrations studied, more SnH_4 was generated as the sodium borohydride concentration was increased. At 2% sodium borohydride concentration, a maximum is reached, and further increase in sodium borohydride concentration leads to decreased SnH_4 production as shown by a decrease in absorbance at 2.5% sodium borohydride. As the hydrochloric acid concentration is increased, the absorbance of the generated tin hydride decreased. L-cysteine was not used in this optimization study.

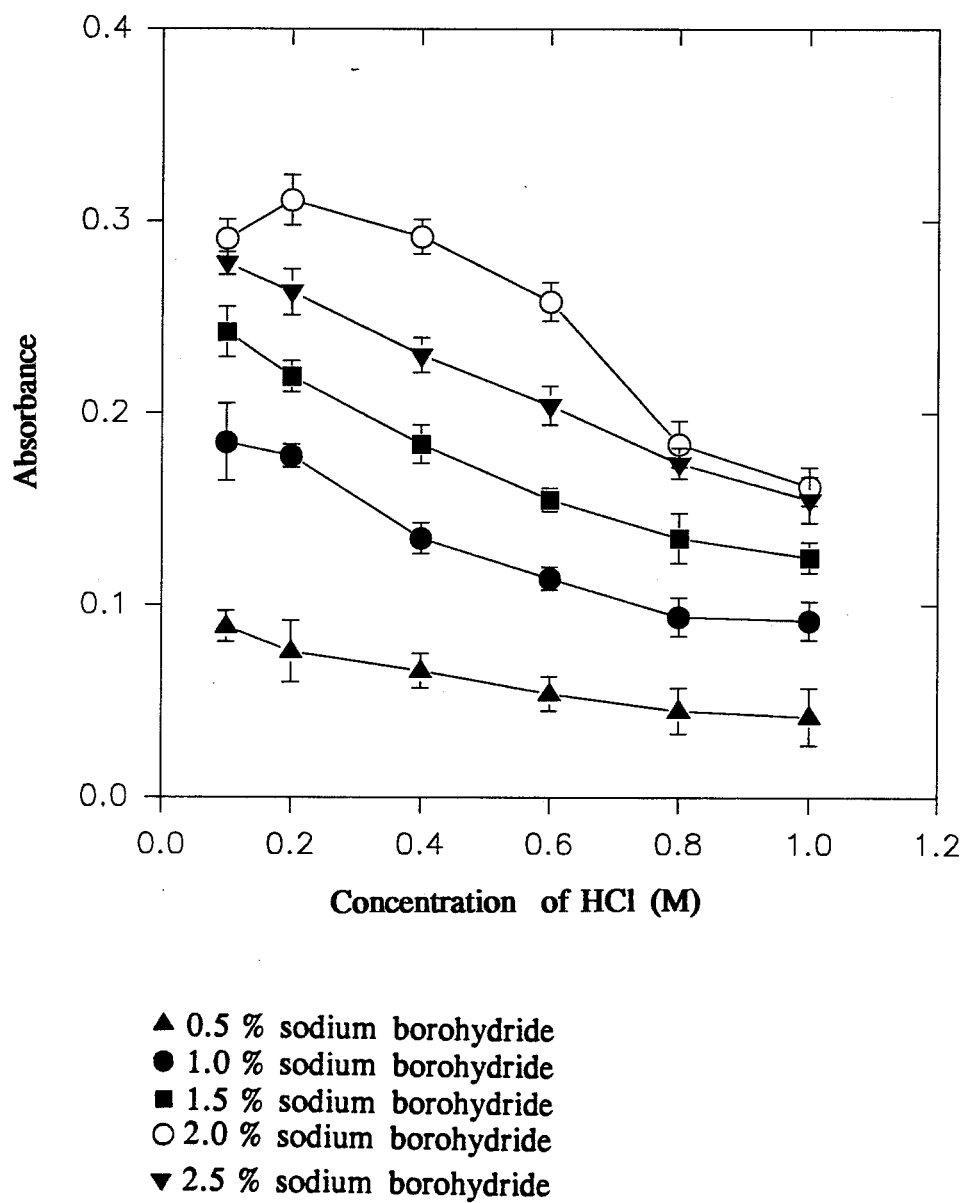


Figure 4.3 Effect of sodium borohydride and HCl on the absorbance of tin hydride produced from 4 $\mu\text{g/mL}$ tin solution.

4.4.2 Optimum concentration of L-cysteine required to eliminate interferences in HG-AAS.

During the HG-AAS analysis of the marine animal samples, the tin absorbance started to decrease as the analysis progressed, especially when the oyster or Tort 1 digested solutions were introduced either into the batch or the continuous hydride generators or when the quartz cell of the continuous hydride generator became dirty with an insoluble material.

Interferences capable of causing the decrease of the tin absorbance signals can be encountered in two stages of the hydride generation-atomic absorption analysis:-

- (a) In the hydride generator, where other metal ions could compete with Sn for borohydride.
- (b) In the heated quartz cell, where the formation of refractory tin carbide, which does not atomize at the temperature of the air-acetylene flame would reduce tin absorption.

Brindle and Le²³⁶, Le et al²³⁷, Nakahara²⁴⁰ and Thompson et al²⁴¹ have reported that transition metal ions such as Fe(II), Fe(III), Co(II), Ni(II), and Cu(II) cause serious reduction of tin absorbance signals. Such interferences that inhibit the formation of SnH_4 had previously been eliminated by using L-cysteine^{113,237} or L-cystine²³⁶. According to these authors^{113,237}, L-cysteine also decreased the pH dependency of the tin hydride formation.

Therefore, a study was carried out to find the optimum concentration of L-cysteine required to improve tin absorbance.

The optimum concentration of L-cysteine was found by analyzing a $0.2 \mu\text{g/mL}$ tin standard solution containing varying concentrations of L-cysteine, and plotting the absorbances against L-cysteine concentrations (Figure 4.4). Figure 4.4 indicates that the optimum concentration of L-cysteine is about 2 % (w/v). The optimum concentration of L-cysteine is higher than the concentration reported by Beach and Shrader¹¹³, and Le *et al*²³⁷ in their methodologies, to improve tin absorbance. Both authors used a 1% L-cysteine solution.

Consequently, all standard tin solutions and digested animal samples were dissolved in solutions containing 2% L-cysteine.

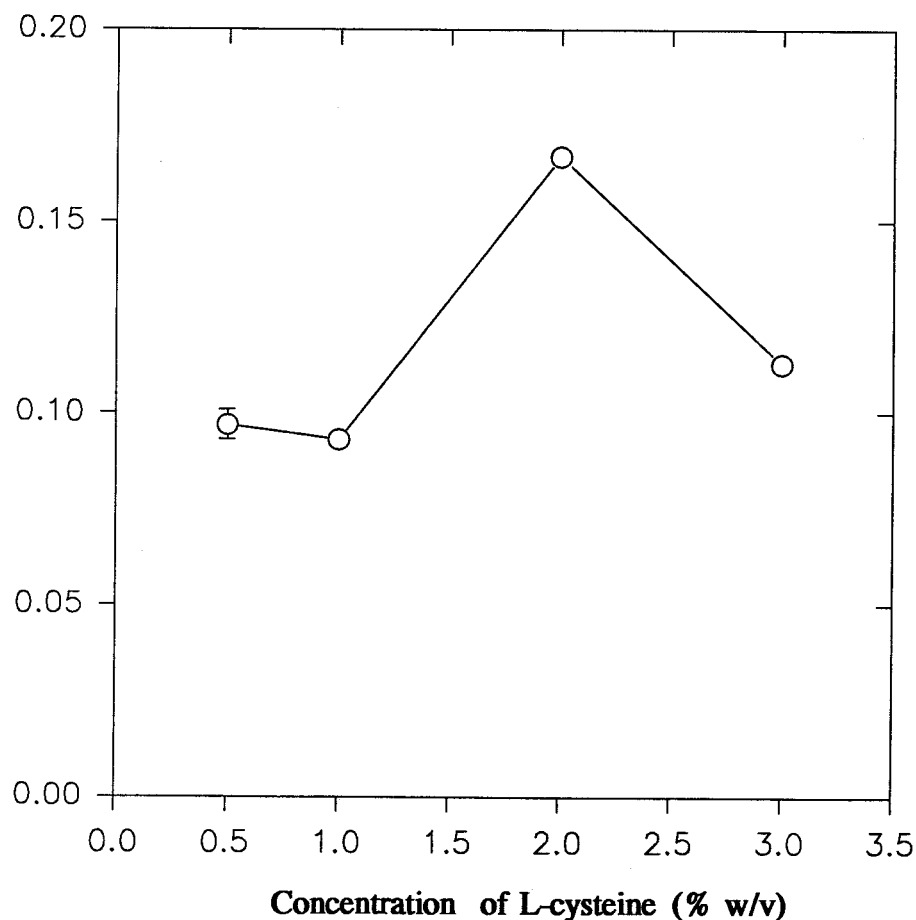


Figure 4.4 Effect of L-cysteine on absorbance of tin hydride.

4.4.3 HG-AAS determination of total tin in oysters and standard reference material (Tort 1).

Digested sample solutions in 2% L-cysteine solution were pumped into the reaction coil of the continuous hydride generator, where a reaction occurred between sodium borohydride and tin, to produce the stannane which was detected by the atomic absorption spectrophotometer. Quantitation of the total tin content of the samples was accomplished by using the standard addition method as follows; 5 mL of the digested sample in 2% L-cysteine solution were spiked into 10 mL of standard tin solutions (0 - 8 $\mu\text{g}/\text{mL}$ Sn) containing 2% L-cysteine in 0.5 M HCl solution. The digested blank solution (5 mL) was also spiked into another set of calibration standards (0 - 8 $\mu\text{g}/\text{mL}$ Sn) containing 2% L-cysteine in 0.5 M HCl. Each mixture of the digested sample solution and the tin standard solution (4 mL) was pumped into the reaction coil of the hydride generator, and the absorbance of the generated tin hydride was measured by the atomic absorption spectrophotometer. Similarly, the absorbance of any tin hydride produced from each mixture of the digested blank and the standard tin solutions was also measured. Two replicate determinations of each sample mixture were carried out. The total tin contents of the samples were then calculated, after the blank values had been subtracted.

Quantitation by using the more difficult and time consuming standard addition method was preferred in this study, because repeated analyses of the certified reference material Tort 1, by the normal calibration method consistently overestimated its total tin content by about three fold. This situation could not be

improved upon, neither by the use of background correction nor blank subtraction. Without the addition of 2% L-cysteine into the sample and standard solutions, quantitation would not be possible, because the tin absorbance was completely suppressed in some determinations. The mechanism of action of L-cysteine is not known with certainty.

The total tin content of the samples and the standard reference materials are shown in Table 4.3.

The total tin content of the standard reference material Tort 1 obtained in this study is in the range previously reported by Sturgeon *et al*²²⁹. Therefore, the digestion method and the HG-AAS method employed in this study are suitable for the determination of total tin in marine animals.

Since the normal calibration method of quantitation gave a much higher total tin value than the certified value for Tort 1, another atomic absorption method capable of reproducing the total tin content of Tort 1, by normal calibration procedure was sought, because of the rapidity and ease of this quantitation method.

Two non-conventional hydride generation-atomic absorption methods; a continuous HG-AAS method developed by Le *et al*²³⁷ and a batch HG-GFAAS method reported by Sturgeon *et al*²²⁹, were considered. The batch HG-GFAAS was preferred over the non-conventional continuous HG-AAS method of Le *et al*²³⁷ because, their method was not validated for the quantitative determination of tin, as neither its reproducibility nor detection limit was reported. Also, the method²³⁷ is not capable of reaching the very high atomization temperatures characteristic of the

Table 4.3 Total tin content of samples analyzed by the HG-AAS method.

Sample	Origin	Total tin content ($\mu\text{g/g}$ dry wt) ^a	Certified value ($\mu\text{g/g}$ dry wt)
Tort 1 ^b	NRC, Canada	0.16 ± 0.04	0.139 ± 0.011^c 0.144 ± 0.016^d
Pacific oyster <u>Crassostrea gigas</u>	Cambell River	0.34 ± 0.09	
Pacific oyster <u>Crassostrea gigas</u>	Fanny Bay	0.35 ± 0.03	
Pacific oyster <u>Crassostrea gigas</u>	Jervis Inlet	0.13 ± 0.01	

a=Total tin content and the standard deviation for 3 replicate determinations

b=Lobster hepatopancrease, a standard reference material from the National Research Council, Canada (NRC).

c=Value certified by NRC, Canada.

d=Value reported by Sturgeon *et al*²²⁹.

batch HG-GFAAS method. Therefore, molecular absorption or non-atomization of refractory tin compounds in the air-acetylene flame, in the quartz furnace of the non-conventional continuous HG-AAS might pose a problem.

Consequently, a batch HG-GFAAS apparatus (Figure 4.2) modelled on the principle reported by Sturgeon *et al*²³⁴, but slightly different in design was constructed and optimized for total tin determination.

4.4.4 Batch hydride generation-graphite furnace atomic absorption spectrophotometry (HG-GFAAS).

The use of the continuous HG-AAS method, has a major disadvantage of consuming large amounts of samples and reagents, and is therefore wasteful and expensive. Conversely, the batch hydride generation method consumes very small amounts of samples and reagents. The small amounts of tin hydride generated are suitable for trapping on a graphite furnace tube, where it is preconcentrated prior to atomization. The preconcentration step, and the ability of the inside surface of the graphite tube to reduce some refractory compounds, are expected to increase the sensitivity and the detection limit of this method.

For normal operation in the graphite furnace mode, the steps involved are: sample drying, ashing, atomization, and tube cleaning. During the drying stage, solvent or water is removed from the sample. At the ashing step, organic and inorganic matrices are removed. However, in the hydride generation-graphite furnace method (HG-GFAAS), organic and inorganic matrices are minimized. At the atomization step, free atoms of the analyte are generated in the graphite tube, and their absorbances are measured by the atomic absorption spectrometer. During the graphite furnace operation, the incandescent graphite tube is protected from

excessive corrosion by an upward flow of an inert gas such as argon or nitrogen (internal purge).

The use of the graphite furnace tube to trap or adsorb tin hydride has been demonstrated by Sturgeon *et al*^{229,235} and was the basis for a HG-GFAAS method reported by these authors^{229,235}. The extension of this methodology to trap tin hydride in graphite furnace tubes precoated with sodium tungstate, and palladium modifiers is described in this section. In the method reported by Sturgeon *et al*²²⁹, no modifiers were used, probably because there was no interference from their sample matrix. In this study, the use of perchloric acid for sample digestion as used by Sturgeon *et al*²²⁹ was avoided because of its explosive nature, instead KOH, HNO₃, H₂SO₄, and HF were used in various stages of the sample digestion (Section 4.3). The difference in reagents used for sample digestion may have contributed to the extent of interferences observed during the HG-GFAAS analysis reported in the present study. The initial approach taken to remove these interferences involved the manual injection of solutions of sodium tungstate or palladium modifiers into the graphite furnace tube prior to every absorbance measurement. Later, the use of graphite furnace tubes pre-treated with solutions of palladium or sodium tungstate, and the presence of L-cysteine in the batch hydride generator, made it possible to analyze the environmental samples. The use of graphite furnace tubes pre-coated with solutions of these modifiers eliminates the inconvenience of manually injecting modifiers into the graphite furnace tube during each analysis.

4.4.4.1 Optimum concentrations of reagents needed for tin hydride production in the HG-GFAAS method.

At a trapping temperature of 700°C, standard tin solution in 0.5M HCl (1 mL of 12 ng/mL Sn), and measured amounts of 0.2 M hydrochloric acid (2 - 20 mL) were pipetted into the batch hydride generator via a B24 joint at the top of the hydride generator. Measured amount of aqueous sodium borohydride (4mL of 2 % w/v in 0.2% KOH solution) was pumped into the batch hydride generator to react with a standard tin solution. The absorbance measurements represent the amount of tin hydride produced (Table 4.4).

Table 4.4 Reagent ratios needed to maximize tin hydride generation

Volume 0.2 M HCl (mL)	Volume 2 % NaBH ₄ (mL)	Absorbance (±) ^a
2	4	0.038 ± 0.007
5	4	0.040 ± 0.003
10	4	0.040 ± 0.007
20	4	0.028 ± 0.001

a=Standard error for three determinations.

All the volume ratios of the reagents examined gave about the same absorbance values when 2 - 10 mL of 0.2 M HCl, and 4 mL sodium borohydride were used for

tin hydride production (Table 4.4). A probable reason for this observation is that in all the cases, the sodium borohydride was present in excess, therefore the reaction went to completion at all the reagent ratios studied. Since the reagent ratios used did not appear to be critical for tin hydride production, provided the sodium borohydride was in excess, all batch hydride generation experiments were carried out at the reagent ratio of 0.2 M HCl (5 mL) : 2% sodium borohydride (4 mL).

4.4.4.2 Optimum flow rate of sodium borohydride into the batch hydride generator.

The effect of the flow rate of sodium borohydride solution into the batch hydride generator, on the absorbance of tin hydride is shown in Figure 4.5. As the

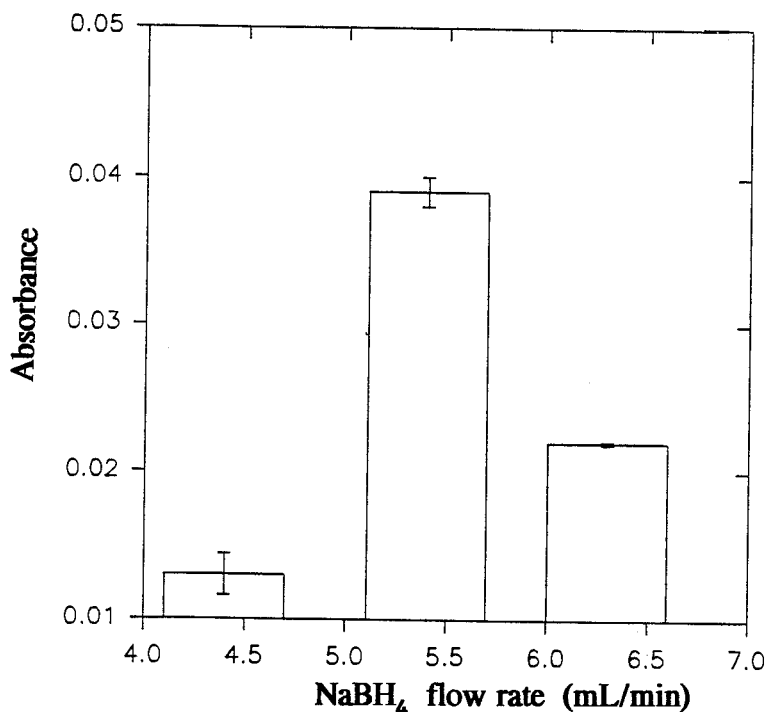


Figure 4.5 Effect of sodium borohydride flow rate on absorbance. (The width of the bars is arbitrary. The error bars are std error for 3 determinations).

sodium borohydride flow rate was increased from 4.4 to 6.3 mL/min, a maximum absorbance was observed at about 5.40 mL/min. This indicates that the flow rate of the sodium borohydride into the hydride generator affects the production of the tin hydride. In their work, Sturgeon *et al*²²⁹ used a flow rate of 4 mL/min to deliver 2 mL of sodium borohydride solution into their hydride generator. The difference in flow rate between the batch hydride generator used in this study and the one reported by Sturgeon *et al*²²⁹ may be due to the difference in the size of the two hydride generators.

4.4.4.3 Optimum temperature for trapping tin hydride in the pre-treated graphite furnace tubes.

The effect of temperature, on the ability of the graphite furnace tubes to trap tin hydride was studied by measuring the absorbance of tin hydride produced from a reaction between standard tin solution (1 mL of 14 $\mu\text{g/mL}$ solution) and sodium borohydride (4 mL of 2% solution), as the temperature of the graphite furnace tube is varied. The result obtained is shown in Figure 4.6.

The absorbance of the tin hydride, as the temperature of the graphite furnace tube is varied, is an indication of the trapping efficiency of the graphite furnace tube. In the temperature range studied, maximum trapping efficiency was obtained at about 700 °C. This trapping temperature is lower than the value reported by Sturgeon *et al*²²⁹, by 100 °C. The lower trapping temperature established in the present study may be due to the pre-treatment of the graphite tubes with sodium

tungstate matrix modifier, and is expected to prolong the "life span" of the graphite tube.

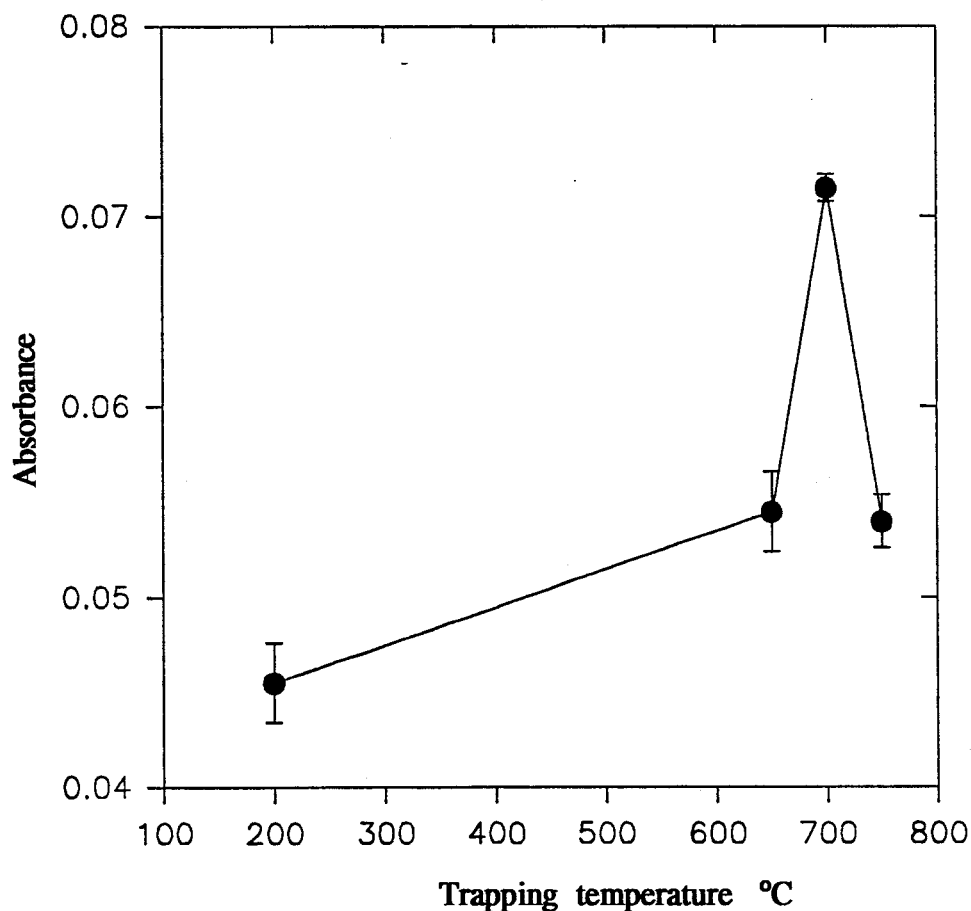


Figure 4.6 Effect of trapping temperature on the atomic absorbance of tin hydride.

4.4.4.4 Optimum trapping time.

A study was carried out to find the trapping time needed to produce maximum absorbance. Figure 4.7 shows the effect of trapping time on the absorbance of tin hydride. Trapping efficiency as monitored by absorbance measurements was maximum at 250-260 seconds. Thereafter, the trapping efficiency decreased. The

decrease in absorbance as trapping time increased beyond 260 seconds may be due to the desorption and escape of the tin hydride from the graphite tube.

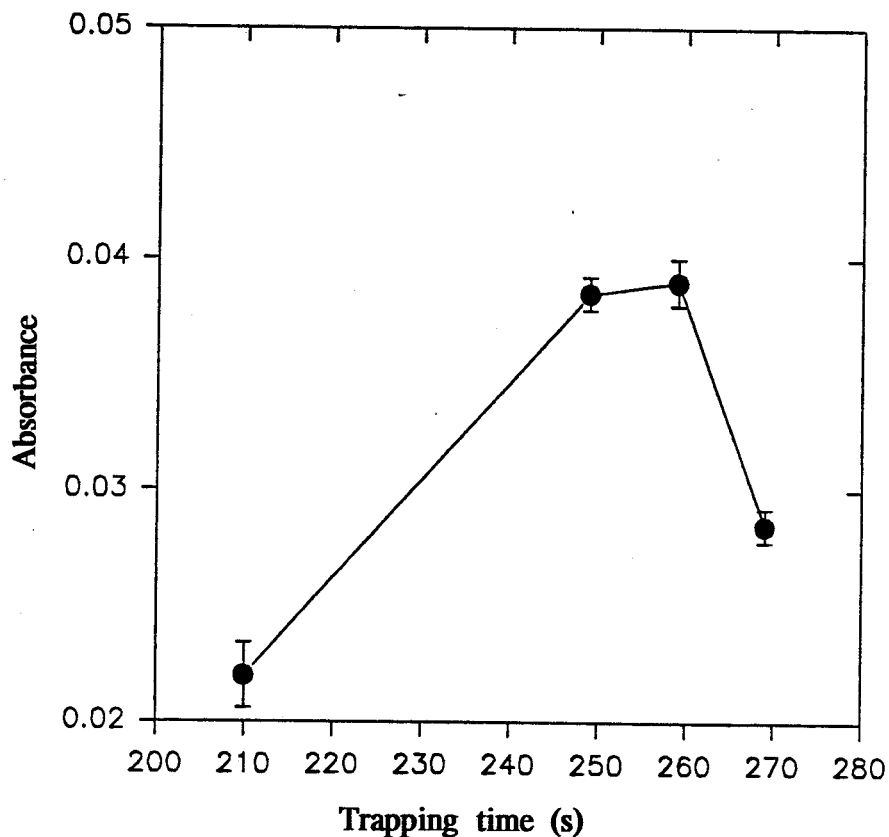


Figure 4.7 Effect of trapping time on absorbance.

4.4.4.5 Pre-treatment of graphite furnace tubes with modifiers.

Vickrey *et al*²⁴² have coated some carbide forming elements such as zirconium, chromium, and molybdenum onto graphite furnace tubes by soaking the graphite furnace tubes in solutions of these elements. This coating method²⁴² was effective in reducing atomization interferences in the GFAAS determination of organotin compounds. Another method of coating graphite furnace tubes with carbide forming elements has been described by Almeida and Seitz²⁴³. This method involved soaking the graphite furnace tubes in solutions of titanium, molybdenum,

or tungsten salts under reduced pressure, in a vacuum line. This method was described by the authors as being more efficient in causing the penetration of the graphite furnace tubes by the modifier, than the method of Vickrey *et al*²⁴². According to Almeida and Seitz²⁴³, the modifiers tungsten and titanium coat on the graphite furnace tubes as oxides, but are converted to the carbides at the high graphite furnace temperatures.

The coating of graphite furnace tubes with carbide forming elements has also been described by Lagas²⁴⁴. His method involved the injection of an aqueous solution of lanthanum chloride into a graphite furnace tube. Drying, ashing, and atomization programs of the graphite furnace converted the injected lanthanum salt to its carbide.

The physical basis for the action of carbide forming elements in GFAAS has been described by Lagas²⁴⁴. According to this author, the carbide coating prevents physical contact between the graphite tube and the analyte thereby preventing carbide formation by the analyte.

Although the use of palladium modifiers to coat GFAAS tubes has not been reported, it was thought feasible to explore such methodology. It is expected that the mechanism of modifier action would be the same as when palladium solution is premixed with the analyte as is normally done in GFAAS. Its use as a modifier in the analyses of an increasing number of elements has been reported^{245,246,247,248}.

Palladium does not act by forming carbides. According to Volynsky²⁴⁹, palladium acts by forming intermetallic compounds and solid solutions with the analyte in the graphite furnace. To function as a modifier, palladium salts are usually

reduced to Pd(0) by using either a solution of citric acid or ascorbic acid.

In the present study, palladium and sodium tungstate modifiers were coated onto graphite furnace tubes, by soaking the graphite furnace tubes in solutions of these modifiers over a period of 26 hours as described in Section 4.2.8

The effect of the concentration of the modifiers on the absorbance of tin hydride, produced by reacting 1 mL of 14 $\mu\text{g/mL}$ tin solution with 4 mL of 2% sodium borohydride in the batch hydride generator is shown in Figures 4.8 and 4.9.

For the graphite furnace tubes coated with sodium tungstate, treatment with 8% sodium tungstate gave maximum absorbance, while treatment with 4% palladium modifier gave maximum absorbance for the palladium-treated graphite tubes.

The exact amount of the modifier coated on each graphite furnace tube was not determined, but it was assumed that the graphite furnace tubes would absorb similar volumes of the modifiers, hence the amount of modifier coated onto these tubes should be proportional to the concentration of the modifier solution in which the graphite furnace tubes were soaked. This assumption seems reasonable because the pre-used graphite furnace tubes were in about the same physical condition, and were from the same batch supplied by the same manufacturer.

Comparatively, at the optimum modifier concentrations, sodium tungstate treated graphite furnace tubes gave better tin absorbance than palladium treated tubes (Table 4.5). Also, analyses with the palladium treated graphite tubes was characterized by a loud popping sound resulting from the ignition of the air-hydrogen mixture in the heated graphite tube. Therefore, the graphite tubes treated with 8%

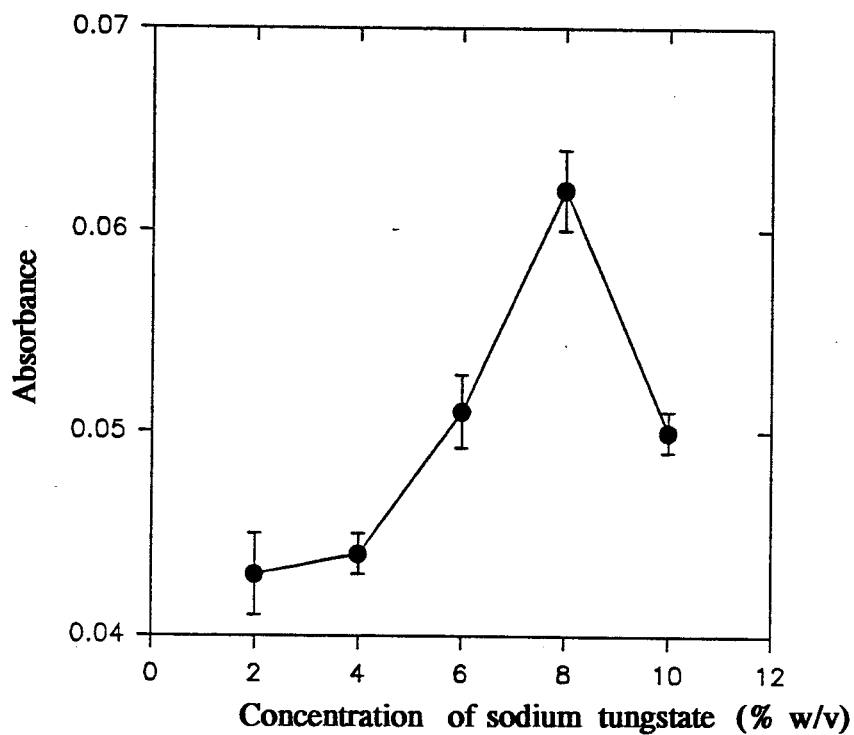


Figure 4.8 Effect of sodium tungstate concentration on absorbance.

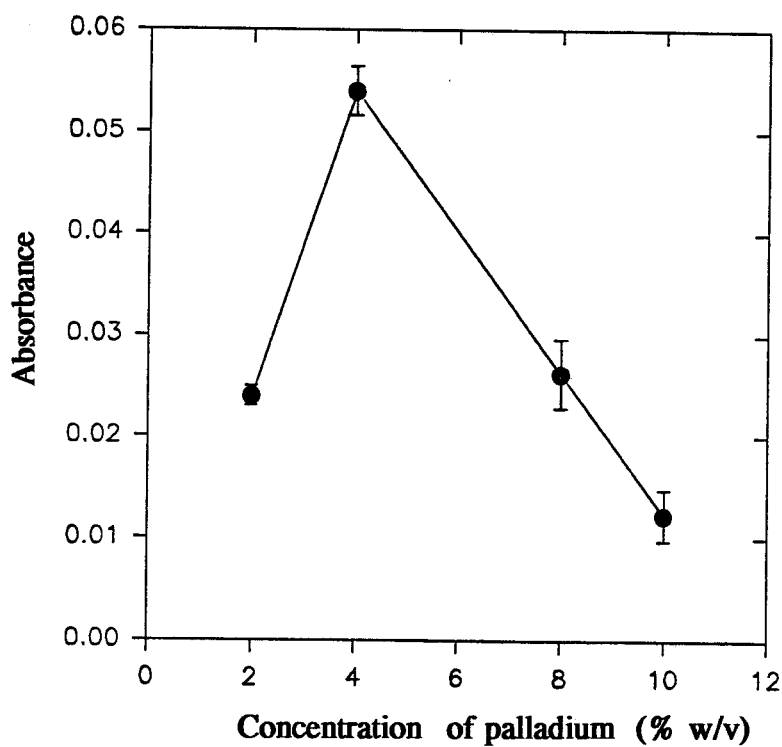


Figure 4.9 Effect of palladium on absorbance.

sodium tungstate were preferred over those treated with the 4% palladium solution.

Table 4.5 Comparison of palladium and sodium tungstate-treated graphite furnace tubes showing the atomic absorbance of tin hydride generated from 14 $\mu\text{g/mL}$ tin solution (1 mL).

Graphite furnace tube treatment	Absorbance (\pm) ^a
4% Palladium treatment	0.054 \pm 0.002
8% Sodium tungstate treatment	0.062 \pm 0.003

a=Standard error for three determinations.

4.4.4.6 Determination of total tin content of a standard reference material by the HG-GFAAS method.

About 2.00 g of Tort 1 (lobster hepatopancrease), a standard reference material was digested as described in Section 4.3. A blank solution of all the reagents used to digest Tort 1 was similarly digested. The digested Tort 1 solution was transferred to a 25 mL volumetric flask containing L-cysteine, and dissolved in de-ionized water, so that the concentration of L-cysteine was 2% w/v. A solution of the digested blank, in 2% L-cysteine was similarly prepared. Aliquots of the digested sample or the digested blank solutions (3 mL), sodium borohydride (4 mL) and HCl (5 mL) were reacted in the batch hydride generator, and the absorbance of the

generated tin hydride was measured.

Quantitation of total tin in Tort 1 was carried out by the normal calibration method, by using the calibration curves obtained as described in Section 4.2.8.2.

The total tin content obtained by using HG-GFAAS is shown in Table 4.6.

Table 4.6 Total tin content of a standard reference material Tort 1 obtained by different authors.

Technique (Source)	Value
HG-GFAAS, (the present study)	0.102 ± 0.018^a
HG-GFAAS, (Sturgeon <i>et al</i> ²³²)	0.144 ± 0.016^b
HG-GFAAS, Isotope dilution ICP-MS (NRC, Canada)	0.139 ± 0.011^b

a= Standard deviation of two replicate determinations.

b= Standard deviation, but number of replicate determinations was not given by the authors.

The total tin content of Tort 1 determined by the batch HG-GFAAS method described in this study lies close to the lower range of values certified for Tort 1 (Table 4.6). The performance of this batch hydride generator may be improved further, by using other optimization techniques, such as the simplex method.

However, the batch HG-GFAAS method described in the present study offers an alternative to the method described by Sturgeon *et al*²²⁹, especially in situations where matrix interferences are a problem. This is because their method²²⁹ was reported to operate without encountering any interferences, therefore its operation in situations such as in the present study where interferences posed a problem, has not been tested.

When the continuous HG-AAS method and the batch HG-GFAAS used in this study are compared, the latter offers a faster method of quantitation by normal calibration. The continuous HG-AAS method is time consuming, involving standard additions. Other comparative data on the two atomic absorption methods of analysis used in the present study are shown in Table 4.7.

Table 4.7 Comparison of figures of merit obtained with the two atomic absorption spectrophotometric methods used in this study.

	HG-AAS	HG-GFAAS
Detection limit	7.5 ng/ mL	1.8 ng/mL
Precision (for 10 runs)	4.3%	3.3%

CHAPTER 5

SUMMARY AND CONCLUSIONS.

Studies involving the analyses of organotin compounds in marine organisms of British Columbia, Canada, and the effect of organotin compounds on the permeability of model biological membranes have been presented in this thesis.

Analysis of organotin compounds in marine organisms by GC-MS SIM affords a very specific technique for the identification and quantitation of these organotin compounds by using the peculiar isotope pattern for tin compounds. This methodology is therefore able to distinguish organotin compounds from other compounds that may co-elute with them from the GC.

The major organotin pollutants found in this study for the coastal areas of British Columbia were tributyltin and dibutyltin species. Dicyclohexyltin levels of 3.5 ng/g (wet wt as Sn) and 21.3 ng/g (wet wt as Sn) were found in only two locations, namely Wreck Beach, Vancouver and Anyox. Therefore, pollution from dicyclohexyltin species is not widespread in the coastal areas studied.

Contamination of mussels and clams by tributyltin and dibutyltin species is widespread, although some locations such as Hastings Arm, Hilton Point Kitimat, Alice Arm and Holberg Sound show no organotin pollution. The butyltin body burden for Blue mussels in the contaminated areas sampled range from 14.4 ng/g to 37.3 ng/g (wet wt as Sn) for tributyltin species and 6.7 to 67.3 ng/g (wet wt as Sn) for dibutyltin species. The trend observed is that most Blue mussels showed the

presence of both dibutyltin and tributyltin. This is expected because dibutyltin species are degradation products of the tributyltin species, and should be present if tributyltin compounds are present. The Soft shell clams analyzed showed tributyltin levels ranging from 0.7 to 19.4 ng/g (wet wt as Sn). The dibutyltin species were mostly not detected even in the Soft shell clams that were contaminated by tributyltin species. This observation is contrary to expectation, and may indicate that dibutyltin species are easily eliminated from the soft shell clams when compared to the Blue mussels. For the other species of mussels and clams analyzed, paucity of samples could not allow for any trend to be established in terms of preferential accumulation of tributyltin or dibutyltin species.

The study of tributyltin body content of Soft shell clams from Quatsino Sound showed a significant reduction in levels from 26.3 ng/g (wet wt as Sn) to 5.5 ng/g (wet wt as Sn) over a period of three years. This reduction in the concentration of tributyltin species may be due to the Canadian Government's regulation of the use of tributyltin compounds, which came into effect in 1989.

When compared to some other locations of the world contaminated by tributyltin species, the mussels analyzed in this study show comparable pollution to mussels from San Diego Bay, U.S.A.¹²² and Tokyo Bay, Japan¹⁷⁴.

The use of ¹H NMR spectroscopy to study the effect of organotin compounds on the permeability properties of model biological membranes was presented in Chapter 3 of this thesis. This represents the first application of proton ¹H NMR to study the permeability properties of butyltin-EPC liposomes. Direct study of the

permeation of the organotin compounds from the model biological membranes was made difficult by their high hydrophobicity and low aqueous solubility. The use of dimethylarsinic acid (DMA) as a permeability probe afforded information on how the organotin compounds affect the permeability of model biomembranes. When tributyltin chloride was added to the extraliposomal compartment of an EPC liposome, the permeability of the liposomes to dimethylarsinic acid greatly increased. The mechanism of the increased permeability could not be determined because the diffusion equations [3.0] and [3.26] (Chapter 3, section 3.9), developed to describe this efflux behavior were unable to distinguish between situations in which there is 100% passive diffusion and 100% facilitated diffusion. However, the increased liposome permeability shows a linear relationship with the concentration of tributyltin chloride present in the extraliposomal compartment according to the relationship $Y = 8.01 \times 10^{-4}X + 1.46 \times 10^{-3}$, where Y is the efflux rate constant and X is the concentration of tributyltin chloride in the extraliposomal compartment.

The permeability coefficient for DMAH efflux from EPC liposomes decreased from 1.7×10^{-8} cm/s to 4×10^{-9} cm/s, when monobutyltin trichloride was added to the extraliposomal compartment of EPC liposomes. The decreased permeability of the EPC liposomes to DMAH in the presence of monobutyltin trichloride does not show a linear relationship. Beyond $16.7 \mu\text{M}$ monobutyltin trichloride added into the extraliposomal compartment, no further decrease in permeability coefficient was observed.

When trimethyltin hydroxide was added to the extraliposomal compartment

of EPC liposomes, the efflux of DMAH was by passive diffusion while the efflux of DMA^- (another species of DMA present in solution at pH 7.4) was by facilitated diffusion mediated by trimethyltin cation. The rate constant for the passive diffusion of DMAH (2.5×10^{-3} /s) when in contact with trimethyl hydroxide was lower than in the absence of trimethyltin hydroxide (1.1×10^{-2} /s).

For the tributyltin chloride-EPC liposomes (TBT-EPC), it was found that DMAH permeated by passive diffusion, while DMA^- permeated by facilitated diffusion if tributyltin chloride was absent in the extraliposomal compartment. This facilitated diffusion was mediated by the tributyltin cations. The rate constant for the passive diffusion of DMAH was dependent on the tributyltin chloride content of the liposomes, and varied from 3.2×10^{-3} /s to 1.7×10^{-3} /s for TBT-EPC A and TBT-EPC B liposomes of composition 5 μg TBT : 0.2 g EPC , and 1.5 μg TBT : 0.2 g EPC respectively.

The rate of facilitated diffusion of DMA^- encountered in this study, was found to be controlled by the ratio of the formation constant to the dissociation constant (β/ϕ), of the trialkyltin-DMA complex. The ratio β/ϕ was found to be 2.5, and 2.1 for the trimethyltin-DMA and tributyltin-DMA complexes respectively. When tributyltin chloride was present in the extraliposomal compartment of a TBT-EPC liposome, the ability of tributyltin cation to mediate facilitated diffusion was removed.

The activation energy for the passive efflux of DMAH from the TBT-EPC liposomes was also concentration dependent and decreased as the tributyltin chloride content of the liposome increased. The activation energies obtained were 64.4

kJ/mol and 52.3 kJ/mol for TBT-EPC A and TBT-EPC B liposomes respectively.

The Arrhenius pre-exponential factor for the TBT-EPC liposomes did not show much variation with the tributyltin chloride content of the liposome, and was calculated to be 2.8×10^{-8} and 4.0×10^{-8} /s for TBT-EPC A and TBT-EPC B respectively.

For the monobutyltin trichloride-EPC liposomes (MBT-EPC), the efflux of DMA was by passive diffusion irrespective of whether monobutyltin trichloride was present in the extraliposomal compartment or not. The permeability coefficient of DMAH for the MBT-EPC liposomes showed slight dependence on the monobutyltin trichloride content of the liposomes, and was 4.9×10^{-9} cm/s and 4.4×10^{-9} cm/s for MBT-EPC A and MBT-EPC B liposomes of composition 0.5 μ g MBT: 0.2 g EPC, and 1.5 μ g MBT: 0.2g EPC respectively. The activation energy for the efflux of DMAH is 106.8 and 121.5 kJ/mol for MBT-EPC A and MBT-EPC B respectively. This indicates that the MBT-EPC liposomes become less permeable with increasing concentration of monobutyltin trichloride in the liposomes. The Arrhenius pre-exponential factors calculated for the these liposomes are 1.1×10^{-8} and 1.0×10^{-8} /s for MBT-EPC A and MBT-EPC B liposomes respectively.

From the results of these permeation experiments, it is concluded that tributyltin chloride and monobutyltin trichloride exert different effects on the permeability of both EPC liposomes and butyltin chloride-EPC liposomes. Whereas tributyltin cation has the ability to act as a carrier for DMA⁻, the monobutyltin cation has no such ability. The present study is the first report of the facilitated transport

of an environmentally important compound, such as dimethylarsinate by trialkyltin cation.

The observation that the Arrhenius pre-exponential factor for the butyltin chloride-EPC liposomes are approximately constant for each type of liposomes, but different for the TBT-EPC and the MBT-EPC liposomes tends to support the conclusion that tributyltin and monobutyltin species exert different effects on the permeability properties of membranes. This difference may contribute to the different toxic effects observed for these butyltin compounds on marine organisms.

Although ^1H NMR spectroscopy is a useful technique for studying the effect of organotin compounds on model membranes, its low sensitivity precludes the direct study of organotin permeation at very low concentrations. There is also the possibility that the spectroscopic shift reagent used to distinguish between the proton resonance inside and outside the liposomes may also modify the properties of the liposomes, thereby influencing the results. The use of a radioisotope technique which would allow for low level organotin permeation studies would be desirable, to check on the results obtained in this investigation.

Chapter 4 of this thesis is concerned with the determination of total tin in oysters from some locations in British Columbia, Canada. Two types of hydride generation-atomic absorption methods were employed for total tin determination: a continuous HG-AAS and a batch HG-GFAAS method. The HG-AAS method was optimized for experimental variables such as reagent concentrations, while the HG-GFAAS method was optimized for reagent concentrations, reagent flow rates,

trapping time and temperatures.

The total tin content of oysters determined by the HG-AAS method, varied from 0.13 $\mu\text{g/g}$ (dry wt) for oysters from Jervis Inlet to 0.35 $\mu\text{g/g}$ (dry wt) for oysters from Fanny Bay, British Columbia, Canada.

Interference effects were minimized by adding L-cysteine into the solution of the analyte. Detection limits of 7.5 and 1.8 ng/mL were obtained for the HG-AAS and HG-GFAAS methods respectively.

REFERENCES

1. Frankland, E., Liebigs Ann. Chem., 71, 171 (1849)
2. Van der Kirk, G.J.M.; Luijten, J.G.A., In "Organotin compounds Vol. 1", Sawyer, A.K., (ed), Marcel Dekker Inc., New York, 1971, p.1.
3. Tin chemicals: The formula for success, International tin research publication No 681.
4. Ward, S.G., Taylor, R.C., Crowe, A.J., Appl. Organomet. Chem. 2, 47 (1988).
5. Huber, F., Vornefeld, M., Preut, H., Von Angerer, E., Ruisi, G., Appl. Organomet. Chem. 6, 597 (1992).
6. Weseloh, R.M., Environ. Entomol., 13, 1371 (1984).
7. Getzendaner, M.E., Corbin, H.E., J. Agr. Food Chem., 20(4), 881 (1972).
8. Jones, P.A., Millson, M.F., Organotins in the Canadian environment; A synopsis, Economic and Technical Review report EPS 3-EC-82-1, Environmental Impact Control Directorate, Ottawa, March 1982, p.6.
9. Hare, J.D., Logan, P.A., Wright, R.J., Environ. Entomol., 12, 1470 (1983).
10. Stewart, C., de More, S.J., Jones, M.R.L., Miller, M.C., Mar Poll. Bull. 24, 204 (1992).
11. Alzieu, C. In "Proc. Organotin Symposium of the Oceans '86" conference, Washington, D.C., September 23-25, 1986, Vol.4, p.1130.
12. Anderson, C.D., Dalley, R., In "Proc. Organotin Symposium of the Oceans '86" Conference, Washington, D.C., September 23-25, 1986, Vol.4, p.1108.
13. Davies, A.G., Smith, P.J., Advances in Inorganic Chemistry and

- Radiochemistry, 23, 1 (1980).
14. Fish, R.H, Kimmel, E.C., Casida, J.E., *J. Organomet. Chem.*, 118, 41 (1976).
 15. Selwyn, M.J., Dawson, A.P., Stockdale, M., Gains, N., *Eur. J. Biochem.* 14, 120 (1970).
 16. Tosteson, M.T., Wieth, J.O., *J. Gen. Physiol.* 73, 789 (1979).
 17. Motais, R., Cousin, J.L., Sola, F., *Biochim. Biophys. Acta*, 467, 357 (1977).
 18. Aldridge, W.N., In "Organotin Compounds: New chemistry and applications", Zuckerman, J.J., (ed) *Adv. Chem. Ser.*, 157, 186 (1976).
 19. Klaus, G.J., Ole, A., Mogens, R., *Appl. Organomet. Chem.*, 3, 225 (1989).
 20. Vitturi, R., Mansueto, C., Catalano, E., Pellerito, L., Girasolo, M.A., *Appl. Organomet. Chem.* 6, 525 (1992).
 21. Spooner, N., Gibbs, P.E., Bryan, G.W., Goad, L.J., *Mar. Environ. Res.* 32, 37 (1991).
 22. Gibbs, P.E., Bryan, G.W., Pascoe, P.L., Burt, G.R., *J. Mar. Biol. Ass. UK*, 67, 507 (1987).
 23. Waldock, M.J., Thain, J.E., *Mar. Poll. Bull.* 14, 411 (1983).
 24. Alzieu, C., Sanjuan, J., Michel, P., Burel, M., Dreno, J.P., *Mar. Poll. Bull.*, 20, 22 (1989)
 25. Beaumont, A.R., Budd, M.D., *Mar. Poll. Bull.*, 15, 402 (1984).
 26. Laughlin, R.B., Norlund, K., Linden, O., *Mar. Environ. Res.*, 12, 243 (1984)
 27. Laughlin, R.B., French, W.J., *Bull. Environ. Contam. Toxicol.*, 25, 802 (1984).
 28. Ward, G.S., Cramm, G.C., Parrish, P.R., Trachman, H., Sleisinger, A., In

- "Aquatic toxicology and hazard assessment: Fourth conference", Branson, D.R., (ed)., American Society for Testing and Materials, Philadelphia, 1981
ASTM STP 737 p.183.
29. Laughlin, R.B., French, W., Guard, H.E., *Water, Air, Soil Pollut.* **20**, 69 (1983).
 30. U'Ren, S.C., *Mar. Poll. Bull.* **14**, 303 (1983).
 31. Maguire, R.J., Paper ENVR-31 presented at the 118th annual meeting of the American Chemical Society, Philadelphia, Pennsylvania, August 26-31, (1984).
 32. Blair, W.R., Olson, G.F., Brinckman, F.E., Iverson, W.P., *Micro. Ecol.*, **8**, 241 (1982).
 33. Laughlin, R.B., Guard, H.E., Coleman, W.M., *Environ. Sci. Technol.*, **20**, 201 (1986).
 34. Chliamovitch, Y.P., Kuhn, C., *J. Fish Biology* **10**, 575 (1977).
 35. Maguire, R.J, Wong, P.T.S, Rhamey, J.S., *Canadian Journal Of Fisheries and Aquatic Sciences.*, **41**, 537 (1984).
 36. Evans, D.W., Laughlin, R.B., *Chemosphere*, **13(1)**, 213 (1984).
 37. Francois, R., Short, T., Weber, J.H., *Environ. Sci. Technol.*, **23(2)**, 191 (1989).
 38. Ward, G.S., Cramm, G.C., Parrish, R.R., Trachman, H., Slesinger, A., Special Technical Publication **734**, American Society for Testing and Materials, Philadelphia, Pennsylvania.
 39. Barug, D., Wonk, J.W., *Pestic. Sci.*, **11**, 77 (1980).
 40. Barug, D., *Chemosphere*, **10**, 1145 (1981).

41. Getzendaner, M.E., Corbin, H.B., *J. Agr. Food Chem.* **20**, 881 (1972).
42. Macek, K.S., Petrocelli, S., Sleight, B., *Aquatic Toxicology ASTM STP 667*, Marking, L.L, Kimerle, R.A., (eds), American Society for Testing and Materials, 1979, p. 251.
43. Cardwell, R.D., Sheldon, A.W., In "Proc. Organotin Symposium of the Oceans '86" Conference, Washington, D.C., September 23-25, 1986, Vol.4, p.1117.
44. Thompson, J.A.J., Sheffer, M.G., Pierce, R.C., Chau, Y.K., Cooney, J.J., Cullen, W.R., Maguire, R.J., "Organotin compounds in the Aquatic Environment". National Research Council of Canada publication No. 22494, 1985, p. 67.
45. Lawson, G., Ostah, N., *Appl. Organomet. Chem.* **7**, 183 (1993).
46. Ford, B.F.E., Liengme, B.V., Sams, J.R., *J. Organomet. Chem.* **19**, 53 (1969).
47. Eng, G., Bathersfield, O., May, L, *Water, Air, and Soil Pollut.*, **27**, 191 (1986).
48. Burke, J.J., Lauterbur, P.C., *J. Am. Chem. Soc.*, **83**, 326 (1961).
49. Hunter, B.K., Reeves, L.W., *Can. J. Chem.*, **46**, 1399 (1968).
50. Harrison, P.G., Ulrich, S.E., Zuckerman, J.J., *J. Am. Chem. Soc.*, **93**, 5398 (1971).
51. Stegmann, H.B., Uber, U., Scheffler, K., *Z. Anal. Chem.*, **286**, 59 (1977).
52. Aldridge, W.N., Cremer, J.E., *Analyst (London)*, **82**, 37 (1957).
53. Havir, J., Vrestal, J., *Vodni Hospod*, **B22(12)**, 323 (1972).
54. Skeel, R.T., Bricker, C.E., *Anal. Chem.*, **33**, 428 (1961).
55. Farnsworth, M., Pekola, J., *Anal. Chem.*, **31**, 410 (1959).

56. Vasundhara, T.S., Parihar, D.B., Fresenius Z. Anal. Chem., **294**, 408 (1979).
57. Farnsworth, M., Pekola, J., In "Treatise on Analytical Chemistry". Part 2, Vol. 3. Kolthoff, I.M., Elving, P.J., Sandell, E.B., (eds), Interscience Publ., New York p. 351.
58. Luke, C.L., Anal. Chem., **28**, 1276 (1956).
59. Ross, W.J., White, J.C., Anal. Chem., **33**, 424 (1961).
60. Omar, M., Bowen, H.J.M., Analyst (London), **107**, 654 (1982).
61. Coyle, C.F., White, C.F., Anal. Chem., **29**, 1486 (1957).
62. Vernon, F., Anal. Chim. Acta, **71(1)**, 192 (1974).
63. Arakawa, Y., Wada, O., Manabe, M., Anal. Chem., **55**, 1901 (1983).
64. Booth, M.D., Fleet, B., Anal. Chem., **42(8)**, 825 (1970).
65. Woggon, H., Sauberlich, H., Unde, W.J., Z. Anal. Chem., **260**, 268 (1972).
66. Laitan, R., Basters, J., Martin, A., Van der Molen, T., Pasma, P., Rabenort, B., Smink, J., J. Assoc. Off. Anal. Chem., **61(6)**, 1504 (1978).
67. Havir, J., Chem. Prum., **24(3)**, 132, (1974). Chem. Abstr., **81**, 9499Z (1974).
68. Riccobi, L., Peboff, P., Chem. Abstr. **44**, 6752a (1950).
69. Tyurin, Y.M., Flerov, V.N., Soviet Electrochem., **6**, 1492 (1970).
70. Toropova, V.F., Saikina, M.K., Chem. Abstr., **48**, 12579g (1954).
71. Hasebe, K., Yamamoto, Y., Kambara, T., Z. Anal. Chem. **310**, 234 (1982).
72. Sulaiman, S.T., Al-Allaf, T.A.K., Abeed, F.A., Microchemical Journal, **35**, 257 (1987).
73. Battais, A., Bensimon, Y., Besson, J., Durand, G., Pietrasanta, Y., Analisis,

- 10(9), 426 (1982).
74. Al-Allaf, T.A.K., Sulaiman, S.T., Hameed, Y.O., *Appl. Organomet. Chem.* **3** 165 (1989).
75. Abeed, F.A., Al-Allaf, T.A.K., Ahmed, K.S., *Appl. Organomet. Chem.*, **4(2)**, 133 (1990).
76. Hodge, V.F., Seidel, S.L., Goldberg, E.D., *Anal. Chem.*, **51(8)**, 1256 (1979).
77. Donard, O.F.X., Rapsomanikis, S., Weber, J.H., *Anal. Chem.* **58**, 772 (1986).
78. Randall, L., Donard, O.F.X., Weber, J.H., *Anal. Chim. Acta* **184**, 197 (1986).
79. Han, J.S., Weber, J.H., *Anal. Chem.* **60**, 316 (1988).
80. Andreae, M.O., Byrd, J.T., *Anal. Chim. Acta* **156**, 147 (1984).
81. Valkirs, A.O., Seligman, P.F., Stang, P.M., Homer, V., Lieberman, S.H., Vafa, G., Dooley, C.A., *Mar. Pollut. Bull.*, **17**, 319 (1986).
82. Balls, P.W., *Anal. Chim. Acta*, **197**, 309 (1987).
83. Michel, P., In "Proc. Organotin Symposium of the Oceans '87" Conference, Halifax, Canada., September 23 - 25, 1987, Vol.4, p.1340.
84. Stang, P.M., Seligman, P.F., In "Proc. Organotin Symposium of the Oceans '86" Conference, Washington, D.C., September 23-25, 1987, Vol. 4, p.1256.
85. Mckie, J.C., *Anal. Chim. Acta.*, **197**, 303 (1987).
86. Stewart, C., de Mora, S.J., *Appl. Organomet. Chem.*, **6**, 507 (1992).
87. Vickrey, T.M., Harrison, G.V., Ramelow, G.J., *Anal. Chem.*, **53(11)**, 1573 (1981).
88. Peetre, I.B., Smith, B.E.F., *Mikrochim Acta*, **1974**, 301.

89. Robbins, W.B., Caruso, J.A., *J. Chromatogr. Sci.*, **17**, 360 (1979).
90. Eckhoff, M.A., McCarthy, J.P., Caruso, J.A., *Anal. Chem.* **54**, 165 (1982).
91. Mulligan, K.J., Hahn, M.H., Caruso, J.A., *Anal. Chem.* **51(12)**, 1935 (1979).
92. Krull, I.S., Panaro, W., Noonan, J., Erickson, D., *Appl. Organomet. Chem.* **3**, 295 (1989).
93. Chromy, L., Mlodzianowska, W., Uhacz, K., Warchol, R., *J. Oil Col. Chem. Assoc.*, **53**, 121 (1970).
94. Krull, I.S., In "The Dahlem Conference on the importance of chemical speciation in environmental processes", Bernhard, M., Brinckman, F.E., Sadlar, P.J., (eds), West Berlin, F.R.G., September 1984, Springer-Verlag, Berlin and Heidelberg, 1986, p.579.
95. Junk, G.A., Richard, J.J., In "Oceans '86 Proceedings Vol. 4, Organotin Symposium, September 1986, Washington, D.C., p. 1160.
96. Gauer, W.O., Seiber, J.N., Crosby, D.G, *J. Agr. Food Chem.*, **22**, 252 (1974).
97. Arakawa, Y., Yu, T.H., Iwai, H., *J. Chromatogr.* **21**, 209 (1981).
98. Tolosa, I., Bayona, J.M., Albaiges, J., Alencastro, L.F., Tarradellas, J., *Fresenius J. Anal. Chem.*, **339**, 646 (1991).
99. Woollins, A., Cullen, W.R., *Analyst*, **109**, 1527 (1984).
100. Hattori, Y., Kobayashi, A., Takemoto, S., Takami, K., Kuge, Y., Sugimae, A., Nakamoto, M., *J. Chromatogr.*, **315**, 341 (1984).
101. Matthias, C.L., Bellama, J.M., Olson, G.J., Brinckman, F.E., *Environ. Sci. Technol.*, **20(6)**, 609 (1986).

102. Clark, S., Craig, P.J., *Appl. Organomet. Chem.*, **2**, 33 (1988).
103. Takami, K., Yamamoto, H., Okumura, T., Sugimae, A., Nakamoto, M., *Analytical Sciences*, **3**, 63 (1987).
104. Soderquist, C.J., Crosby, D.G., *Anal. Chem.*, **50**, 1435 (1978).
105. Valkirs, A.O., Seligman, P.F., Olson, G.J., Brinckman, F.E., Matthias, C.L., Bellama, J.M., *Analyst*, **112**, 17 (1987).
106. Jackson, J.A., Blair, W.R., Brinckman, F.E., Iverson, W.P., *Environ. Sci. Technol.*, **16**, 110 (1982).
107. Andreae, M.O., Byrd, J.T., Froehlich, P.N.Jr, *Environ. Sci. Technol.*, **17**(12), 731 (1983).
108. Hallas, L.E., Means, J.C., Cooney, J.J., *Science*, **215**, 1505 (1982).
109. Ishii, T., *Bull. Jpn Soc. Sci. Fish.*, **48**(11), 1609 (1982).
110. Andreae, M.O., In "Trace metals in sea water (NATO Conf. Ser., 4:9), Wong, C.S., Boyle, E., Bruland, K.W., Burton, J.D., and Goldberg, E.D., (eds)., Plenum Press, New York, p. 1, (1983).
111. Quevauviller, P., Donard, O.F.X., *Appl. Organomet. Chem.*, **4**, 353 (1990).
112. Quevauviller, P., Martin, F., Belin, C., Donard, O.F.X., *Appl. Organomet. Chem.*, **7**, 149 (1993).
113. Beach, C., Shrader, D., *Varian 1991 Seventh Annual Spring Optical Spectroscopy workshop Richmond, B.C., Canada, 1991*, p.111.
114. Neubert, G., Wirth, H.O., *Z. Anal. Chem.*, **273**(1), 19 (1975).
115. Maguire, R.J., Huneault, H., *J. Chromatogr.*, **209**(3), 458 (1981).

116. Meinema, H.A., Burger-Wiersma, T., Versluis-de Haan, G., Gevers, E.C., *Environ. Sci. Technol.* **12(3)**, 288 (1978).
117. Cullen, W.R., Eigendorf, G.K., Nwata, B.U., Takatsu, A., *Appl. Organomet. Chem.* **4(6)**, 585 (1990).
118. Michel, P., Averty, B., *Appl. Organomet. Chem.*, **5**, 393 (1991).
119. Maguire, R.J., Tkacz, R.J., Chau, Y.K., Bengert, G.A., Wong, P.T.S., *Chemosphere*, **15(3)**, 253 (1986).
120. Martin-Landa, I., Pablos, F., Marr, I.L., *Appl. Organomet. Chem.*, **5**, 399 (1991).
121. Gomez-Ariza, J.L., Morales, E., Ruiz-Benite, Z., *Appl. Organomet. Chem.*, **6**, 279 (1992).
122. Stallard, M.O., Cola, S.Y., Dooley, C.A., *Appl. Organomet. Chem.*, **3**, 105 (1989).
123. Aue, W.A., Flinn, G.G., *J. Chromatogr.*, **142**, 145 (1977).
124. Maguire, R.J., Huneault, H., *J. Chromatogr.*, **209(3)**, 458 (1981).
125. Maguire, R.J., *J. Environ. Sci. Technol.*, **18(4)**, 291 (1984).
126. Braman, R.S., Tompkins, M.A., *Anal. Chem.*, **51(1)**, 12 (1979).
127. Maguire, R.J., Tkacz, R.J., *J. Chromatogr.*, **268(1)**, 99 (1983).
128. Aue, W.A., Flinn, C.G., *Can. J. Spectrosc.*, **25**, 141 (1980).
129. Jang, Maxwell, P.S., Siu, K.W.M., Luong, V.T., Berman, S.S., *Anal. Chem.* **63**, 1506 (1991).
130. Forsyth, D.S., Weber, D., Barlow, L., *Appl. Organomet. Chem.*, **6**, 579 (1992).

131. Mueller, M.D., *Fresenius Z. Anal. Chem.* **317**, 32 (1984).
132. Unger, M.A., MacIntyre, W.G., Greaves, J., Huggett, R.J., *Chemosphere*, **15**, 461 (1986).
133. Whang, C., Yang, L., *Analyst (London)*, **113**, 1393 (1988).
134. McLaren, J.W., Siu, K.W.M., Lam, J.W., Willie, S.N., Maxwell, P.S., Palepu, A., Koether, M., Berman, S.S., *Fresenius Z. Anal. Chem.*, **337**, 721 (1990).
135. Suyani, H., Creed, J., Davidson, T., Caruso, J., *J. Chromatogr. Sci.*, **27**, 139 (1989).
136. Garcia-Alonso, J.I., Sanz-Medel, A., Ebdon, L., *Anal. Chim. Acta*, **283**, 261 (1993).
137. Jewett, K.L., Brinckman, F.E., *J. Chromatogr. Sci.*, **19**, 583 (1981).
138. Parks, E.J., Brinckman, F.E., Jewett, K.L., Blair, W.R., Weiss, C.S., *Appl. Organomet. Chem.*, **2**, 441 (1988).
139. Parks, E.J., Brinckman, F.E., Blair, W.R., *J. Chromatogr.* **185**, 563 (1979).
140. Nygren, O., Nilsson, C., Frech, W., *Anal. Chem.* **60**, 2204 (1988).
141. Vickrey, T.M., Howell, H.E., Harrison, G.V., Ramelow, G., *Anal. Chem.*, **52**, 1743 (1980).
142. McGuffin, V.L., Novotny, M., *Anal. Chem.*, **53**(7), 946 (1981).
143. Epler, K.S., O'Haver, T.C., Turk, G.C., MacCrehan, W.A., *Anal. Chem.*, **60**, 2062 (1988).
144. Burns, D.T., Glockling, F., Harriott, M., *Analyst (London)*, **106**, 921 (1981).
145. Jessen, E.B., Taugbol, K., Greibrokk, T., *J. Chromatogr.*, **168**, 139, (1979).

146. Ferri, T., Cardarelli, E., Petronio, B.M., *Talanta*, **36(4)**, 513 (1989).
147. Langseth, W., *J. Chromatogr.*, **315**, 351 (1984).
148. Laughlin, R.B., Guard, H.E., Coleman, W.M., *Environ. Sci. Technol.*, **20(2)**, 201 (1986).
149. Kimmel, E.C., Fish, R.H., Casida, J.E., *J. Agr. Food Chem.*, **25(1)**, 1 (1977).
150. Ohlsson, S.V., Hintze, W.W., *J. High Resol. Chrom. and Chrom. Comm.*, **6**, 69 (1983).
151. Tombouliau, P., Walters, S.M., Brown, K.K., *Mikochim. Acta. [Wien]*, **11**, 11 (1987).
152. Alzieu, C "In Proc. Organotin Symposium of the Oceans'86" conference, Washington D.C., September 23-25, 1986, Vol. 4, p. 1130.
153. Abel, R., King, N.J., Vossler, J.L., Wilkinson, T.G., In "Proc. Organotin Symposium of the Oceans'87" conference, Halifax, Nova Scotia, Canada, September 28-October 1, 1987, Vol.4, p.1314.
154. Champ, M.A., Proc. In "Organotin Symposium of the Oceans'86" conference, Washington, D.C., September 23-25, 1986, Vol.4, p.1135.
155. Maguire, R. J., *Water Poll. Res. J. Canada* **26 (3)**, 243 (1991).
156. Tosteson, M.T., Weith, J.O., *J. Gen. Physiol.* **73**, 789 (1979).
157. Arakawa, Y., Iizuka, T., Matsumoto, C., *Biomed. Res. Trace Elements*, **2(3)**, 321 (1991).
158. Arakawa, Y., Wada, O., In "Metal ions in biological systems" Vol 29, Sigel, H. and Sigel, A., (eds), Marcel Dekker Inc, New York, 1993, p. 101-136.

159. Van der Kirk, G.J.M., Luijten, J.G.A., In "Organic Synthesis", Leonard, N.J., (ed) 36, 86 (1956).
160. Oaks, V., Hutton, R.E., J. Organomet. Chem. 3, 472 (1965).
161. Vogel, A.I., Elementary Practical Organic Chemistry Part III, Quantitative Organic Analysis 3rd edition, Longmans, Green and Co, London, 1957, p.787.
162. The Stadtler handbook of proton NMR spectra, Sadtler Research laboratories Inc., Philadelphia, U.S.A., p.24 & 162.
163. Miller, J. C, Miller, J. N. Statistics for Analytical Chemistry, Ellis Horwood Ltd., England, 1984, p. 57-99.
164. Stewart, C., Thompson, J.A.J., Extensive butyltin contamination in Southwestern Coastal British Columbia, Canada. Paper submitted to Mar. Poll. Bull. (1994).
165. Rice, C. D., Espourteille, F. A., Huggett, R. J., Appl. Organomet. Chem. 1, 541 (1987).
166. Wolniakowski, K. U., Stephenson, M. D., Ichikawa, G. S., In Proc. organotin Symposium of the Oceans '87 conference, Halifax, Nova Scotia, Canada, September 28 - Oct 1, 1987, Vol 4, p.1438.
167. Waldock, M. J., Miller, D., Marine Environmental quality committee report CM 1983/E:12, Ministry of Agriculture, Fisheries and Food, Fisheries Laboratory, Remembrance Avenue, Burnham-on-Crouch, Essex CMO 8HA, U.K., (1983).
168. Rapsomanikis, S., Harrison, R. M., Appl. Organomet. Chem. 2(2), 151 (1988).

169. King, N., Miller, M., de Mora, S., N.Zealand J. Mar. Freshwater Res. **23**, 287, (1989).
170. Bright, D., Personal communication to Professor W.R. Cullen.
171. Chau, Y.K., Yang, F., Maguire, R.J., 24th International Symposium on Environmental Analytical chemistry, Carleton University, Ottawa, Canada, May 16 - 19, 1994.
172. Cai, Y., Bayona, J.M., Albaiges, J., 24th International Symposium on Environmental Analytical chemistry, Carleton University, Ottawa, Canada, May 16 - 19, 1994.
173. Garriet, C., Personal communication to Professor W.R. Cullen.
174. Higashiyama, T., Shiraishi, H., Otsuki, A., Hashimoto, S., Mar. Poll. Bull. **22**(12), 585 (1991).
175. Mayo, B.C., Chem. Soc. Rev. **2**, 49 (1973).
176. Herring, F.G., Cullen, W.R., Nelson, J.C., Philips, P.S., Bull. Mag. Res. **14**, 289 (1992).
177. Lehninger, A.L., Principles of Biochemistry, Worth Publishers Inc., New York, 1984, p. 318.
178. Singer, S.J., Nicholson, G.L., Science, **175**, 720 (1972).
179. Deamer, D.W., Bramhall, J., Chemistry and physics of lipids **40**, 167 (1986).
180. Hope, M.J., Bally, M.B., Mayer, L.D., Janoff, A.S., Cullis, P.R., Chem. Phys. Lipids **40**, 89, (1986)
181. Szoka, F., Papahadjopoulos, D., Ann. Rev. Biophys. Bioeng. **9**, 467 (1980).

182. Bangham, A.D., De Gier, J., Greville, G.D., *Chem. Phys. Lipids* **1**, 225 (1967).
183. Gruner, S.M., Lenk, R.P., Janoff, A.S., Ostro, M.J., *Biochemistry* **24**, 2833 (1985)
184. Mayer, L.D., Hope, M.J., Cullis, P.R., Janoff, A.S., *Biochim. Biophys. Acta* **817**, 193 (1985)
185. Kirby, C., Gregoriadis, G., in "Liposome Technology" Vol 1 Gregoriadis, G (ed) CRC press, 1984, p. 19-27.
186. Johnson, S.M., *Biochim. Biophys. Acta* **307**, 27 (1973).
187. Barrenholtz, Y., Amselem, S., Lichtenberg, D., *FEBS lett.*, **99**, 210 (1986).
188. Kremer, J.M.H, Esker, M.W.J.V.D, Pathmamanoharan, C., Wiersema, P.H., *Biochemistry* **16**, 3932 (1977).
189. Szoka, F., Papahadjopoulos, D., *Proc. Natl. Acad. Sci.* **75**, 4194 (1978).
190. Deamer, D.W., Bangham, A.D., *Biochim. Biophys. Acta* **443**, 629 (1976).
191. Madden, T.D., *Chem. Phys. Lipid* **40**, 207 (1986).
192. Olson, F., Hunt, C.A., Szoka, E.C., Vail, W.J., Papahadjopoulos, D., *Biochim. Biophys. Acta* **557**, 9 (1979).
193. Hope, M.J., Bally, M.B., Webb, G., Cullis, P.R., *Biochim. Biophys. Acta* **812**, 55 (1985).
194. Transport across biological membranes, Hofer, M., (Translated by J.G. Hogget), Pitman Advanced Publishing program, Boston, U.S.A., 1981.
195. Heinz, E., "In Molecular biology, Biochemistry and Biophysics", Kleinzeller, A., Springer, G.F. and Wittmann, H.G., (eds), Springer-Verlag Publishers New

- York, 1978, Vol. 29, p. 10.
196. Hall, J.L., Baker, D.A., Cell membranes and ion transport, Longman Publishers New York, 1977, p.62.
 197. Stein, W.D.,Transport and diffusion across cell membranes, Academic Press, New York, 1986.
 198. Walter, A., Gutknecht, J.J., J. Membrane Biol., **90**, 207 (1986).
 199. Jain, M.K., The bimolecular lipid membrane:A system, Van Nostrand Reinhold Company, New York, 1972, p. 115.
 200. Lieb, W.R., Stein, W.D.,In "Current topics in membranes and transport Vol 2", Bonner, F and Klinzeller, A. (eds), 1971, p. 1-39.
 201. Poznansky, M., Tong, S., White, P.C., Milgram, J.M., Solomon, A.K., J. Gen. Physiol. **67**, 45 (1976).
 202. De Gier, J., Mandersloot, J.G., Hupkes, J.V., McElhaney, R.N., Van Beek, W.P., Biochim. Biophys. Acta **233**, 610 (1970).
 203. Orbach, E., Finkelstein, A., J. Gen. Physiol. **75**, 427 (1980).
 204. Hauser, H., Oldani, D., Philips, M.C., Biochemistry **2**, 4507 (1973).
 205. Parsegian, V.A., Nature **221**, 844 (1969).
 206. Flewelling, R.F., Hubbell, W.L., Biophys. J. **49**, 541, (1986).
 207. Gruner, S.M., In "Liposomes", Ostro, J., (ed), Marcel Dekker Inc. New York, 1987, p. 1.
 208. Selwyn, M.J., Adv. in Chem. Series **157**, 204 (1976).
 209. Heywood, B.R., Molley, K.C., Waterfield, P.C., Appl. Organomet. Chem., **3**,

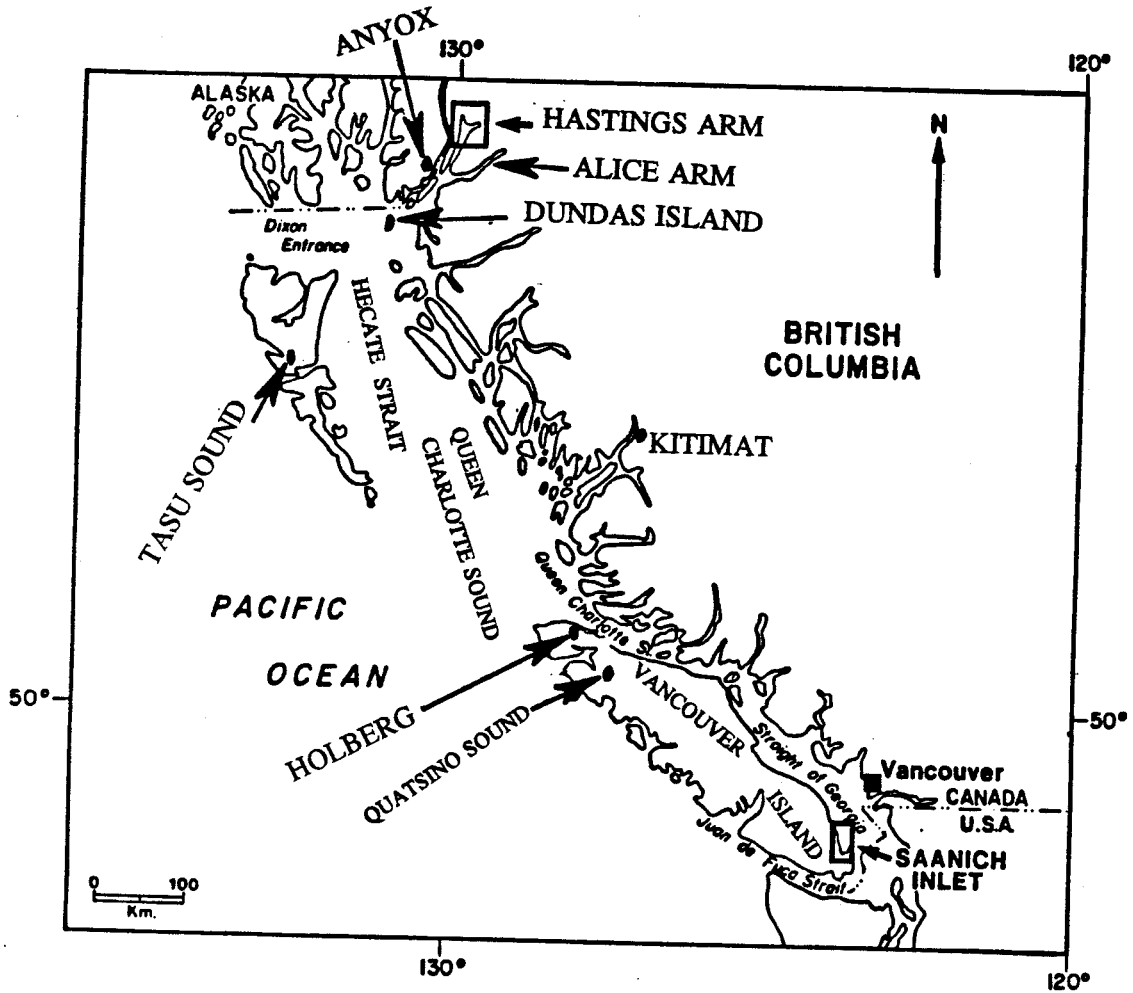
- 443 (1989).
210. Nelson, J.C., Ph.D thesis submitted to the University of British Columbia, Vancouver, Canada, 1993.
 211. Langmuir, I., *J. Amer. Chem. Soc.* **40**, 1361 (1918).
 212. Widdas, W.F., *J. Physiol.* **118**, 23 (1952).
 213. Hall, J.L., Baker, D.A., *Cell membranes and ion transport*, Longman Publishers, New York, 1977, p.46.
 214. Michaelis, L., Menten, M.L., *Biochem. Z.*, **49**, 333 (1913).
 215. Fiske, C.H., Subborow, Y., *J. Biol. Chem.* **66**, 375 (1925).
 216. Bottcher, C.J.F., Vam Gent, C.M., Pries, C., *Anal. Chim. Acta* **24**, 203, (1961).
 217. Houslay, M.D., Stanley, K.K., *Dynamics of biological membranes*, John Wiley and Sons, New York, 1982, p.71-81.
 218. Fukuzawa, K., Ikeno, H., Tokumura, A., Tsukatani, H., *Chemistry and Physics of lipids.* **23**, 13 (1979).
 219. Arakawa, Y., *Main Group metal chemistry*, **12**, 37 (1989).
 220. Arakawa, Y., *Japan J. Hyg.*, **44(1)**, 439 (1986).
 221. Cohen, B.E., *J. Membrane Biol.* **20**, 205 (1975).
 222. Rosenberg, D.W., Kappas, A., *Main Group Metal Chemistry*, **12**, 17 (1989).
 223. Porvaznik, M., Gray, B.H., Mattie, D., Jackson, A.G., Omlor, R.E., *Lab. Invest.*, **54**, 254 (1986).
 224. Juliano, P.O., Harrison, W.W., *Anal. Chem.*, **42**, 84 (1970).
 225. Levine, J.R., Moore, S.G., Levine, S.L., *Anal. Chem.*, **42**, 412 (1970).

226. Rubaska, I., Mikowsky, M., *At. Absorp. Newsl.*, **11**, 57 (1972).
227. Vijan, P.N., Chan, C.Y., *Anal. Chem.*, **48**, 1788 (1976).
228. Subramanian, K.S., *American Laboratory*, p.127 (1980).
229. Sturgeon, R.E., Willie, S.N., Berman, S.S., *Anal. Chem.*, **59**, 2441 (1987).
230. Lee, D., *Anal. Chem.*, **54**, 1682 (1982).
231. Sturgeon, R.E., Willie, S.N., Berman, S.S., *Anal. Chem.*, **57**, 2311 (1985).
232. Willie, S.N., Sturgeon, R.E., Berman, S.S., *Anal. Chem.*, **58**, 1140 (1986).
233. Cullen, W.R., Dodd, M., *Appl. Organomet. Chem.*, **3**, 79 (1989).
234. Sturgeon, R.E., Willie, S.N., Berman, S.S., *Fresenius Z. Anal. Chem.* **323**, 788 (1986).
235. Sturgeon, R.E., Willie, S.N., Sproule, G.I., Berman, S.S., *J. Anal. At. Spec.*, **2**, 719 (1987).
236. Brindle, I.D., Le, X.C., *Analyst* **113**, 1377 (1988).
237. Le, X.C., Cullen, W.R., Reimer, K.J., Brindle, I.D., *Anal. Chim. Acta* **258**, 307 (1992).
238. Fritzsche, H., Wegscheider, W., Knapp, G., Ortner, H.M., *Talanta* **26**, 219 (1979).
239. Dodd, M., Ph.D thesis submitted to the University of British Columbia, Canada (1989).
240. Nakahara, T., *Appl. Spectrosc.* **37**, 539 (1983).
241. Thompson, M., Pahlavanpour, B., *Anal. Chim. Acta* **109**, 251 (1979).
242. Vickrey, T.M., Harrison, G.V., Ramelow, G.J., Carver, J.C., *Anal. Letts.*

- 13(A9), 781 (1980).
243. Almeida, M.C., Seitz, W.R., *Appl. Spectrosc.* **40(1)**, 4 (1986).
244. Lagas, P., *Anal. Chim. Acta* **98**, 261 (1978).
245. Shan, X.Q., Ni, Z.M., Zhang, L., *Anal. Chim. Acta* **151**, 179 (1983).
246. Weibust, G., Langmyhr, F.T., Thomassen, Y., *Anal. Chim. Acta* **128**, 23 (1981).
247. Jin, L.Z., Ni, Z.M., *Can. J. Spectrosc.* **26**, 219 (1981).
248. Schlemmer, G., Wertz, B., *Spectrochim. Acta* **41B**, 1157 (1968).
249. Volynsky, A., *Analyst* **116**, 145 (1991).

APPENDIX A

MAP OF BRITISH COLUMBIA, CANADA, SHOWING SOME LOCATIONS
SAMPLED FOR ORGANOTIN POLLUTION.



APPENDIX B

THE NMR SPECTRAL ACQUISITION AND WATER SUPPRESSION
PARAMETERS FOR THE EFFLUX OF DIMETHYLARSINIC ACID FROM
LIPOSOMES.

;Baz:AU PROGRAM FOR DIFFUSION EXPERIMENTS

II

2ZE

VD

1 DO HG

GO=1 DO

WR #1

IF #1

IN=2

EXIT

VD VDLIST.001

1-27 appropriate delays (seconds)

1	0.001	10	1116.8	19	1716.8
2	216.8	11	1116.8	20	3516.8
3	216.8	12	1116.8	21	3516.8
4	216.8	13	1116.8	22	3516.8
5	216.8	14	1716.8	23	3516.8
6	516.8	15	1716.8	24	3516.8

7	516.8	16	1716.8	25	3516.8
8	516.8	17	1716.8	26	3516.8
9	516.8	18	716.81	27	3516.8

VD; the variable delay was obtained by subtracting the time required to obtain 48 scans from the intended delay. The time required for the NMR spectrometer to obtain 48 scans was 83.2 seconds.

Other NMR parameters were:-

PW=3

DP=0L

DR INITIAL=16 FINAL =8

D1 =0.5

D3 =30 μ S

PW=PO=3.00

NS=48

DE=77.50

DS=2

D1 is the duration of the presaturation pulse

D3 is the pulse delay time

DS is the dummy scan

PW is the pulse width

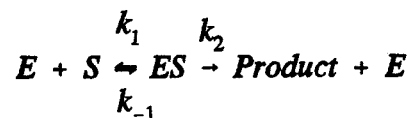
DR is the digitizer resolution

DP is the decoupler power

APPENDIX C

MICHAELIS-MENTONS EQUATIONS FOR ENZYME KINETICS

For enzyme catalyzed reaction:-



where E is the enzyme and S is the substrate.

$$[ES] = \frac{k_1 [E][S]}{k_{-1} + k_2}$$

[ES] is the concentration of complexed enzyme

where $(k_{-1} + k_2)/k_1 = k_m$

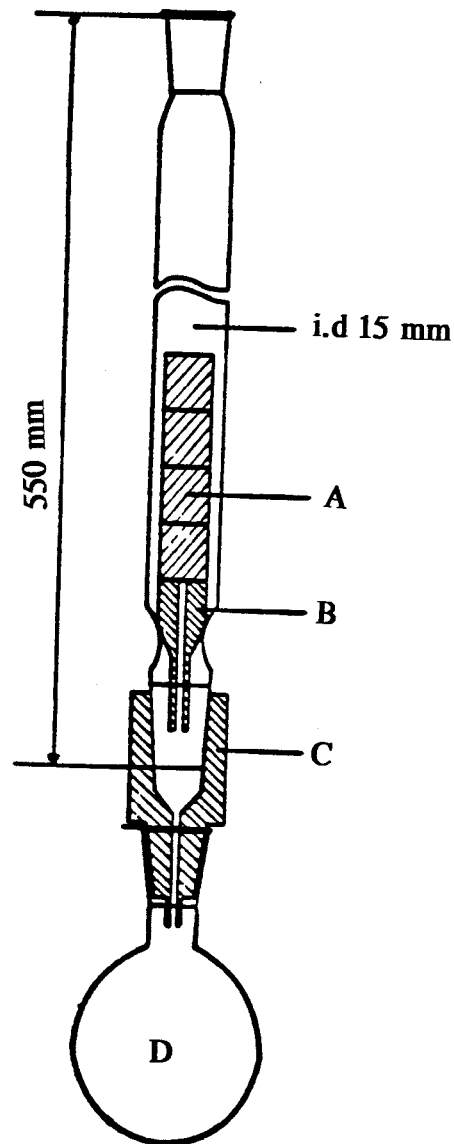
k_m is Michaelis constant.

The rate of the forward reaction is:-

$$v = \frac{V_{\max} [S]}{k_m + [S]}$$

APPENDIX D

WET ASHING APPARATUS WITH AIR COOLED REFLUX CONDENSER
USED FOR DIGESTION OF MARINE ANIMALS.



Wet ashing apparatus (Taken from reference 242) showing the following parts (A) Teflon cylindrical plugs, (B) Teflon diffusion funnel, (C) Teflon stopper with capillary, (D) 500 mL round bottom flask